

AN APPROACH TO GOING HIGHER THAN 1+1
DIMENSIONS WITH SUPERSYMMETRIC DISCRETE
LIGHT CONE QUANTIZATION

DISSERTATION

Presented in Partial Fulfillment of the Requirements for
the Degree Doctor of Philosophy in the
Graduate School of The Ohio State University

By

Motomichi Harada, B.S.

* * * * *

The Ohio State University

2006

Dissertation Committee:

Professor Stephen Pinsky, Adviser

Professor Gregory Kilcup

Professor Robert Perry

Professor Brian Winer

Approved by

Adviser
Graduate Program in
Physics

ABSTRACT

A new technique is proposed in the context of Supersymmetric Discrete Light Cone Quantization (SDLCQ). SDLCQ is a well-established numerical technique to solve supersymmetric theories non-perturbatively. However, it is difficult to apply SDLCQ to theories in the space-time dimensions higher than 1+1 dimensions. This is mainly because in many cases the size of the basis grows exponentially as we increase the number of transverse directions, making it exponentially difficult to solve the theories numerically. Our technique is to circumvent this difficulty by combining the conventional transverse lattice formulation with SDLCQ. Within our formalism, with the help of the large N_c limit, where N_c is the number of color, we treat the transverse degrees of freedom as new 1+1 dimensional field degrees of freedom. This then allows us to regard a theory in $(n+1)+1$ dimensions as a theory in 1+1 dimensions with many more fields and some non-trivial interactions among them, where n is some positive integer. Utilizing this technique, we successfully find the mass spectrum of low-lying energy states for $\mathcal{N} = 1$ Super Yang-Mills theory both in 2+1 dimensions and 3+1 dimensions. Solving supersymmetric theories with SDLCQ in higher than 2+1 dimensions is done for the first time. It is shown that we are free from the species doubling problem in this formulation, even though we have a transverse lattice. Remaining issues and future possible applications of this technique are also discussed.

Dedicated to my mom

ACKNOWLEDGMENTS

First of all, I would like to acknowledge my adviser, Stephen Pinsky for his supervision throughout the course of my research. Without his help, guidance, patience, understanding, insight, knowledge, and wisdom, this work would not have been accomplished in any way. I would also like to show my gratitude to the colleagues, John Hiller, Nathan Salwen, and Uwe Trittman for their insightful comments and help.

I owe so many thanks to so many friends for their support, encouragement, help, advice and prayers. Especially to David and Emily Bressette am I greatly indebted for their consistent care and love. Lastly, I would like to express my sincerest appreciation to my mom for always being a mom for me.

VITA

February 25, 1978 Born - Kochi, Japan.
2000 B. S. Physics, Kobe University, Japan.
2000 - present Graduate Teaching and Research Associate,
The Ohio State University.

PUBLICATIONS

Research Publications

1. M. Harada and S. Pinsky, “ $N = (1,1)$ super Yang-Mills on a $(2+1)$ dimensional transverse lattice with one exact supersymmetry,” *Phys. Lett. B* **567**, 277 (2003) [arXiv:hep-lat/0303027].
2. M. Harada, J. R. Hiller, S. Pinsky and N. Salwen, “Improved results for $N = (2,2)$ super Yang-Mills theory using supersymmetric discrete light-cone quantization,” *Phys. Rev. D* **70**, 045015 (2004) [arXiv:hep-th/0404123].
3. M. Harada and S. Pinsky, “A solution to the fermion doubling problem for supersymmetric theories on the transverse lattice,” *Phys. Rev. D* **70**, 087701 (2004) [arXiv:hep-lat/0408026].
4. M. Harada and S. Pinsky, “ $N = 1$ super Yang-Mills on a $(3+1)$ dimensional transverse lattice with one exact supersymmetry,” *Phys. Rev. D* **71**, 065013 (2005) [arXiv:hep-lat/0411024].
5. J. R. Hiller, M. Harada, S. S. Pinsky, N. Salwen and U. Trittmann, “Two-dimensional super Yang-Mills theory investigated with improved resolution,” *Phys. Rev. D* **71**, 085008 (2005) [arXiv:hep-th/0411220].

FIELDS OF STUDY

Major Field: Physics

TABLE OF CONTENTS

	Page
Abstract	ii
Dedication	iii
Acknowledgments	iv
Vita	v
List of Tables	ix
List of Figures	x
Chapters:	
1. Introduction	1
2. Brief Review of SDLCQ	8
2.1 SDLCQ = SUSY + DLCQ	8
2.2 What is DLCQ?	9
2.2.1 Discretization of momentum	9
2.2.2 Light Cone coordinates	10
2.2.3 Quantization of fields	11
2.2.4 Solving the eigenvalue problem	12
2.3 What is super-algebra?	13
2.4 What can we do with SDLCQ?	14
2.5 Summary	14

3.	Application of SDLCQ to $\mathcal{N} = (2, 2)$ SYM	16
3.1	Introduction	16
3.2	Review of $\mathcal{N}=(2,2)$ SYM theory	18
3.2.1	$\mathcal{N}=(2,2)$ SYM theory and SDLCQ	18
3.2.2	Mass gap	23
3.2.3	Massless states	25
3.3	Correlation functions	31
3.3.1	Correlation functions in supergravity	32
3.3.2	Correlation functions in SUSY with 4 supercharges	33
3.3.3	Numerical results	34
3.4	Discussion	36
4.	SDLCQ meets Transverse Lattice in 2+1 Dimensions	40
4.1	Introduction	40
4.2	Transverse lattice model in 2+1 dimensions	43
4.3	SDLCQ of the transverse lattice model	49
4.4	Numerical results for the cyclic ($W \neq 0$) states	53
4.5	Numerical results for the non-cyclic ($W = 0$) states	57
4.6	Discussion	58
5.	A Solution to Fermion Doubling Problem	62
5.1	Introduction	62
5.2	Fermion species doubling problem on a transverse lattice	63
5.3	Transverse lattice with SDLCQ	65
5.4	Discussion	66
6.	SDLCQ and Transverse Lattice in 3+1 Dimensions	69
6.1	Introduction	69
6.2	Transverse lattice model in 3+1 dimensions	73
6.3	SDLCQ of the transverse lattice model	80
6.4	Coupling dependence of the mass spectrum	89
6.5	Numerical results for the cyclic ($W_I \neq 0$) bound states	92
6.6	Numerical results for the non-cyclic bound states ($W_I = 0$)	94
6.7	Eguchi-Kawai Reduction	95
6.8	Discussion	98

Appendices:

A.	$\mathcal{N}=1$ super-algebra in Majorana representation	106
A.1	D=1	107
A.2	D=2	107
A.3	D=3	107
B.	Formulas	109
	Bibliography	111

LIST OF TABLES

Table	Page
3.1 The mass squared M^2 of the first few lowest massive states in the S -even sector in units of $g^2 N_c / \pi$ for a series of resolutions K	23
3.2 Same as Table 1 but for the S -odd sector.	24
4.1 Number of massive and massless cyclic eigenstates.	54
4.2 Number of massive and massless non-cyclic eigenstates	57
6.1 Parameter sets used for our toy model to get each of the spectra in Fig. 6.3.	91
6.2 Extrapolated values for m^2 in units of $\frac{g'^2}{\pi a^2}$ as $K \rightarrow \infty$ for State A, B, and C in Fig. 6.6 represented by its dominant Fock state.	95

LIST OF FIGURES

Figure	Page	
3.1	Plots of the mass squared in units of $g^2 N_c / \pi$ for the lowest massive states, excluding the anomalously light states, with a polynomial fit constrained to go through the origin. The plot in (a) corresponds to the sector where S and K have the same parity, and the plot in (b) to the sector where S and K have opposite parity.	24
3.2	Plots of log of the scaled correlation function f as a function of $\log_{10}(r)$ for (a) $K = 3, 4, \dots, 12$, (c) K odd, and (e) K even, and plots of $d \log_{10}(f) / d \log_{10}(r)$ as a function of $\log_{10}(r)$ for (b) $K = 3, 4, \dots, 12$, (d) K odd, and (f) K even.	39
4.1	(a) The color charge for the state $ phys\ 1\rangle \equiv d_{i,rs}^\dagger(k_1^+) a_{i,rs}^\dagger(k_2^+) 0\rangle$. The planes represent the color space. a_i carries color r at site i to s at site $i + 1$ and d_i carries it back to r at site i . (b) The color for the state $ phys\ 2\rangle \equiv a_{i+N_{sites}-1,ru}^\dagger(k_{N_{sites}}^+) \cdots a_{i+1,ts}^\dagger(k_2^+) \cdot a_{i,rs}^\dagger(k_1^+) 0\rangle$. The lines which intersect a circle represent the color planes at sites. The color goes all the way around the transverse lattice.	48
4.2	Plots of m^2 in units of $\frac{N_c g^2}{\pi a}$ of low energy cyclic states versus $1/(K - W)$ with a linear fit for $W=1$ (top diamond), 2(top star), 3(top square), 4(top triangle), 5(middle diamond), 6(bottom star), 7(bottom square), 8(bottom triangle), 9(bottom diamond), (a) state A and, (b) state B.	55
4.3	Plots of $K \rightarrow \infty$ limit of m^2 in units of $\frac{N_c g^2}{\pi a}$ of low energy cyclic states versus $1/W$ with a quadratic fit to the data. The diamonds correspond to state A and squares correspond to the state B in Fig. 4.2	56
4.4	Plots of m^2 of low-energy non-cyclic states against $1/K$ with a linear fit in units of $\frac{N_c g^2}{\pi a}$	58

6.1	(a) The color charge for the state $ phys\ 1\rangle \equiv d_{n,rs}^{I\dagger} a_{n,rs}^{I\dagger} 0\rangle$. The planes represent the color space. $a_n^{I\dagger}$ carries color r at site n to s at site $n+i_I$ and $d_n^{I\dagger}$ carries it back to r at site n . (b) The color charge for the state $ phys\ 2\rangle \equiv a_{n+(N_{sites}-1)i_I,ru}^{I\dagger} \cdots a_{n+i_I,ts}^{I\dagger} a_{n,rs}^{I\dagger} 0\rangle$. The lines which intersect a circle represent the color planes at sites. The color goes all the way around the transverse lattice.	79
6.2	Log-log plots of the mass spectrum m^2 in units of $\frac{g'^2}{\pi a^2}$ versus $g' \equiv g\sqrt{N_c}$ with $K = 4, 5, 6$ for (a),(c),(e), respectively. (b), (d), and (f) are the same as (a), (c) and (e), respectively but on a different scale so that one can see the crossings in more detail. 10^{-8} or less is the numerical zero in our code.	102
6.3	Sample spectra obtained from our toy model. (a) and (b) can be seen in the actual full spectrum in Fig. 6.2, while (c) and (d) cannot. . . .	103
6.4	Plots of m^2 in units of $\frac{g'^2}{\pi a^2}$ of low-energy cyclic bound states versus $1/(K - W_1)$ for $W_1=1$ (circle), 2(square), 3(diamond), 4(triangle up), 5(triangle left). Also shown are a linear fit for (a), (b), and (c) and a quadratic fit for (d). The coupling $g' \equiv g\sqrt{N_c} = 1$	104
6.5	Plots of $K \rightarrow \infty$ limit of m^2 in units of $\frac{g'^2}{\pi a^2}$ of low energy cyclic bound states versus W_1 with a fit to the data of the form $b + cW_1^2 + d/W_1^2$ in (a) and of the form $b + c/W_1 + d/W_1^2$ in (b). The circles correspond to the bound state in Fig. 6.4(a), squares in 6.4(b), diamonds in 6.4(c), and triangles in 6.4(d).	105
6.6	Plots of m^2 in units of $\frac{g'^2}{\pi a^2}$ of low-energy non-cyclic bound states against $1/K$ with a linear fit to the data. The coupling $g' \equiv g\sqrt{N_c} = 1$. The circles correspond to bound state A, squares to the state B, diamonds to state C	105

CHAPTER 1

INTRODUCTION

When one is asked to explain what supersymmetry(SUSY) is, there are many ways to answer the question. The most popular one, however, is that it is a symmetry between bosons and fermions. Bosons are particles with integer spin, in particular the ones which mediate the forces in the world of elementary particles, while fermions are particles of half integer spin, and they make up the matter in nature. Interestingly, however, when Golfand and Likhtman discovered SUSY for the first time in their paper [1], they were not looking for the symmetry between bosons and fermions. Rather the question they addressed was what happens if we extend the Poincaré algebra by including some spinorial operators. The Poincaré algebra gives the relation among the generators of translations, rotations and Lorentz boosts. By spinorial operators we mean the ones which anticommute with one another in contrast to the ordinary ones, which commute with one another. It was a few years after their remarkable observation that Wess and Zumino independently constructed the theory of a self-interacting chiral supermultiplet in their seminal paper [2]. For more detail of the early history of how SUSY was discovered and how its formulation has been developed since then, we would like to refer the reader to [3] and the references therein.

Supersymmetric theories¹ have some nice features; for instance, many are not renormalized [4, 5], which means that theories are finite and get no quantum corrections if they are finite at tree level. This feature is the one that plays the central role when we try to resolve the gauge hierarchy problem with SUSY. The gauge hierarchy problem is the problem that we apparently have a huge difference in fundamental energy scale in nature. To put it in another way, it is the problem that in order for the mass of Higgs, which is the scalar (spinless) particle and thought to be responsible for the origin of the mass, to be stable against some quantum corrections, we would have to *fine-tune* the bare mass parameter to compensate for the quantum corrections to about one part of 10^{17} , which seems *unnatural*. Supersymmetry by virtue of the non-renormalization theorem solves the problem because we know that Higgs mass be stable if it exists². In other words, it is because the mass of Higgs is finite at tree level, and therefore we get no quantum corrections and have no need to fine-tune the bare mass parameter.

One more attractive feature that SUSY provides is the following. Suppose there is a unified theory that treats three out of the four forces between elementary particles, the electromagnetic force, weak force, and strong force on an equal footing. Then it is well-known that the unification of the forces does not quite occur without SUSY, whereas it does with SUSY [10]. This fact is probably the most suggestive indirect evidence for the existence of SUSY. Unfortunately we do not yet have *any* direct evidence for it.

¹There is ample literature on SUSY. See for instance [6] and the references therein for a formal introduction. [7, 8] is more related to phenomenology. For more recent review, see for instance [9].

²Higgs particle has not been observed yet, although Large Hadron Collider is eagerly awaited to discover it once it starts collecting data in a couple of years.

Just like many other new ideas, SUSY solved some problems, but also caused some new problems. For instance we must explain how to break SUSY since obviously nature does not respect SUSY (at least) up to some energy scale, say the energy scale that we have been able to explore with the current experiment. There are many ways proposed for breaking SUSY; gauge-mediated, gravity-mediated, and anomaly-mediated SUSY breaking mechanisms to name a few. Also since the Standard Model for the elementary particles without SUSY explains the experiment very well, we must come up with some mechanism to suppress contributions from SUSY in flavor changing neutral current (FCNC) processes to be consistent with the experiment, which is non-trivial. For more discussions of the constraints from the FCNC processes on supersymmetric theories, see for example [11] and the references therein.

All those issues associated with SUSY should be settled once the results from Large Hadron Collider (LHC) are in hand. LHC is an enormous accelerator being built between the Jura mountain range in France and Lake Geneva in Switzerland and is going to be able to generate head-on collisions between particles with enough energies to prove or disprove SUSY. As LHC is expected to start operating in 2007, now is the most exciting time without any doubt to investigate SUSY in full detail.

Enough about the motive to investigate SUSY from the phenomenological point of view. Now let us turn our attention to the reasons why it is of great interest to study supersymmetric theories from the pure theoretical point of view. With regard to this, perhaps one of the greatest discoveries in particle physics in the past decade would be that there appear to be the equivalence between some class of string theories and some class of supersymmetric field theories in the large N_c limit, where N_c is the number of color. This is called AdS/CFT correspondence in literature [12]. For direct numerical

evidence for the AdS/CFT correspondence, see [13]. This correspondence is intriguing because it connects apparently different two fields of study in physics; string theory and field theory. It is well known that string theories have had little to do with any practical application due to the energy scale that they are embedded in, the Planck scale³. However, thanks to the correspondence, now it could be made possible to draw some experimentally testable physical conclusions from the string theory side. Also, understanding supersymmetric theories could help understand string theories as well. This is welcome since the string theory has become one of the most promising candidates for the fundamental theory in nature, with which all the four different interactions among the elementary particles can be unified in a consistent way.

Furthermore, it has been conjectured recently by Armoni, Shifman and Veneziano that in the large N_c limit a non-supersymmetric gauge theory with a Dirac fermion in the antisymmetric tensor representation is equivalent, both perturbatively and nonperturbatively, to $\mathcal{N}=1$ super Yang-Mills (SYM) theory in its bosonic sector [14, 15], where \mathcal{N} stands for the number of SUSYs in theory. Notice here that for $N_c = 3$ the non-supersymmetric gauge theory with a Dirac fermion is just one-flavor QCD. Therefore, even though we have to keep in mind $1/N_c$ corrections, investigating $\mathcal{N}=1$ SYM can be made contact with phenomenology once the conjecture is proven right.

The technique we use to investigate supersymmetric theories throughout in this thesis is called Supersymmetric Discrete Light Cone Quantization (SDLCQ) [16, 17]. A brief review of SDLCQ is given in the following chapter. SDLCQ is a well-established, powerful technique and has been used exclusively to solve SYM in 1+1 dimensions [17] and in 2+1 dimensions [18, 19, 20]. What is remarkable about SDLCQ

³The Planck scale $M_P \simeq 10^{19}$ GeV is of about 10^{17} orders of magnitude bigger than the energy scale the current experiment can attain.

is that it allows one to numerically explore the *nonperturbative* regime of supersymmetric theories. When it comes to solving theories non-perturbatively, one would probably first think of lattice calculations. Unfortunately, however, there are some well-known obstacles that one has to overcome when trying to put SUSY on a lattice; the lack of translational invariance on a lattice; the notorious doubling of fermion states [21]; and the breakdown of the Leibniz rule [22]. Because of them, the progress in putting supersymmetry on a lattice has been rather slow. This fact alone makes the SDLCQ technique even more valuable since SDLCQ does not suffer from these obstacles. Recently, however, some interesting new approaches have shed some light on this issue [23, 24, 25, 26, 27, 28, 29, 30, 31, 32, 33]⁴. These approaches make possible the restoration of supersymmetry in a continuum limit without fine-tuning of parameters and even without introducing some “sophisticated” fermions such as domain-wall [36] or overlap fermions [37, 38]. However, these techniques seem to be applicable to only some subset of all supersymmetric theories.

Therefore, it is interesting to present some results using SDLCQ that can be compared with lattice calculations that make use of these new lattice techniques. This is done in chapter 3 for $\mathcal{N}=(2,2)$ SYM in 1+1 dimensions. The chapter 3 also gives the reader a taste of what we can compute with SDLCQ, which include, but not exhaustively, the calculation of mass spectrum, and two-point correlation function of the stress energy tensor. In particular, we will see that the mass gap closes for the theory as expected by Witten [39], and that there appear to be two different representations in SDLCQ, which coincide in the continuum limit.

⁴These references are only for SYM formulation on a lattice. For other recent progress in an effort to realize (non-gauged) SUSY on a lattice, see for example Ref. [34, 35].

What makes this thesis unique is the development of a technique to apply SDLCQ to theories in higher than 1+1 dimensions in the large N_c limit. Without this newly developed technique, one had to introduce one numerical parameter for the case of 2+1 dimensions, two for 3+1 dimensions and n for $(n+1)+1$ dimensions in addition to the one called K also known as “harmonic resolution” [40]. Then the continuum, desired results are obtained by extrapolating the limit of all the parameters going to infinity. However, there is a strong limitation inherent in the conventional approach because the number of states increases exponentially in each of these parameters⁵, making it difficult to get any sensible extrapolations. The breakthrough, however, comes when we treat the transverse components as new field degrees of freedom and thus regard a theory in $(n+1)+1$ dimensions as a theory in 1+1 dimensions with many fields and some non-trivial interactions. Therefore, we have no need introducing additional parameters besides the harmonic resolution K . This idea was motivated by the notion dubbed “(de)construction” [42], and has been realized by combining the conventional transverse lattice formulation [43, 44, 45] with SDLCQ and making most use of the large N_c limit. The full detail of the technique is given in chapter 4 and 6 for the case of 2+1 dimensional SYM and 3+1 dimensional SYM, respectively.

In chapter 4, we will first derive some physical constraints for states to satisfy, which along with *partially* conserved SUSY will be shown to be enough to resolve, at least for the massive states, the problem associated with the “linearization” of unitary link variables. We will also calculate the mass spectrum of low energy states with different winding numbers. The winding number tells us how many times the

⁵For 1+1 dimensional cases, it turns out that the number of states grows as $(1+l)^K$, where l is the number of types of particles [41].

color flux of a bound state winds around in the transverse direction. The discussion of the apparent similarity of our model and the model in [24] is also given.

Chapter 5 is devoted to dealing with a subtle issue of the species doubling associated with the new technique and we will show that there is no species doubling with our formulation.

The last chapter consists of the generalization of our technique presented in chapter 4 to 3+1 dimensional SYM. It is worthwhile to note that this is the first attempt in literature to solve supersymmetric theories with SDLCQ in higher than 2+1 dimensions. We will find some similarities between 2+1 dimensional case and 3+1 dimensional case as well as some differences. For instance, as in 2+1 dimensions, we *partially* preserve SUSY. What is different in 3+1 dimensions is that the mass spectrum shows much richer behavior with varying the coupling; in fact we see bound states go through some sort of “transition” as we vary the coupling. We will give a toy model to explain the underlying reason for the behavior. The relation between the mass spectrum and winding number is investigated and it appears that the relation can be better explained by considering the bound state as a string constrained in the transverse direction. We end the chapter with discussions of future directions of research regarding this new technique.

CHAPTER 2

BRIEF REVIEW OF SDLCQ

2.1 SDLCQ = SUSY + DLCQ

In this chapter, we give a brief review of Supersymmetric Discrete Light Cone Quantization (SDLCQ). For simplicity we constrain ourselves to 1+1 dimensions. However, the generalization to arbitrary dimensions is straightforward. We write $P^\mu = (E, p)$ and $X^\mu = (t, x)$, where E , p , t , and x are the energy, momentum, usual time coordinate, and space coordinate of a particle in consideration, respectively,

SDLCQ is very similar to the well-known technique called Discrete Light Cone Quantization (DLCQ) first introduced by Pauli and Brodsky in 1985 [40]. As we will see in some detail in the following section, DLCQ (and SDLCQ) is a technique to solve the eigenvalue equation $P^2|\Psi\rangle = m^2|\Psi\rangle$ in quantum field theory. Here $P^2 = E^2 - p^2$ with m being the invariant mass of the particle, and $|\Psi\rangle$ is the state vector describing the particle. The only difference between SDLCQ and DLCQ lies in the fact that, when we try to solve the equation, we express P^2 in terms of the supercharges Q in SDLCQ, while we do not in DLCQ. The relation between P and Q is given by the super-algebra, which will be discussed in some detail later. Thus, roughly speaking, one can say that SDLCQ is a supersymmetric version of DLCQ, or

$$SDLCQ = SUSY + DLCQ.$$

2.2 What is DLCQ?

Here let us discuss DLCQ in some detail. For a complete review of DLCQ, we would like the reader to refer to [46]. As we mentioned above, DLCQ is a technique to solve the eigenvalue problem $P^2|\Psi\rangle = m^2|\Psi\rangle$ in quantum field theory. To this end, we need

- **Discrete** \implies Discretization of momentum;
- **Light Cone** \implies Working in the light cone coordinates; and
- **Quantization** \implies Quantization of fields.

In the following let us take a closer look at each component of DLCQ.

2.2.1 Discretization of momentum

The way to discretize momentum is to impose a periodic or antiperiodic boundary condition on the wave function, so that

$$\Psi(x) = \pm\Psi(x + 2L), \tag{2.1}$$

where the plus (minus) is for the periodic (antiperiodic) condition, x stands for the spatial coordinate, and $2L$ is the period. For definiteness let us employ the periodic condition here. Then, Eq. (2.1) means that the particle described by $\Psi(x)$ has the momentum

$$p = \frac{\pi}{L}n,$$

where $n = 0, 1, 2, \dots$. Note here that n is *non-negative*, which is true only because we work in the light cone coordinates as we will see below.

2.2.2 Light Cone coordinates

The light cone coordinates are defined in 1+1 dimensions as

$$x^\pm \equiv \frac{t \pm x}{\sqrt{2}},$$

where x and t are the usual space and time coordinates, respectively. Similarly we define the light cone momentum and energy as

$$p^\pm \equiv \frac{E \pm p}{\sqrt{2}}. \quad (2.2)$$

By convention x^+ is to describe the light cone “time”, while x^- the light cone “space”. This convention then implies that p^+ is the light cone “momentum” and p^- the light cone “energy” due to the identity

$$P \cdot X \equiv P^\mu X_\mu = Et - px = p^- x^+ + p^+ x^-, \quad (2.3)$$

and the prevalent conception that when we dot P^μ into X_μ , energy is multiplied by time coordinate and momentum by space coordinate. It is a straightforward exercise to find the metric in the light cone coordinates

$$g^{\mu\nu} = \begin{pmatrix} 0 & 1 \\ 1 & 0 \end{pmatrix},$$

which is consistent with Eq. (2.3). With this metric we get

$$m^2 \equiv P^2 = p^+ p^- + p^- p^+ = 2p^+ p^-.$$

Also, one should notice that since $E \geq |p|$, we have $p^\pm \geq 0$ by construction Eq. (2.2) as we noted in the previous section.

2.2.3 Quantization of fields

There is nothing drastically different in the light cone coordinates as far as the field quantization process is concerned. As usual, we upgrade fields to operators by imposing commutation/anticommutation relation; for bosonic fields $A(x)$ at $x^+ = 0$

$$[\hat{A}(x^+ = 0, x^-), \hat{\Pi}_A(y^+ = 0, y^-)] = \frac{i}{2}\delta(x^- - y^-), \quad (2.4)$$

where the hat on top of fields is to remind us that we are now treating fields as operators, and $\hat{\Pi}_A$ is the conjugate momentum of \hat{A} . Similarly for fermionic fields $\hat{\psi}(x)$ at $x^+ = 0$, we have

$$\{\hat{\psi}(x^+ = 0, x^-), \hat{\Pi}_\psi(y^+ = 0, y^-)\} = \frac{i}{2}\delta(x^- - y^-). \quad (2.5)$$

In order for us to proceed further to write A and ψ in terms of creation and annihilation operators \hat{a} , \hat{a}^\dagger , \hat{b} , \hat{b}^\dagger , we need to know what the conjugate momenta are. For instance consider the theory in Ref. [16], where we have SYM dimensionally reduced from 2+1 to 1+1 dimensions. In this case we have⁶ $\hat{\Pi}_A = \partial_- \hat{A}$ and $\hat{\Pi}_\psi = i\hat{\psi}$, so that Eqs. (2.4,2.5) become

$$[\hat{A}(x^-), \partial_- \hat{A}(y^-)] = \{\hat{\psi}(x^-), i\hat{\psi}(y^-)\} = \frac{i}{2}\delta(x^- - y^-). \quad (2.6)$$

The mode expansion of \hat{A} and $\hat{\psi}$ is then given, respectively, by

$$\hat{A}(x^+ = 0, x^-) = \frac{1}{\sqrt{2\pi}} \int_0^\infty \frac{dk^+}{\sqrt{2k^+}} [\hat{a}(k^+)e^{-ik^+x^-} + \hat{a}^\dagger(k^+)e^{ik^+x^-}], \quad (2.7)$$

$$\hat{\psi}(x^+ = 0, x^-) = \frac{1}{2\sqrt{\pi}} \int_0^\infty dk^+ [\hat{b}(k^+)e^{-ik^+x^-} + \hat{b}^\dagger(k^+)e^{ik^+x^-}] \quad (2.8)$$

with

$$[\hat{a}(k^+), \hat{a}^\dagger(p^+)] = \{\hat{b}(k^+), \hat{b}^\dagger(p^+)\} = \delta(k^+ - p^+). \quad (2.9)$$

⁶Here and hereafter we have omitted the color indices from the fields for the sake of simplicity

Note that the momentum k^+ runs from 0 to infinity in the momentum integral above and because of that we have somewhat different coefficients in front of the mode expansion Eqs. (2.7,2.8) than usual. One can verify that Eqs. (2.7,2.8) with the help of (2.9) satisfy (2.6).

As far as the gauge fixing is concerned, it is customary to choose the light cone gauge where $A^+ = A_- = 0$.

2.2.4 Solving the eigenvalue problem

Now we are in a position to solve the eigenvalue problem

$$P^2|\Psi\rangle = m^2|\Psi\rangle = 2p^+p^-|\Psi\rangle. \quad (2.10)$$

We take Fock states as the basis states, so that all the states are obtained by acting on the vacuum $|0\rangle$ with the creation operators a^\dagger and b^\dagger . Remember that each operator carries some unit of momentum π/L . Then it is almost evident that any Fock state is an eigenstate of the total momentum operator p^+ . For instance a state $a^\dagger(\pi/L)b^\dagger(\pi/L)|0\rangle$ is an eigenstate of p^+ with the eigenvalue of $2\pi/L$. Thus, by construction, p^+ is *diagonal* in this basis, and the problem of finding the eigenvalues of $m^2 = 2p^+p^-$ reduces to that of finding the eigenvalues of p^- alone.

One more great feature in this formalism comes from the fact that the light cone momentum is positive definite, that is, $p^+ \geq 0$. Suppose we wish to look for states with a fixed momentum, say $p^+ = K\pi/L$, where K is some positive integer. Then it is not difficult to convince oneself that the number of possible states with the momentum $p^+ = K\pi/L$ obtained by acting on the vacuum with the creation operators, each of which carries some positive momentum, is *finite*. Therefore, when one writes the light

cone energy operator p^- in the matrix form, the matrix becomes *finite*, and thus can be diagonalized in the usual way to find its eigenvalues.

2.3 What is super-algebra?

The super-algebra is an extension of the Poincaré algebra. The Poincaré algebra gives the relation among the generators of the translations, rotations and Lorentz boosts. We extend the Poincaré algebra by including some anticommuting generators which we call supercharges Q . Since the energy-momentum is the generator of the space-time translation, one would expect that the extended algebra would give rise to some relations between the energy-momentum and supercharges. In fact, we have such relations, that for $\mathcal{N} = 1$ SUSY in 1+1 dimensional light cone coordinates turn out to be

$$\{Q^\pm, Q^\pm\} = 2\sqrt{2}p^\pm, \quad \{Q^+, Q^-\} = 0.$$

See Appendix A for more detail of how to derive the relation. In particular, we have

$$(Q^+)^2 = \sqrt{2}p^+, \quad (Q^-)^2 = \sqrt{2}p^-.$$

Thus, plugging $p^+ = K\pi/L$ and $p^- = (Q^-)^2/\sqrt{2}$ into the eigenvalue equation Eq. (2.10), we find

$$m^2|\Psi\rangle = 2p^+p^-|\Psi\rangle = \frac{\sqrt{2}\pi K}{L}(Q^-)^2|\Psi\rangle.$$

Hence, now instead of finding the eigenvalues of p^- , we are to find the eigenvalues of $(Q^-)^2$. This way of solving the eigenvalue problem is what we call Supersymmetric Discrete Light Cone Quantization (SDLCQ).

2.4 What can we do with SDLCQ?

One can calculate many physical quantities with SDLCQ. Most obvious one is the mass spectrum, which is nothing but the solution of the eigenvalue problem Eq. (2.10). Also, since we solve the theory completely by finding the wavefunctions, we can compute the structure function[20], parton number distribution[47], two point correlation function[19, 48, 49], some thermodynamic functions[50] and so forth. The structure function is the probability of finding a parton with specific momentum in a bound state of partons. The probability of finding a specific number of partons in a bound state is called the parton number distribution. By some thermodynamic functions, we mean for example the free energy, internal energy, and specific heat. Thus, the applications of this technique has been proved extremely fruitful. We will give the results of applying SDLCQ to $\mathcal{N} = (2, 2)$ SYM in 1+1 dimensions in the following chapter so as to demonstrate the power of SDLCQ.

2.5 Summary

We reviewed briefly the formulation of SDLCQ in this chapter. SDLCQ is the same as the well-established technique called DLCQ except for the fact that we express the light cone energy p^- in terms of the supercharges Q in SDLCQ to solve the eigenvalue problem Eq. (2.10). We imposed the (anti-)periodic condition in the x^- direction to have discrete momentum p^+ . The field quantization was done by upgrading fields to operators in the usual manner. The advantage of working in the light cone is that the momentum is positive definite and, therefore, the Fock space spanned by Fock states with a fixed momentum becomes finite. This then reduces the infinite dimensional eigenvalue problem to a finite dimensional one. Therefore in

DLCQ (SDLCQ) formalism solving the Eq. (2.10) is to diagonalize the finite matrix $P^-(Q^-)^2$.

CHAPTER 3

APPLICATION OF SDLCQ TO $\mathcal{N} = (2, 2)$ SYM

3.1 Introduction

After briefly reviewing the formulation of SDLCQ, we are going to give some detailed results of the application of SDLCQ in this chapter. The theory we consider is the $\mathcal{N} = (2, 2)$ Super Yang-Mills (SYM) theory in 1+1 dimensions in the large- N_c limit, which is discussed in Ref. [51]. However, the published results are primitive compared to what can be obtained today because of our greatly improved hardware and software. In this chapter we are able to reach a resolution of $K = 12$, while in Ref. [51] we could reach only $K = 5$. Here we will present new and more detailed results on this theory against which the lattice community can compare the results of their new techniques [23, 24, 25, 26, 27, 28, 29, 30, 31, 32, 33]. The results given here have been published in Ref.[52].

An interesting new result of the calculation we present here is that finite dimensional representations of the SDLCQ with odd and even values of K result in very distinct solutions of the $\mathcal{N} = (2, 2)$ SYM theory, which only become identical as K approaches infinity. One might initially think that this is a shortcoming of the SDLCQ approach, but it turns out to be an advantage because it provides an internal measure of convergence.

We will give some numerical results of the low-energy spectrum. There we will see that as we go to higher and higher resolutions, we find bound states with lower and lower mass. We have seen this behavior in the $\mathcal{N} = (1, 1)$ theory where the lowest mass state converges linearly to zero as a function of $1/K$. This closing of the mass gap as $K \rightarrow \infty$ was predicted by Witten [39] for the $\mathcal{N} = (1, 1)$ and $\mathcal{N} = (2, 2)$ theories. We find that in the latter case the convergence is not linear in $\frac{1}{K}$, and, while our results are consistent with the mass gap going to zero, they are not conclusive.

We have also been able to solve analytically for the wave functions of some of the pure bosonic massless states, and we will present the exact form of the wave function for some cases. We will show that the states must have certain properties to be massless, which then enable us to count the number of the states for a given resolution K . In addition, we will present the formulae to count a minimum total number of massless states.

Finally, we will look at the two-point correlation function of the stress-energy tensor $\langle T^{++}(r)T^{++}(0) \rangle$. We see the expected $1/r^4$ -behavior in the UV and IR regions, and, interestingly, we find that the correlator behaves as $1/r^{4.75}$ in the intermediate region. We know of no predictions for this behavior; however, for $\mathcal{N} = (8, 8)$ SYM theory there is a prediction that this correlator should behave like $1/r^5$ in the intermediate region.

The structure of this chapter is the following. In Sec. 3.2 we focus our attention on the low-energy states. After giving a quick review of $\mathcal{N} = (2, 2)$ SYM theory with SDLCQ, we give some numerical results for the low-energy states, discuss analytically some properties of pure bosonic massless states, and present the formulae to count a minimum total number of massless states. We discuss the numerical results for the

two-point correlation function of the stress-energy tensor in Sec. 3.3. A summary and some additional discussion are given in Sec. 3.4.

3.2 Review of $\mathcal{N}=(2,2)$ SYM theory

3.2.1 $\mathcal{N}=(2,2)$ SYM theory and SDLCQ

Before giving the numerical results, let us quickly review some analytical work on $\mathcal{N}=(2,2)$ SYM theory for the sake of completeness. For more details see Ref. [51]. This theory is obtained by dimensionally reducing $\mathcal{N}=1$ SYM theory from four dimensions to two dimensions. In light cone gauge, where $A_- = 0$, we find for the action

$$S_{1+1}^{LC} = \int dx^+ dx^- \text{tr} \left[\partial_+ X_I \partial_- X_I + i\theta_R^T \partial^+ \theta_R + i\theta_L^T \partial^- \theta_L \right. \\ \left. + \frac{1}{2}(\partial_- A_+)^2 + gA_+ J^+ + \sqrt{2}g\theta_L^T \epsilon_2 \beta_I [X_I, \theta_R] + \frac{g^2}{4} [X_I, X_J]^2 \right], \quad (3.1)$$

where x^\pm are the light-cone coordinates in two dimensions, the trace is taken over the color indices, X_I with $I = 1, 2$ are the scalar fields and the remnants of the transverse components of the four-dimensional gauge field A_μ , two-component spinor fields θ_R and θ_L are remnants of the right-moving and left-moving projections of the four-component spinor in the four-dimensional theory, and g is the coupling constant. We also define the current $J^+ = i[X_I, \partial_- X_I] + 2\theta_R^T \theta_R$, and use the Pauli matrices $\beta_1 \equiv \sigma_1$, $\beta_2 \equiv \sigma_3$, and $\epsilon_2 \equiv -i\sigma_2$.

After eliminating all the non-dynamical fields using the equations of motion, we find for $P^\alpha = \int dx^- T^{+\alpha}$

$$P^+ = \int dx^- \text{tr}(\partial_- X_I \partial_- X_I + i\theta_R^T \partial_- \theta_R), \quad (3.2)$$

and

$$P^- = g^2 \int dx^- \text{tr} \left(-\frac{1}{2} J^+ \frac{1}{\partial_-^2} J^+ - \frac{1}{4} [X_I, X_J]^2 + \frac{i}{2} (\epsilon_2 \beta_I [X_I, \theta_R])^T \frac{1}{\partial_-} \epsilon_2 \beta_J [X_J, \theta_R] \right). \quad (3.3)$$

The supercharges are found by dimensionally reducing the supercurrent in the four-dimensional theory. They are

$$Q_\alpha^+ = 2^{5/4} \int dx^- \text{tr} (\partial_- X_I \beta_{I\alpha\eta} u_\eta), \quad (3.4)$$

$$Q_\alpha^- = g \int dx^- \text{tr} \left(-2^{3/4} J^+ \frac{1}{\partial_-} \epsilon_{2\alpha\eta} u_\eta + 2^{-1/4} i [X_I, X_J] (\beta_I \beta_J \epsilon_2)_{\alpha\eta} u_\eta \right), \quad (3.5)$$

where $\alpha, \eta = 1, 2$ and u_α are the components of θ_R .

We expand the dynamical fields X_I and u_α in Fourier modes as

$$X_{I pq}(x^-) = \frac{1}{\sqrt{2\pi}} \int_0^\infty \frac{dk^+}{\sqrt{2k^+}} [A_{I pq}(k^+) e^{-ik^+ x^-} + A_{I qp}^\dagger(k^+) e^{ik^+ x^-}], \quad (3.6)$$

$$u_{\alpha pq}(x^-) = \frac{1}{\sqrt{2\pi}} \int_0^\infty \frac{dk^+}{\sqrt{2}} [B_{\alpha pq}(k^+) e^{-ik^+ x^-} + B_{\alpha qp}^\dagger(k^+) e^{ik^+ x^-}], \quad (3.7)$$

where $p, q = 1, 2, \dots, N_c$ stand for the color indices, and A, B satisfy the usual commutation relations

$$[A_{I pq}(k^+), A_{J rs}^\dagger(k'^+)] = \delta_{IJ} \delta_{pr} \delta_{qs} \delta(k^+ - k'^+), \quad (3.8)$$

$$\{B_{\alpha pq}(k^+), B_{\beta rs}^\dagger(k'^+)\} = \delta_{\alpha\beta} \delta_{pr} \delta_{qs} \delta(k^+ - k'^+). \quad (3.9)$$

We work in a compactified x^- direction of length $2L$ and ignore zero modes. With periodic boundary conditions we restrict to a discrete set of momenta [16]

$$k^+ = \frac{\pi}{L} k, \quad k = 1, 2, 3, \dots, \quad \int dk^+ \rightarrow \frac{\pi}{L} \sum_{k=1}^\infty, \quad \delta(k^+ - k'^+) \rightarrow \frac{L}{\pi} \delta_{kk'} \quad (3.10)$$

Relabeling the operator modes $\sqrt{\frac{L}{\pi}} a(k) = A(k^+ = \frac{\pi k}{L})$ and $\sqrt{\frac{L}{\pi}} b(k) = B(k^+ = \frac{\pi k}{L})$, so that

$$[a_{I pq}(k), a_{J rs}^\dagger(k')] = \delta_{IJ} \delta_{pr} \delta_{qs} \delta_{kk'}, \quad \{b_{\alpha pq}(k), b_{\beta rs}^\dagger(k')\} = \delta_{\alpha\beta} \delta_{pr} \delta_{qs} \delta_{kk'}. \quad (3.11)$$

the expansion is

$$X_{Ipq}(x^-) = \frac{1}{\sqrt{2\pi}} \sum_{k=1}^{\infty} \frac{1}{\sqrt{2k}} [a_{Ipq}(k) e^{-i\frac{\pi}{L}kx^-} + a_{Iqp}^\dagger(k^+) e^{i\frac{\pi}{L}kx^-}], \quad (3.12)$$

$$u_{\alpha pq}(x^-) = \frac{1}{\sqrt{2L}} \sum_{k=1}^{\infty} \frac{1}{\sqrt{2}} [b_{\alpha pq}(k) e^{-i\frac{\pi}{L}kx^-} + b_{\alpha qp}^\dagger(k) e^{i\frac{\pi}{L}kx^-}]. \quad (3.13)$$

In terms of a and b , the supercharges are given by

$$Q_\alpha^+ = 2^{1/4} i \sqrt{\frac{\pi}{L}} \sum_{k=1}^{\infty} \sqrt{k} \beta_{I\alpha\eta} [a_{Iij}^\dagger(k) b_{\eta ij}(k) - b_{\eta ij}^\dagger(k) a_{Iij}(k)], \quad (3.14)$$

and

$$\begin{aligned} Q_\alpha^- &= \frac{i2^{-1/4}g}{\pi} \sqrt{\frac{L}{\pi}} \sum_{k_1, k_2, k_3=1}^{\infty} \delta_{(k_1+k_2), k_3} \left\{ (\epsilon_2)_{\alpha\eta} \right. \\ &\times \left[\frac{1}{2\sqrt{k_1 k_2}} \left(\frac{k_2 - k_1}{k_3} \right) [b_{\eta ij}^\dagger(k_3) a_{Iim}(k_1) a_{Imj}(k_2) - a_{Iim}^\dagger(k_1) a_{Imj}^\dagger(k_2) b_{\eta ij}(k_3)] \right. \\ &+ \frac{1}{2\sqrt{k_1 k_3}} \left(\frac{k_1 + k_3}{k_2} \right) [a_{Iim}^\dagger(k_1) b_{\eta mj}^\dagger(k_2) a_{Iij}(k_3) - a_{Iij}^\dagger(k_3) a_{Iim}(k_1) b_{\eta mj}(k_2)] \\ &+ \frac{1}{2\sqrt{k_2 k_3}} \left(\frac{k_2 + k_3}{k_1} \right) [a_{Iij}^\dagger(k_3) b_{\eta im}(k_1) a_{Imj}(k_2) - b_{\eta im}^\dagger(k_1) a_{Imj}^\dagger(k_2) a_{Iij}(k_3)] \\ &- \frac{1}{k_1} [b_{\eta ij}^\dagger(k_3) b_{\eta im}(k_1) b_{\eta mj}(k_2) + b_{\eta im}^\dagger(k_1) b_{\eta mj}^\dagger(k_2) b_{\eta ij}(k_3)] \\ &- \frac{1}{k_2} [b_{\eta ij}^\dagger(k_3) b_{\eta im}(k_1) b_{\eta mj}(k_2) + b_{\eta im}^\dagger(k_1) b_{\eta mj}^\dagger(k_2) b_{\eta ij}(k_3)] \\ &\left. + \frac{1}{k_3} [b_{\eta ij}^\dagger(k_3) b_{\eta im}(k_1) b_{\eta mj}(k_2) + b_{\eta im}^\dagger(k_1) b_{\eta mj}^\dagger(k_2) b_{\eta ij}(k_3)] \right] \\ &+ 2(\epsilon_2)_{IJ} \left(\frac{1}{4\sqrt{k_1 k_2}} [b_{\alpha ij}^\dagger(k_3) a_{Iim}(k_1) a_{Jmj}(k_2) + a_{Jim}^\dagger(k_1) a_{Imj}^\dagger(k_2) b_{\alpha ij}(k_3)] \right. \\ &+ \frac{1}{4\sqrt{k_2 k_3}} [a_{Iij}^\dagger(k_3) b_{\alpha im}(k_1) a_{Imj}(k_2) + b_{\alpha im}^\dagger(k_1) a_{Jmj}^\dagger(k_2) a_{Iij}(k_3)] \\ &\left. + \frac{1}{4\sqrt{k_3 k_1}} [a_{Iij}^\dagger(k_3) a_{Jim}(k_1) b_{\alpha mj}(k_2) + a_{Iim}^\dagger(k_1) b_{\alpha mj}^\dagger(k_2) a_{Jij}(k_3)] \right) \left. \right\}. \end{aligned} \quad (3.15)$$

using the relation $([\beta_I, \beta_J] \epsilon_2)_{\alpha\eta} = \delta_{\alpha\eta} (\epsilon_2)_{IJ}$.

They satisfy the superalgebra conditions for anticommutators involving Q_α^+ ,

$$\{Q_\alpha^+, Q_\beta^+\} = \delta_{\alpha\beta} 2\sqrt{2} P^+, \quad \{Q_\alpha^+, Q_\beta^-\} = 0. \quad (3.16)$$

but do not satisfy the condition $\{Q_\alpha^-, Q_\beta^-\} = \delta_{\alpha\beta} 2\sqrt{2}P^-$. Instead, in SDLCQ we find

$$\{Q_\alpha^-, Q_\beta^-\} \neq 0 \text{ if } \alpha \neq \beta, \quad (Q_1^-)^2 = \sqrt{2}P_1^- \neq \sqrt{2}P_2^- = (Q_2^-)^2. \quad (3.17)$$

Although we have different P_α^- for different Q_α^- , we can define a unitary, self-adjoint transformation C , such that

$$Ca_{1ij}C = a_{2ij}, \quad Cb_{1ij}C = -b_{2ij}. \quad (3.18)$$

and find that $CP_1^-C = P_2^-$. Thus the eigenvalues of P_α^- are the same. We may choose either one of the two Q_α^- 's, at least for our purposes, and in what follows we will use Q_1^- and will suppress the subscript unless it is needed for clarity.

The momentum, P^+ , is given by

$$P^+ = \frac{1}{\sqrt{2}}(Q_1^+)^2 = \frac{\pi}{L} \sum_k k (a_{Iij}^\dagger a_{Iij} + b_{\nu ij}^\dagger b_{\nu ij}) \quad (3.19)$$

We work with a fixed value of momentum

$$P^+ = \frac{\pi}{L}K, \quad K = 1, 2, \dots \quad (3.20)$$

We call K the resolution because larger values of K allow larger values of L while leaving the momentum P^+ fixed.

The next thing to note is that there are three Z_2 symmetries of Q_1^- . The first one is R_1 -symmetry, where R_α acts as follows

$$a_{1ij} \leftrightarrow a_{2ij}, \quad b_\alpha \rightarrow -b_\alpha \quad (3.21)$$

The second is S -symmetry

$$a_{Iij} \rightarrow -a_{Iji}, \quad b_{\alpha ij} \rightarrow -b_{\alpha ji}. \quad (3.22)$$

The third is what we call T -symmetry

$$a_{Iij} \rightarrow -a_{Iij}, \quad b_\alpha \text{ unchanged.} \quad (3.23)$$

It is easy to see that under these symmetries Q_1^- is invariant.

Using the relations,

$$R_1 Q_1^+ R_1 = -Q_2^+, \quad T Q_\alpha^+ T = -Q_\alpha^+,$$

we find

$$R_1(Q_1^+ \pm Q_2^+)R_1 = \mp(Q_1^+ \pm Q_2^+), \quad T(Q_1^+ \pm Q_2^+)T = -(Q_1^+ \pm Q_2^+). \quad (3.24)$$

Also note that

$$\{Q_1^+ \pm Q_2^+, Q_1^+ \pm Q_2^+\} = \{Q_1^+, Q_1^+\} + \{Q_2^+, Q_2^+\} + \pm 2\{Q_1^+, Q_2^+\} = 4\sqrt{2}P^+. \quad (3.25)$$

We work in a subspace of definite momentum so $(Q_1^+ \pm Q_2^+)$ must have non zero eigenvectors. Since Q_α^+ and Q_α^- are fermionic operators we see that a bosonic energy eigenstate $|\Psi_B\rangle_{++}$ which is even under R and T -symmetry, can be transformed into

$$|\Psi_B\rangle_{\mp-} = Q_1^-(Q_1^+ \pm Q_2^+)|\Psi_B\rangle_{++}, \quad |\Psi_B\rangle_{-+} = (Q_1^+ + Q_2^+)(Q_1^+ - Q_2^+)|\Psi_B\rangle_{++} \quad (3.26)$$

which are all degenerate with $|\Psi_B\rangle_{++}$. One should notice here that we cannot use Q_1^- and Q_2^- at the same time since they do not commute with each other. Thus, including the supersymmetry, we have an 8-fold degeneracy. Utilizing the remaining S -symmetry, which does not give us a mass degeneracy, we can divide the mass spectrum into 16 independent sectors. This significantly reduces the size of the computational problem. It will be convenient to refer to bound states of this theory as having S , T , or R even or odd parity and to refer to a state as having even or odd resolutions if K is an even or odd integer.

$K=3$	4	5	6	7	8	9	10	11	12
1.308	4.009	0.0067	2.144	0.0040	1.415	0.0026	1.040	0.0018	0.8188
12.62	12.24	0.6304	2.514	0.0060	1.5999	0.0038	1.138	0.0026	0.8790
22.06	15.04	1.0813	2.645	0.4366	1.712	0.0048	1.212	0.0026	0.9312
	15.28	1.1099	2.773	0.6016	1.729	0.3515	1.256	0.0039	0.9397
	22.53	1.5732	2.807	0.6308	1.811	0.4372	1.347	0.3062	1.0072

Table 3.1: The mass squared M^2 of the first few lowest massive states in the S -even sector in units of $g^2 N_c / \pi$ for a series of resolutions K .

3.2.2 Mass gap

Tables 3.1 and 3.2 show the first few low-mass states. We find anomalously light states in the sectors with opposite K and S parity for K larger than 4. Furthermore, the number of extremely light states increases by one as we increase K by two. We believe that these anomalously light states should be exactly massless states, but for some reason there is an impediment preventing SDLCQ from achieving this result. Some of the evidence for this comes from a study of the average number of partons $\langle n \rangle$ in the bound states. For example, in the sector with S and K even, for each even integer r less than K , there is exactly one bosonic massless state with $\langle n \rangle = r$. For K odd we do not see massless states of this type, but we do find $\langle n \rangle = r$ for the anomalously light bound states in this sector. This is also the first sign of the distinction between representations of the supersymmetry algebra in different symmetry sectors, namely those with anomalously light states (with opposite S and K parity) and those without anomalously light states (with matching S and K parity).

In our discussion of the mass gap we will not include the anomalously light states as part of the massive spectrum for the reason given above. To study the mass gap

$K=4$	5	6	7	8	9	10	11	12
1.2009	3.1876	0.00674	1.8427	0.00440	1.2687	0.00302	0.95786	0.00217
1.2009	3.1887	0.6402	1.9305	0.00538	1.3266	0.00317	0.99795	0.00218
12.296	3.3239	0.6747	2.0413	0.45529	1.4087	0.00431	1.0302	0.00219
12.296	11.489	0.9900	2.1415	0.48010	1.5107	0.36858	1.1036	0.00356
19.502	11.492	1.0313	2.3603	0.55873	1.5219	0.38647	1.1345	0.32053

Table 3.2: Same as Table 1 but for the S -odd sector.

we will look at the lowest massive state in each sector as a function of $1/K$ as shown in Fig. 3.1. There we also show polynomial fits in all four sectors separately. The

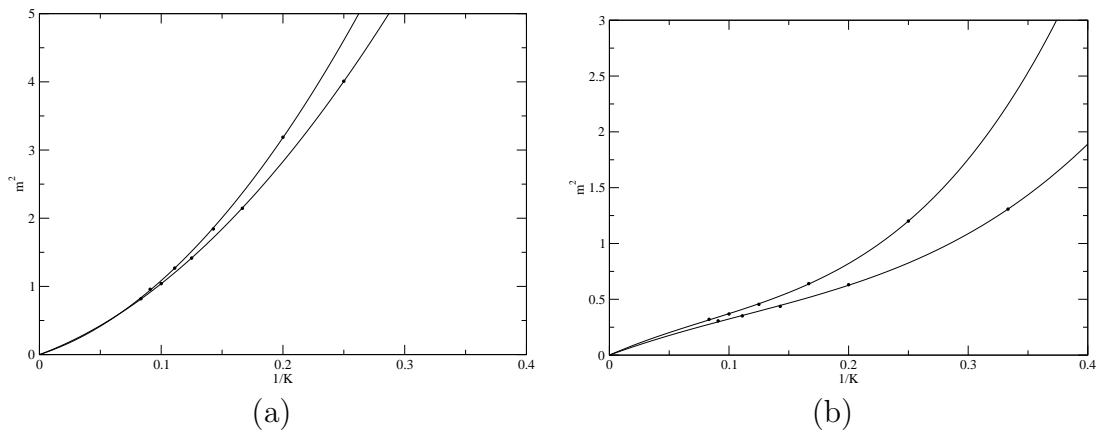


Figure 3.1: Plots of the mass squared in units of $g^2 N_c / \pi$ for the lowest massive states, excluding the anomalously light states, with a polynomial fit constrained to go through the origin. The plot in (a) corresponds to the sector where S and K have the same parity, and the plot in (b) to the sector where S and K have opposite parity.

fits are constrained to go through the origin. The quadratic fits look very good in Fig. 3.1(a). but Fig. 3.1(b) required a cubic. The two fits with opposite S and K parity look very similar as do the two fits with same S and K parity. In each case we could have fit all the points with one curve if we were to include a small oscillatory

function in the fit. We should note here that oscillatory behavior has been observed before in different theories [53, 54]. The explanation given there is that those states which show the oscillatory behavior comprise non-interacting two-body states. This, however, does not seem applicable in our case since the states in Fig. 3.1 are the lowest energy states; thus there are no lower energy states available to form two-body states.

The distinct character of the mass gap serves as another piece of evidence that we have two different classes of representations. The data is consistent with the mass gap closing to 0 as $K \rightarrow \infty$, especially for the case where S and K have the same parity. The odd and even representations approach each other as K increases and we hypothesize that they become identical in the continuum limit of $K \rightarrow \infty$. When we present the correlation function in Sec. 3.3, we will see further evidence for this claim.

3.2.3 Massless states

Pure bosonic massless states

Let us investigate the properties of pure bosonic massless states in full detail in the $N_c \rightarrow \infty$ limit. This is done by generalizing the discussion of the bound states in SDLCQ for $\mathcal{N}=(1,1)$ SYM theory, as given in Refs. [17, 55], to $\mathcal{N}=(2,2)$ SYM theory.

For simplicity, let us consider the states consisting of a fixed n number of partons only. A pure bosonic massless state is given by

$$|\Psi, 0\rangle = N \sum_{q_1, \dots, q_n} \sum_A \delta_{(q_1 + \dots + q_n), K} \bar{f}_{[A_1 \dots A_n]}^{(0)}(q_1 \dots q_n) \text{tr}[a_{A_1}^\dagger(q_1) \dots a_{A_n}^\dagger(q_n)] |0\rangle,$$

where N is the normalization factor, $q_i = 1, 2, \dots$ is the unit of the light-cone momentum $p_i = q_i \pi / L$ carried by the i -th parton, $A_i = 1, 2$ indicates the flavor index for each

parton, the sum \sum_A is the summation over all possible permutations of the flavor indices A_i 's, \bar{f} is the wave function, and the trace is taken over the color indices. Note that we don't have the symmetry factor coming from the cyclic property of the trace in the above notation; one has to put in the symmetry factor by hand if one would like it to be in there as we will do so for an example given later in this subsection. In other words, Fock states with non-zero symmetry factor are not normalized.

Due to the cyclic property of the trace, we have

$$\bar{f}_{[A_1 \dots A_n]}(q_1, \dots, q_n) = \bar{f}_{[A_2 \dots A_n A_1]}(q_2, \dots, q_n, q_1) = \dots = \bar{f}_{[A_n A_1 \dots A_{n-1}]}(q_n, \dots, q_{n-1}).$$

Since $P^- = (Q^-)^2/\sqrt{2}$, all the massless states should vanish upon the action of Q^- . Thus, we must have $Q^-|\Psi, 0\rangle = 0$. This identity, however, can be simplified somewhat for pure bosonic massless states. That is, the terms to consider in Q^- are those which annihilate one boson and create one boson and one fermion, and those which annihilate two bosons and create one fermion. Both the former and latter class of terms in Q^- separately annihilates $|\Psi, 0\rangle$. In the large- N_c limit the former class gives, writing $f(q_1, \dots, q_n) \equiv \sqrt{q_1 \dots q_n} \bar{f}(q_1, \dots, q_n)$,

$$\begin{aligned} 0 &= (\epsilon_2)_{\alpha\beta} \left\{ \frac{2q_{n-1} + t}{(q_{n-1} + t)t} f_{[A_1 \dots A_n]}^{(0)}(q_1, \dots, q_{n-1} + t, q_n) \right. \\ &\quad \left. - \frac{2q_n + t}{(q_n + t)t} f_{[A_1 \dots A_n]}^{(0)}(q_1, \dots, q_{n-1}, q_n + t) \right\} \\ &\quad + \frac{M_{IA_n}^{\alpha\beta}}{2(q_n + t)} f_{[A_1 \dots A_{n-1}, I]}^{(0)}(q_1, \dots, q_{n-1}, q_n + t) \\ &\quad - \frac{M_{IA_{n-1}}^{\alpha\beta}}{2(q_{n-1} + t)} f_{[A_1 \dots A_{n-2}, I, A_n]}^{(0)}(q_1, \dots, q_{n-1} + t, q_n), \end{aligned} \quad (3.27)$$

and the latter yields

$$0 = \sum_{A_{n-1}, A_n} \sum_k \left((\epsilon_2)_{\alpha\beta} \frac{t - 2k}{tk(t - k)} \delta_{A_{n-1}, A_n} + \frac{M_{A_{n-1} A_n}^{\alpha\beta}}{k(t - k)} \right) f_{[A_1 \dots A_n]}^{(0)}(q_1, \dots, q_{n-2}, k, t - k), \quad (3.28)$$

where $M_{IJ}^{\alpha\beta} \equiv [(\beta_I\beta_J - \beta_J\beta_I)\epsilon_2]_{\alpha\beta}$, t is the momentum of the created fermion, and the momentum conserving Kronecker's delta $\delta_{(q_1+\dots+q_n),K}$ is understood implicitly. These are the necessary and sufficient conditions for a pure bosonic state to be massless. One should notice that the above equations reduce to the corresponding equations found in Ref. [17, 55] with $(\epsilon_2)_{\alpha\beta} = 1$, $A_i = 1$ for all i 's, and $M_{IJ}^{\alpha\beta} = 0$, as expected.

In principle, we could find the properties of all kinds of pure bosonic massless states using Eqs. (3.27) and (3.28). However, we limit ourselves here to the investigation of only two special types. To simplify the notation, we omit the superscript (0) from the wave function f hereafter.

The simplest case is where $n = K$, that is to say, all the partons have one unit of momentum π/L and, thus, $f = \bar{f}$. In this case Eq. (3.27) is trivially satisfied since we cannot have states with $(K + 1)$ partons. From Eq. (3.28) we get

$$0 = f_{[A_1\dots A_{n-2},1,2]} - f_{[A_1\dots A_{n-2},2,1]}, \quad (3.29)$$

where we have omitted $(q_1, \dots, q_n) = (1, \dots, 1)$. Eq. (3.29) means, with the help of the cyclic property of f , that the wave function is unchanged after moving *any* flavor index to *any* location in the list of indices. For instance, we find, writing $f_{[A_1\dots A_n]} \equiv [A_1 \dots A_n]$,

$$[1212] = [1221] = [2121] = [2211] = [2112] = [1122].$$

It is clear that the state with the above six wave functions being the same and all others zero satisfies (3.29), or equivalently Eqs. (3.27) and (3.28), the necessary and sufficient conditions to be massless. Therefore, writing $\text{tr}[a_{A_1}^\dagger(1) \dots a_{A_n}^\dagger(1)]|0\rangle \equiv A_1 \dots A_n$, we find the state

$$N[1212](1212 + 1221 + 2121 + 2211 + 2112 + 1122) = N[1212](2(1212) + 4(1122))$$

is massless, where we used the cyclic property of f . In terms of the normalized Fock states $\text{tr}[a_{A_1}^\dagger(1) \dots a_{A_n}^\dagger(1)]|0\rangle/(\sqrt{s}N_c^{n/2}) \equiv \underline{A_1 \dots A_n} = A_1 \dots A_n/(\sqrt{s}N_c^{n/2})$, where s is the symmetry factor, we find, after normalizing properly, that

$$\frac{1}{\sqrt{3}}(\underline{1212}) + \sqrt{\frac{2}{3}}(\underline{1122})$$

is massless since s for 1212 and 1122 equals two and one, respectively. Indeed we have found the very same massless state in our numerical results.

As we have seen above, there is a one-to-one correspondence between a massless state and a given set of flavor indices, which has a *fixed* number of 1's and 2's. This means that every time we change the number of 1's (or 2's) in the flavor indices, we find a new massless state. Since we can have $K + 1$ such different sets of flavor indices, we have $K + 1$ massless states of this kind. As verification of our argument, we enumerated all the massless states for K up to six and found all of them with the correct coefficients in our numerical results.

The next case to consider is where $n = K - 1$. In this case only one of the partons has two units of momentum, so that $f = \sqrt{2}\bar{f}$. However, since all the f 's have the same factor of $\sqrt{2}$, we can absorb $\sqrt{2}$ into the normalization factor N and practically can set $f \equiv \bar{f}$. We have $t = 1$ and $q_i = 1$ with $i = 1, \dots, n$ in Eq. (3.27) and find, writing $(q_1, \dots, q_n) = (1, \dots, 1, 1, 2) \equiv (1, 2)$ and so on,

$$0 = [A_1 \dots A_n](2, 1) - [A_1 \dots A_n](1, 2), \quad (3.30)$$

$$0 = [A_1 \dots A_{n-2}, A_{n-1}, A_n](1, 2) - [A_1 \dots A_{n-2}, A_n, A_{n-1}](2, 1), \quad (3.31)$$

$$0 = [A_1 \dots A_{n-2}, A_{n-1}, A_{n-1}](1, 2) + [A_1 \dots A_{n-2}, A_n, A_n](2, 1), \quad (3.32)$$

where $A_{n-1} \neq A_n$ in Eqs. (3.31) and (3.32). For Eq. (3.28) we have $t = 2$, $k = 1, 2$ and $q_i = 1$ with $i = 1, \dots, n - 2$, and we get

$$0 = [A_1 \dots A_{n-2}, A, A](1, 2) - [A_1 \dots A_{n-2}, A, A](2, 1), \quad (3.33)$$

$$\begin{aligned} 0 = & [A_1 \dots A_{n-2}, 1, 2](1, 2) + [A_1 \dots A_{n-2}, 1, 2](2, 1) \\ & - [A_1 \dots A_{n-2}, 2, 1](1, 2) - [A_1 \dots A_{n-2}, 2, 1](2, 1). \end{aligned} \quad (3.34)$$

Apparently, we have five equations for the massless states to satisfy, but it is easy to see that Eq. (3.33) is incorporated into Eq. (3.30) and that if Eqs. (3.30) and (3.31) are true, so is Eq. (3.34) automatically. Hence, the three equations Eqs. (3.30), (3.31), and (3.32) are in fact the equations for massless states to satisfy for $n = K - 1$.

In order to see what the three equations allow us to do, let us first write

$$[A_1, \dots, A_n](1, 2) \equiv [A_1, \dots, A'_n].$$

That is, let us put a prime on top of an index whose corresponding parton has two units of momentum. Then, Eq. (3.30) allows us to move the “prime” to any index. Eq. (3.31), along with this fact, then also allows us to move the index with a prime to any location in the index list. For example, we have

$$[112'] = [11'2] = [1'12] = [12'1] = [1'21] = [121'] = [2'11] = [21'1] = [211'].$$

Furthermore, Eq. (3.32) allows us to replace $11'$ by $2'2$ (or $22'$ using Eq. (3.30)) as long as a minus sign is inserted. Thus, for the above example we get

$$[112'] = [11'2] = [1'12] = -[22'2],$$

where we have omitted the wave functions related by cyclic permutations. This means that the state

$$(112' + 11'2 + 1'12 - 22'2)/2$$

is massless. Note that the symmetry factor in this case is equal to one for all the Fock states above.

Since Eqs. (3.30), (3.31), and (3.32) relate all the sets of flavor indices with an even/odd number of 1's to one another, we have only *two* independent sets of flavor indices: the one with even numbers of 1's and the other with an odd number. This means that there are *two* massless states of this type. Again we have confirmed this statement numerically for K up to six.

To summarize, we have found in the large- N_c limit the necessary and sufficient conditions, Eqs. (3.27) and (3.28), that pure bosonic massless states are to satisfy. As an application we considered two special cases and found that there are $K + 1$ massless states of the type

$$\text{tr}[a_{A_1}^\dagger(1) \dots a_{A_K}^\dagger(1)]$$

and two of the type

$$\text{tr}[a_{A_1}^\dagger(1) \dots a_{A_{K-2}}^\dagger(1) a_{A_{K-1}}^\dagger(2)]$$

. Also, we gave a way to enumerate all such massless states for a given K .

Count of massless states

It is possible to predict a minimum number of massless states by comparing the number of states in the different symmetry sectors. Since $(Q^-)^2$ takes a state from one symmetry sector to another and then back it must have 0 eigenvalues if the dimensionality of the intermediate sector is less than that of the original sector. It is possible to create a simple recursive formula for the number of states in each sector. For the case when K is prime and odd, the formula is particularly simple. We present the results here but refer to the other publication for justification [41]. We

define $A_{bes^+}(K, n)$ as the number of states in the bosonic sector with an even number of partons and even S symmetry, where n indicates how many types of particles we have in a SYM theory, i.e. $n = 4$ for $\mathcal{N} = (2, 2)$ SYM. Then

$$A_{bes^+}(K, n) = A_{fes^+}(K, n) = \frac{A_f(K, n) + A_f(K, -n) + W}{2} \quad (3.35)$$

$$A_{bes^-}(K, n) = A_{fes^-}(K, n) = \frac{A_f(K, n) + A_f(K, -n) - W}{2}$$

$$A_{bos^+}(K, n) = A_{fos^+}(K, n) = A_{bos^-}(K, n) = A_{fos^-}(K, n)$$

$$= \frac{A_f(K, n) - A_f(K, -n)}{2} \quad (3.36)$$

where

$$A_f(K, n)_{\text{prime}} = \frac{1}{2K}((1+n)^K - (1-n)^K) \quad (3.37)$$

$$W = \left(\frac{n}{2}\right)^2(K-1) \quad (3.38)$$

Q^- goes from bosonic to fermionic and from even to odd.

$$A_{fos^+}(K, n) - A_{bes^+}(K, n) = A_{bos^+}(K, n) - A_{fes^+}(K, n) = -A_f(K, -n) - \frac{W}{2} \quad (3.39)$$

$$A_{fos^-}(K, n) - A_{bes^-}(K, n) = A_{bos^-}(K, n) - A_{fes^-}(K, n) = -A_f(K, -n) + \frac{W}{2} \quad (3.40)$$

The minimum total number of massless states must therefore be

$$-4A_f(K, -n) = -\frac{2}{K}((1-n)^K - (1+n)^K) = \frac{2}{K}(3^K - 3) \quad (3.41)$$

For $K = 5$, this comes to 96 states which is way more than the 8 purely bosonic states with 4 or 5 partons that we have found in this section.

3.3 Correlation functions

One of the physical quantities we can calculate nonperturbatively is the two-point function of the stress-energy tensor. Previous calculations of this correlator in this

and other theories can be found in [48, 49, 19]. Ref. [48] gives results for the theory considered here but only for resolutions K up to 6. We can now reach $K = 12$.

We will show that there is a distinct behavior for even and odd K in the correlation function, just as in the energy spectrum. Then we will argue, by taking a closer look at the data, that we have two different classes of representations at finite K , which become identical as $K \rightarrow \infty$.

3.3.1 Correlation functions in supergravity

Let us first recall that there is a duality that relates the results for the two-point function in $\mathcal{N}=(8,8)$ SYM theory to the results in string theory [49]. The correlation function on the string-theory side, which can be calculated with use of the supergravity approximation, was presented in [48], and we will only quote the result here. The computation is essentially a generalization of that given in [56, 57]. The main conclusion on the supergravity side was reported in [58]. Up to a numerical coefficient of order one, which we have suppressed, it was found that

$$\langle \mathcal{O}(x)\mathcal{O}(0) \rangle = \frac{N_c^{\frac{3}{2}}}{g_{YM}x^5}. \quad (3.42)$$

This result passes the following important consistency test. The SYM theory in two dimensions with 16 supercharges has conformal fixed points in both the UV and the IR regions, with central charges of order N_c^2 and N_c , respectively. Therefore, we expect the two-point function of the stress-energy tensor to scale like N_c^2/x^4 and N_c/x^4 in the deep UV and IR regions, respectively. According to the analysis of [59], we expect to deviate from these conformal behaviors and cross over to a regime where the supergravity calculation can be trusted. The crossover occurs at $x = 1/g_{YM}\sqrt{N_c}$

and $x = \sqrt{N_c}/g_{YM}$. At these points, the N_c scaling of (3.42) and the conformal result match in the sense of the correspondence principle [60].

We should note here that this property for the correlation functions is expected *only* for $\mathcal{N}=(8,8)$ SYM theory, not for the theory in consideration in this chapter. However, it would be natural to expect some similarity between $\mathcal{N}=(8,8)$ and $\mathcal{N}=(2,2)$ theories. Indeed, we will find numerically that (3.42) is *almost* true in $\mathcal{N}=(2,2)$ SYM theory.

3.3.2 Correlation functions in SUSY with 4 supercharges

We wish to compute a general expression of the form

$$F(x^-, x^+) = \langle \mathcal{O}(x^-, x^+) \mathcal{O}(0, 0) \rangle$$

where \mathcal{O} is T^{++} . In DLCQ, where we fix the total momentum in the x^- direction, it is more natural to compute the Fourier transform and express the transform in a spectral decomposed form [48, 49]

$$\begin{aligned} \tilde{F}(P_-, x^+) &= \frac{1}{2L} \langle T^{++}(P_-, x^+) T^{++}(-P_-, 0) \rangle \\ &= \sum_i \frac{1}{2L} \langle 0 | T^{++}(P_-, 0) | i \rangle e^{-iP_+^i x^+} \langle i | T^{++}(-P_-, 0) | 0 \rangle. \end{aligned} \quad (3.43)$$

The position-space form of the correlation function is recovered by Fourier transforming with respect to $P_- = P^+ = K\pi/L$. We can continue to Euclidean space by taking $r = \sqrt{2x^+x^-}$ to be real. The result for the correlator of the stress-energy tensor was presented in [48], and we only quote the result here:

$$\begin{aligned} F(x^-, x^+) &\equiv \langle T^{++}(\mathbf{x}) T^{++}(0) \rangle \\ &= \sum_i \left| \frac{L}{\pi} \langle 0 | T^{++}(K) | i \rangle \right|^2 \left(\frac{x^+}{x^-} \right)^2 \frac{M_i^4}{8\pi^2 K^3} K_4(M_i \sqrt{2x^+x^-}), \end{aligned} \quad (3.44)$$

where \mathbf{x} has light cone coordinates x^-, x^+ , M_i is a mass eigenvalue and $K_4(x)$ is the modified Bessel function of order 4. In [51] we found that the momentum operator $T^{++}(\mathbf{x})$ is given by

$$T^{++}(\mathbf{x}) = \text{tr} \left[(\partial_- X^I)^2 + \frac{1}{2} (i u^\alpha \partial_- u^\alpha - i (\partial_- u^\alpha) u^\alpha) \right], \quad I, \alpha = 1, 2, \quad (3.45)$$

where X and u are the physical adjoint scalars and fermions, respectively, following the notation of [51]. When written in terms of the discretized operators, a and b , (Eqs. (3.12,3.13)), we find

$$T^{++}(K)|0\rangle = \frac{\pi}{2L} \sum_{k=1}^{K-1} \left[-\sqrt{k(K-k)} a_{Iij}^\dagger(K-k) a_{Iji}^\dagger(k) + \left(\frac{K}{2} - k \right) b_{\alpha ij}^\dagger(K-k) b_{\alpha ji}^\dagger(k) \right] |0\rangle. \quad (3.46)$$

The matrix element $(L/\pi)\langle 0|T^{++}(K)|i\rangle$ is independent of L and can be substituted directly to give an explicit expression for the two-point function. We see immediately that the correlator behaves like $1/r^4$ at small r , for in that limit, it asymptotes to

$$\left(\frac{x^-}{x^+} \right)^2 F(x^-, x^+) = \frac{N_c^2(2n_b + n_f)}{4\pi^2 r^4} \left(1 - \frac{1}{K} \right). \quad (3.47)$$

On the other hand, the contribution to the correlator from strictly massless states is given by

$$\left(\frac{x^-}{x^+} \right)^2 F(x^-, x^+) = \sum_i \left| \frac{L}{\pi} \langle 0|T^{++}(K)|i\rangle \right|_{M_i=0}^2 \frac{6}{K^3 \pi^2 r^4}. \quad (3.48)$$

That is to say, we would expect the correlator to behave like $1/r^4$ at both small and large r , assuming massless states have non-zero matrix elements.

3.3.3 Numerical results

To compute the correlator using Eq. (3.44), we approximate the sum over eigenstates by a Lanczos [61] iteration technique, as described in [49, 19]. Only states with

positive R_α , T and S parity contribute to the correlator. The results are shown in Fig. 3.2, which includes a log-log plot of the scaled correlation function

$$f \equiv \langle T^{++}(\mathbf{x})T^{++}(0) \rangle \left(\frac{x^-}{x^+} \right)^2 \frac{4\pi^2 r^4}{N_c^2(2n_b + n_f)} \quad (3.49)$$

and a plot of $\frac{d\log_{10}(f)}{d\log_{10}(r)}$ versus $\log_{10}(r)$, with r measured in units of $\sqrt{\pi/g^2 N_c}$. Let us discuss the behavior of the correlator at small, large, and intermediate r , separately in the following.

First, at small r , the graphs of f for different K approach 0 as K increases. This follows Eq. (3.47) which gives the form $f = \log(1 - \frac{1}{K})$. Second, at large r , obviously, the behavior is different for odd K , in Fig. 3.2(c) and (d), and even K , in (e) and (f). However, the difference gets smaller as K gets bigger, as seen in Fig. 3.2(a). The reason for this is as follows. Looking at the detailed information of the computation of the correlator, we found that for even K there is exactly one massless state that contributes to the correlator, while there is no massless state nor even an anomalously light state that makes any contribution for odd K . Instead, it is the lowest massive state that contributes the most for odd K . This observation serves as another piece of evidence for the claim that we have two distinct classes of representations for odd and even K .

In the intermediate- r region, for the $\mathcal{N}=(8,8)$ theory we expected from Eq. (3.42) that the behavior is $1/r^5$, and in [49] we found that the correlator may be approaching this behavior. We indicated in [49] that conclusive evidence would be a flat region in the derivative of the scaled correlator at a value of -1 . Our resolution was not high enough to see this in the $\mathcal{N}=(8,8)$ case. Here we find such a flat region, indicating that the correlator in fact behaves like $1/r^{-4.75}$ for $\mathcal{N}=(2,2)$ SYM theory. Also, note that the region of flattening around -0.75 extends farther out as K gets bigger, for

both odd and even K , implying again that the representations appear to agree as K goes to infinity. For any fixed value of r the correlators for odd and even K approach each other as K increases and the flat region extends further. This indicates that it is only in the region of r where the correlators for even and odd K agree that we have sufficient convergence for the results to be meaningful.

3.4 Discussion

To demonstrate the power of SDLCQ, and to respond to the increasing interest in calculating supersymmetric theories on a lattice [24, 25, 27, 28], we have presented detailed numerical results for the low-energy spectrum and the two-point correlation function of the stress-energy tensor, using SDLCQ for $\mathcal{N}=(2,2)$ SYM theory in $1+1$ dimensions in the large- N_c approximation. Our hope is that these results will serve as benchmarks for others to compare and check their results.

In addition, we found an important new aspect of the SDLCQ approximation in this calculation. There seem to be two distinct classes of representations for $\mathcal{N}=(2,2)$ SYM theory, one where S and K have the same parity and one where S and K have opposite parity; these representations become identical as $K \rightarrow \infty$. We found evidence for this feature of $\mathcal{N}=(2,2)$ SYM theory in both the mass spectrum and the correlator. We also found that there are some anomalously light states that appear only in the sectors where S and K have opposite parity. We argued that the anomalously light states should be exactly massless, but have acquired a tiny mass because of some impediment to having them exactly massless in the SDLCQ approximation. In the calculation of the correlator where only positive S parity contribute we found that there is exactly one massless state that contributes to the

correlator when K has positive parity and that no massless state or anomalously light state contributes when K has negative parity. The lightest massive state in the sector where K has negative parity does contribute to the correlator, but because the mass gap appears to close at infinite resolution this state appears to become massless, as expected [39].

The two-point correlator of the stress-energy tensor was found to show $1/r^4$ -behavior in the UV (small r) and IR (large r , K even) regions as expected. The large r behavior for K odd, on the other hand, has an exponential decay. Surprisingly, the correlator behaves like $1/r^{4.75}$ at intermediate values of r . In $\mathcal{N}=(8,8)$ SYM theory in $1+1$ dimensions, the correlator is expected to behave like $1/r^5$ in the intermediate region, and it is interesting that $\mathcal{N}=(2,2)$ behaves similarly but with a different exponent. We were able to confirm this power law behavior with a flat region in the derivative of the scaled correlator.

Analytically, we investigated the properties of pure bosonic massless states and found the necessary and sufficient conditions to determine their wave function. Then we explored some special cases to find that there are $K+1$ massless states of type

$$\text{tr}[a_{A_1}^\dagger(1)a_{A_2}^\dagger(1)\dots a_{A_K}^\dagger(1)]|0\rangle,$$

where A_i is a flavor index and the number in the parentheses tells how many units of momentum each parton carries, and that there are two massless states of the type

$$\text{tr}[a_{A_1}^\dagger(1)a_{A_2}^\dagger(1)\dots a_{A_{K-1}}^\dagger(2)]|0\rangle.$$

We also gave the formulae to count a minimum total number of massless states for a SYM theory which is dimensionally reduced to one spatial and one time dimensions.

What prevents us from reaching even higher K is obviously the fact that, as one can show [41], the total number of basis states grows like $\sim (1+n)^K$, where n is the total number of particle types and $n = 4$ for $\mathcal{N}=(2,2)$ SYM theory. Our numerical results were obtained using one single PC with memory of 4 GB. The problem that we now face is that we do not have enough memory to store all the states in one PC. However, as we make use of a cluster of PCs and find ways to split and share the information among them, we are able to reach even higher K . This is the direction of our future work, with the ultimate goal being to achieve sufficient numerical precision to detect the correspondence between $\mathcal{N} = (8,8)$ SYM theory and supergravity conjectured by Maldacena [12]⁷.

⁷Recently this correspondence for $\mathcal{N} = (8,8)$ SYM theory has been confirmed numerically in Ref. [13].

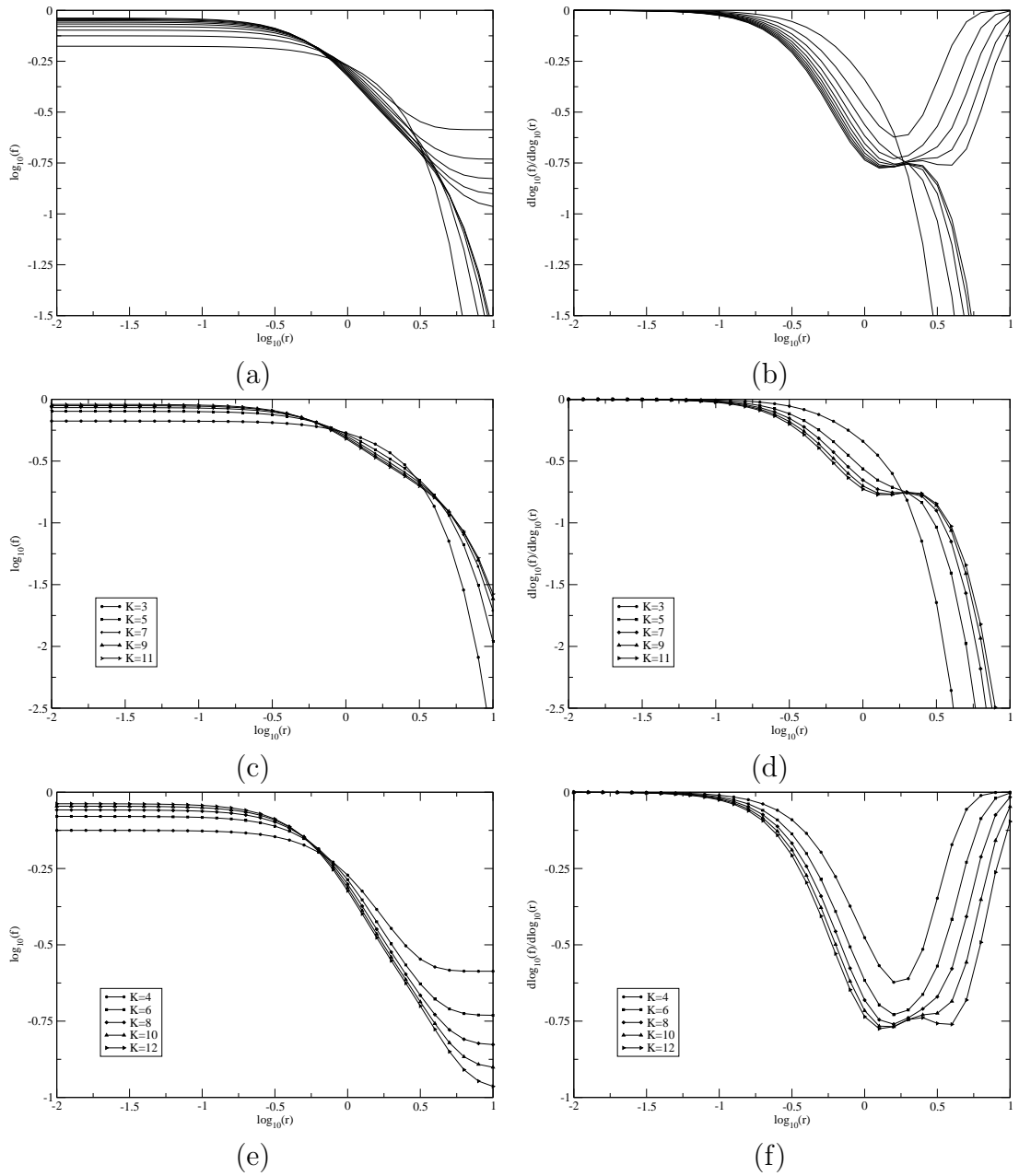


Figure 3.2: Plots of \log of the scaled correlation function f as a function of $\log_{10}(r)$ for (a) $K = 3, 4, \dots, 12$, (c) K odd, and (e) K even, and plots of $d \log_{10}(f) / d \log_{10}(r)$ as a function of $\log_{10}(r)$ for (b) $K = 3, 4, \dots, 12$, (d) K odd, and (f) K even.

CHAPTER 4

SDLCQ MEETS TRANSVERSE LATTICE IN 2+1 DIMENSIONS

4.1 Introduction

As we have seen in the previous chapter, SDLCQ is a very powerful tool to solve supersymmetric theories in the non-perturbative regime. However, it turns out that going to higher than 1+1 dimensions is not an easy task. This is mainly because the number of states increases exponentially [41] as we increase the numerical resolutions and the number of parameters associated with the resolutions is typically n for $n+1$ dimensional theory. This chapter discusses a new technique to circumvent this difficulty in SDLCQ formulation [62]. This approach is motivated by the newly developed idea of "(de)construction" [42] and the key idea is to introduce a transverse lattice [43, 44, 63, 64, 65, 66] in the transverse spatial dimensions, and to fully utilize the consequences of the large N_c limit. For a review of transverse lattice formulation see [45].

To be more specific, in this chapter we will attempt to formulate a (2+1) dimensional $\mathcal{N} = 1$ Super Yang–Mills (SYM) theory as a SDLCQ theory in 1+1 dimensions with a transverse spatial lattice in the one transverse direction. The challenge is to

formulate it such that it is supersymmetric exactly at every order of the numerical approximation.

We will not be able to fully realize this goal. There are several fundamental problems that prevent complete success. In formulating this theory with gauge invariance in the one transverse dimension the gauge field is replaced by a complex unitary link field. Within the context of DLCQ this field is quantized as a linear complex field. This then disturbs the supersymmetry which usually requires the same number of fundamental fermion and boson fields. In some sense this is a restatement of the error we are making by treating a unitary field as a general complex field. There are simply too many boson degrees of freedom relative to the number of fermion degrees of freedom. Conventionally one adds a potential to a transverse lattice theory to enforce the unitarity of this complex boson field, but this is not possible within the context of an exactly supersymmetric theory. However, in the formulation of Gauss's law on the transverse lattice, one finds that color conservation must be enforced at every lattice site. This greatly reduces the number of allowed boson degrees of freedom. It is unclear however if this constraint is sufficient to reduce the number of boson degrees of freedom to the number required by unitarity.

We will be able to partially formulate SDLCQ for this theory and write the Hamiltonian as the square of a supercharge. Previously we considered this situation in a different class of theories [69]. We will show that this produces a different and simpler discrete Hamiltonian than the standard lagrangian formulation. When we solve this theory using this partial formulation of SDLCQ we find that all of the massive states have exact fermion-boson degeneracy as required by full supersymmetry. Our partial SDLCQ does not require degeneracy between the massless fermion and boson states.

We find however that they are nearly equal in number. The solution can be viewed as a unitary transformation from the constrained basis to an unconstrained basis and we see that in this new basis the number of fermion and boson degrees of freedom are very nearly equal. In effect, the partial supersymmetry and Gauss's law are sufficient to approximately enforce the same symmetry in the spectrum that we would have obtained had we been able to enforce unitarity. Recently Dalley and Van de Sande [66, 70] have also pointed out the importance of Lorentz symmetry in enforcing the constraint of unitarity.

Since color is conserved at every transverse lattice site, there are two fundamentally different types of states. For one class of states the color flux winds around the space one or more times. We refer to these as cyclic states and to the other class of states as non-cyclic states. The spectrum for both classes of states are presented. For the cyclic states we present the spectrum as a function of the number of windings.

In Section 4.2, we present the standard lagrangian formulation of this theory of adjoint fermions and adjoint bosons. We show that Hamiltonian is sixth order in the field. In Section 4.3, we present the SDLCQ formulation which turns out to be only fourth order in the field. We show that there are two types of allowed states. One type loops the entire transverse space, and we study these state in Section 4.4. The states of the other type are localized, and we study these states in Section 4.5. In Section 4.6 we discuss our conclusions

4.2 Transverse lattice model in 2+1 dimensions

In this section we present the standard formulation of a transverse lattice model in 2+1 dimensions of an $\mathcal{N} = (1, 1)$ supersymmetric $SU(N_c)$ theory with *both* adjoint bosons and adjoint fermions in the large- N_c limit.

We work in light cone coordinates so that $x^\pm \equiv (x^0 \pm x^1)/\sqrt{2}$. The metric is specified by $x^\pm = x_\mp$ and $x^2 = -x_2$. Suppose that there are N_{sites} sites in the transverse direction x^2 with lattice spacing a . With each site, i , we associate one gauge boson field $A_{\nu,i}(x^\mu)$ and one spinor field $\Psi_i(x^\mu)$, where $\nu, \mu = \pm$. $A_{\nu,i}$'s and Ψ_i 's are in the adjoint representation. The adjacent sites, say i and $i+1$, are connected by what we call the link variables $M_i(x^\mu)$ and $M_i^\dagger(x^\mu)$, where $M_i(x^\mu)$ stands for a link which goes from the i -th site to the $(i+1)$ -th site and $M_i^\dagger(x^\mu)$ for a link from the $(i+1)$ -th to the i -th site. We impose the periodic condition on the transverse sites so that $A_{N_{sites}+1} = A_1$, $\Psi_{N_{sites}+1} = \Psi_1$, $M_{N_{sites}+1} = M_1$ and $M_{N_{sites}+1}^\dagger = M_1^\dagger$. Under the transverse gauge transformation [45] the fields transform as

$$gA_i^\mu \longrightarrow U_i gA_i^\mu U_i^\dagger - iU_i \partial^\mu U_i^\dagger, \quad M_i \longrightarrow U_i M_i U_{i+1}^\dagger, \quad \Psi_i \longrightarrow U_i \Psi_i U_i^\dagger, \quad (4.1)$$

where g is the coupling constant and $U_i \equiv U_i(x^\mu)$ is a $N_c \times N_c$ unitary matrix. In all earlier work on the transverse lattice [45] Ψ_i was in the fundamental representation.

The link variable can be written as

$$M_i(x^\mu) = \exp\left(ia g A_{i+1/2,\perp}(x^\mu)\right), \quad (4.2)$$

where $A_{i,\perp} \equiv A_{i,2}$ is the transverse component of the gauge potential at site i and as $a \rightarrow 0$ we can formally expand Eq. (4.2) in powers of a as follows:

$$\begin{aligned} M_i(x^\mu) &= 1 + iagA_{i+1/2,\perp}(x^\mu) - \frac{1}{2} (agA_{i+1/2,\perp}(x^\mu))^2 + \dots \\ &= 1 + iagA_{i,\perp}(x^\mu) + \frac{a^2}{2} [ig\partial_\perp A_{i,\perp}(x^\mu) - g^2 (A_{i,\perp}(x^\mu))^2] + O(a^3). \end{aligned} \quad (4.3)$$

In the limit $a \rightarrow 0$, with the substitution of the expansion Eq. (4.3) for M_i , we expect everything to coincide with its counterpart in *continuum* (2+1)-dimensional theory.

The discrete Lagrangian is then given by

$$\begin{aligned} \mathcal{L} &= \text{tr} \left\{ -\frac{1}{4} F_i^{\mu\nu} F_{i,\mu\nu} + \frac{1}{2a^2 g^2} (D_\mu M_i) (D^\mu M_i)^\dagger \right. \\ &\quad \left. + \bar{\Psi}_i i\gamma^\mu D_\mu \Psi_i + \frac{i}{2a} \bar{\Psi}_i \gamma^\perp (M_i \Psi_{i+1} M_i^\dagger - M_{i-1}^\dagger \Psi_{i-1} M_{i-1}) \right\}, \end{aligned} \quad (4.4)$$

where the trace has been taken with respect to the color indices, $F_{i,\mu\nu} = \partial_\mu A_{i,\nu} - \partial_\nu A_{i,\mu} + ig[A_{i,\mu}, A_{i,\nu}]$, $\mu, \nu = \pm$ and γ 's are defined as follows

$$\gamma^+ \equiv \frac{\gamma^0 + \gamma^1}{\sqrt{2}} \equiv \frac{\sigma_2 + i\sigma_1}{\sqrt{2}}, \quad \gamma^- \equiv \frac{\gamma^0 - \gamma^1}{\sqrt{2}} \equiv \frac{\sigma_2 - i\sigma_1}{\sqrt{2}}, \quad \gamma^\perp \equiv i\sigma_3,$$

and the covariant derivative D_μ is defined as

$$\begin{aligned} D_\mu \Psi_i &= \partial_\mu \Psi_i + ig[A_{i,\mu}, \Psi_i], \\ D_\mu M_i &= \partial_\mu M_i + igA_{i,\mu} M_i - igM_i A_{i+1,\mu} \xrightarrow{a \rightarrow 0} igF_{\mu\perp}, \\ (D^\mu M_i)^\dagger &= \partial^\mu M_i^\dagger - igM_i^\dagger A_i^\mu + igA_{i+1}^\mu M_i^\dagger \xrightarrow{a \rightarrow 0} igF^{\mu\perp}. \end{aligned} \quad (4.5)$$

Thus, in the limit $a \rightarrow 0$ one finds, as expected,

$$\mathcal{L} \xrightarrow{a \rightarrow 0} \text{tr} \left(-\frac{1}{4} F^{\alpha\beta} F_{\alpha\beta} + i\Psi i\gamma^\alpha D_\alpha \Psi \right),$$

where $\alpha, \beta = \pm, \perp$. Of course the form of this Lagrangian is slightly different from that in Ref. [45] since the fermions are in the adjoint representation. This Lagrangian is hermitian and invariant under the transformation in Eq. (4.1) as one would expect.

The following Euler-Lagrange equations in the light cone gauge, $A_{i,-} = 0$, are constraint equations.

$$\partial_-^2 A_i^- \equiv gJ_i^+, \quad \partial_- \chi_i = \frac{1}{2\sqrt{2}a} (M_i \overleftrightarrow{\partial}_- M_i^\dagger - M_{i-1}^\dagger \overleftrightarrow{\partial}_- M_{i-1}) \xrightarrow{a \rightarrow 0} \frac{1}{\sqrt{2}} D_\perp \psi, \quad (4.6)$$

where

$$J_i^+ \equiv \frac{i}{2g^2 a^2} (M_i \overleftrightarrow{\partial}_- M_i^\dagger + M_{i-1}^\dagger \overleftrightarrow{\partial}_- M_{i-1}) + 2\psi_i \psi_i \quad (4.7)$$

$$\xrightarrow{a \rightarrow 0} i[A_\perp, \partial_- A_\perp] + \frac{1}{g} \partial_- \partial_\perp A_\perp + 2\psi\psi, \quad (4.8)$$

$$\Psi_i \equiv \frac{1}{2^{1/4}} \begin{pmatrix} \psi_i \\ \chi_i \end{pmatrix}. \quad (4.9)$$

Since these equations only involve the spatial derivative we can solve them for A_i^- and χ_i , respectively. Thus the dynamical field degrees of freedom are M_i , M_i^\dagger and ψ_i .

The first of the equations in Eq. (4.6) gives a constraint on physical states $|phys\rangle$, since the zero mode of J_i^+ acting on any physical state must vanish,

$$J_i^+ |phys\rangle = \int dx^- J_i^+(x^\mu) |phys\rangle = 0 \quad \text{for any } i. \quad (4.10)$$

The physical states must be color singlet at *each* site.

It is straightforward to derive $P^\pm \equiv \int dx^- T^{+\pm}$, where $T^{\mu\nu}$ is the stress-energy tensor. We have

$$P^+ = a \sum_{i=1}^{N_{sites}} \int dx^- \text{tr} \left(\frac{1}{a^2 g^2} \partial_- M_i^\dagger \partial_- M_i + i\psi_i \partial_- \psi_i \right) \quad (4.11)$$

$$\xrightarrow{a \rightarrow 0} \int dx^- dx^\perp \text{tr} \left((\partial_- A_\perp)^2 + i\psi \partial_- \psi \right), \quad (4.12)$$

and

$$\begin{aligned}
P^- &= a \sum_{i=1}^{N_{sites}} \int dx^- \text{tr} \left[\frac{1}{2} (\partial_- A_i^-)^2 + i \chi_i \partial_- \chi_i \right] \\
&= a \sum_{i=1}^{N_{sites}} \int dx^- \text{tr} \left[-\frac{g^2}{2} J_i^+ \frac{1}{\partial_-^2} J_i^+ \right. \\
&\quad \left. - \frac{i}{8a^2} (M_i \psi_{i+1} M_i^\dagger - M_{i-1}^\dagger \psi_{i-1} M_{i-1}) \frac{1}{\partial_-} (M_i \psi_{i+1} M_i^\dagger - M_{i-1}^\dagger \psi_{i-1} M_{i-1}) \right] \\
&\xrightarrow{a \rightarrow 0} \int dx^- dx^+ \text{tr} \left[-\frac{g^2}{2} J^+ \frac{1}{\partial_-^2} J^+ - \frac{i}{2} D_\perp \psi \frac{1}{\partial_-} D_\perp \psi \right]. \tag{4.14}
\end{aligned}$$

When one quantizes the dynamical fields, unitarity of M_i is lost and M_i becomes an $N_c \times N_c$ imaginary matrix [63, 64, 65, 66, 70, 45]. Some have suggested the addition of an effective potential $V(M_i)$ to force M_i to be a unitary matrix in the limit $a \rightarrow 0$ [43, 44, 45]. We will approach this issue using supersymmetry.

Having linearized M_i , we can expand M_i and ψ_i in their Fourier modes as follows; at $x^+ = 0$

$$M_{i,rs}(x^-) = \frac{ag}{\sqrt{2\pi}} \int_0^\infty \frac{dk^+}{\sqrt{k^+}} (d_{i,rs}(k^+) e^{-ik^+x^-} + a_{i,rs}^\dagger(k^+) e^{ik^+x^-}), \tag{4.15}$$

$$\psi_{i,rs}(x^-) = \frac{1}{2\sqrt{\pi}} \int_0^\infty dk^+ (b_{i,rs}(k^+) e^{-ik^+x^-} + b_{i,rs}^\dagger(k^+) e^{ik^+x^-}), \tag{4.16}$$

where r, s indicate the color indices, $a_{i,rs}^\dagger(k^+)$ creates a link variable with momentum k^+ which carries color r at site i to s at site $(i+1)$, $d_{i,rs}^\dagger(k^+)$ creates a link with k^+ which carries color r at site $(i+1)$ to s at site i and $b_{i,rs}^\dagger$ creates a fermion at the i -site which carries color r to s . Quantizing at $x^+ = 0$ we have

$$\begin{aligned}
[M_{i,rs}(x^-), \pi_{M_j,pq}(y^-)] &= [M_{i,rs}^\dagger(x^-), \pi_{M_j,pq}^\dagger(y^-)] \\
&= \{\psi_{i,rs}(x^-), \pi_{\psi_j,pq}(y^-)\} = \frac{i}{2} \delta(x^- - y^-) \frac{\delta_{ij}}{a} \delta_{rp} \delta_{sq}. \tag{4.17}
\end{aligned}$$

Note that we divided δ_{ij} by a because $\delta_{ij}/a \rightarrow \delta(x^\perp - y^\perp)$ as $a \rightarrow 0$. The conjugate momentum are

$$\pi_{M_i} = \frac{1}{2a^2 g^2} \partial_- M_i^\dagger, \quad \pi_{M_i^\dagger} = \frac{1}{2a^2 g^2} \partial_- M_i, \quad \pi_{\psi_i} = i\psi_i.$$

Thus we must have

$$\begin{aligned} [M_{i,rs}(x^-), \partial_{-y} M_{j,pq}^\dagger(y^-)] &= [M_{i,rs}^\dagger(x^-), \partial_{-y} M_{j,pq}(y^-)] = ia^2 g^2 \delta(x^- - y^-) \frac{\delta_{ij}}{a} \delta_{rp} \delta_{sq}, \\ \{\psi_{i,rs}(x^-), \psi_{j,pq}(y^-)\} &= \frac{1}{2} \delta(x^- - y^-) \frac{\delta_{ij}}{a} \delta_{rp} \delta_{sq}. \end{aligned} \quad (4.18)$$

Then, one can easily see that these commutation relations are satisfied when a 's, d 's and b 's satisfy the following:

$$\begin{aligned} [a_{i,rs}(k^+), a_{j,pq}^\dagger(p^+)] &= [d_{i,rs}(k^+), d_{j,pq}^\dagger(p^+)] \\ &= \{b_{i,rs}(k^+), b_{j,pq}^\dagger(p^+)\} = \delta(k^+ - p^+) \frac{\delta_{ij}}{a} \delta_{rp} \delta_{sq}, \end{aligned} \quad (4.19)$$

with others all being zero. Physical states can be generated by acting on the Fock vacuum $|0\rangle$ with these a^\dagger 's, d^\dagger and b^\dagger 's in such a manner that the constraint Eq. (4.10) is satisfied.

Let us complete this section by discussing the physical constraint (4.10) in more detail. The states are all constructed in the large- N_c limit, and therefore we need only consider single-trace states. In order for a state to be color singlet at each site, *each color index has to be contracted at the same site*. As an example consider a state represented by $|phys\ 1\rangle \equiv d_{i,rs}^\dagger(k_1^+) a_{i,rs}^\dagger(k_2^+) |0\rangle$. For this state the color r at site i is carried by a_i^\dagger to s at site $(i+1)$ and then brought back by d_i^\dagger to r at site i . The color r is contracted at site i *only* and the color s at site $(i+1)$ *only*. Therefore, this is a physical state satisfying Eq. (4.10). A picture to visualize this case is shown in Fig.

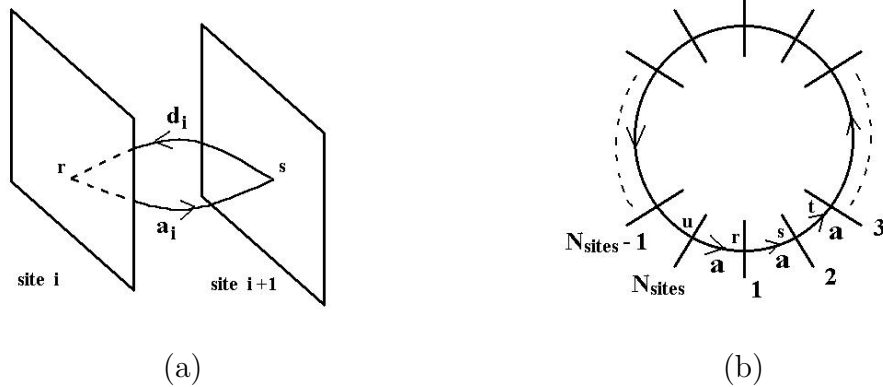


Figure 4.1: (a) The color charge for the state $|phys\ 1\rangle \equiv d_{i,rs}^\dagger(k_1^+) a_{i,rs}^\dagger(k_2^+) |0\rangle$. The planes represent the color space. a_i carries color r at site i to s at site $i+1$ and d_i carries it back to r at site i . (b) The color for the state $|phys\ 2\rangle \equiv a_{i+N_{sites}-1,ru}^\dagger(k_{N_{sites}}^+) \cdots a_{i+1,ts}^\dagger(k_2^+) \cdot a_{i,rs}^\dagger(k_1^+) |0\rangle$. The lines which intersect a circle represent the color planes at sites. The color goes all the way around the transverse lattice.

4.1a. One also needs to be careful with operator ordering. One can show that the state $d_{i,rs}^\dagger(k_1^+) a_{i,rs}^\dagger(k_2^+) b_{i,tr}^\dagger(k_3^+) |0\rangle$ is physical, while the state $b_{i,rs}^\dagger(k_1^+) a_{i,rs}^\dagger(k_2^+) d_{i,tr}^\dagger(k_3^+) |0\rangle$ is unphysical.

We should, however, note that a true physical state be summed over all the transverse sites since we have discrete translational symmetry in the transverse direction. That is, for example, the states $d_{1,rs}^\dagger(k_1^+) a_{1,rs}^\dagger(k_2^+) |0\rangle$ and $d_{2,rs}^\dagger(k_1^+) a_{2,rs}^\dagger(k_2^+) |0\rangle$ are the same up to a phase factor given by $\exp(iP^\perp a)$. We set the phase factor to one since we take physical state to have $P^\perp = 0$. The physical state $|phys\ 1\rangle$ is in fact $\sum_{i=1}^{N_{sites}} d_{i,rs}^\dagger(k_1^+) a_{i,rs}^\dagger(k_2^+) |0\rangle$ with the appropriate normalization constant. From a computational point of view this is a great simplification because we can drop the site index i from the representation.

Periodic conditions on the fields, allow for physical states of the form $|phys\ 2\rangle \equiv \sum_i a_{i+N_{sites}-1,ru}^\dagger(k_{N_{sites}}^+) \cdots a_{i+1,ts}^\dagger(k_2^+) \cdot a_{i,rs}^\dagger(k_1^+) |0\rangle$. The color for this state is carried around the transverse lattice, as shown in Fig. 4.1b. We will refer to these states as cyclic states. The states where the color flux does not go all the way around the transverse lattice we will refer to as non-cyclic states. We characterize states by what we call the winding number defined by $W = n/N_{sites}$, where $n \equiv \sum_i (a_i^\dagger a_i - d_i^\dagger d_i)$. Using the Eguchi–Kawai[71] reduction which applies in the large- N_c limit we can always take $N_{sites} = 1$. The winding number simply gives us the excess number of a^\dagger over d^\dagger in a state. We use the winding number to classify states since the winding number is a good quantum number commuting with P_{SDLCQ}^- . In the language of the winding number the non-cyclic states are those states with $W = 0$ and cyclic states have non-zero W .

It is straight forward to show that $|phys\rangle$ satisfies Eq. (4.10) but $|unphys\rangle$ does not using

$$\begin{aligned} (J_i^+)_{pq} &= \int dk^+ a_{i,rp}^\dagger(k^+) a_{i,rq}(k^+) - d_{i,pr}(k^+) d_{i,qr}^\dagger(k^+) - a_{i-1,pr}(k^+) a_{i-1,qr}^\dagger(k^+) \\ &\quad + d_{i-1,rp}^\dagger(k^+) d_{i-1,rq}(k^+) + b_{i,pr}(k^+) b_{i,qr}^\dagger(k^+) + b_{i,rp}^\dagger(k^+) b_{i,rq}(k^+). \end{aligned} \quad (4.20)$$

Diagrammatically, one can say that at every point in color space at any site one has to have either no lines or *two* lines, one of which goes into and the other of which comes out of the point, so that the color indices are contracted at the same site.

4.3 SDLCQ of the transverse lattice model

The transverse lattice formulation of $\mathcal{N} = 1$ SYM theory in 2+1 dimension presented in the previous section has several undesirable features. The supersymmetric

structure of the theory is completely hidden and the resulting Hamiltonian is 6^{th} order in the fields. From the numerical point of view a 6^{th} order interaction makes the theory considerably more difficult to solve. Also the underlying (2+1)-dimensional supersymmetric Hamiltonian is only 4^{th} order making this discrete formulation of the theory very different than the underlying theory. There can, of course, be many discrete formulations that correspond to the same continuum theory and it is therefore desirable to search for a better one. In the spirit of SDLCQ we will attempt a discrete formulation based on the underlying super-algebra of this theory,

$$\{Q^\pm, Q^\pm\} = 2\sqrt{2}P^\pm, \quad \{Q^+, Q^-\} = 2P^\perp. \quad (4.21)$$

In this effort there are some fundamental limits to how far one can go. As we discussed in the previous section the physical states of this theory must conserve color at every point on the transverse lattice. Experience with other supersymmetric theories indicates that each term in Q^+ has to be either the product of *one* M_i and *one* ψ_i or of *one* M_i^\dagger and *one* ψ_i therefore Q^+ is *unphysical*, by which we mean that Q^+ transforms a physical state into an unphysical one, so that $\langle phys|Q^+|phys\rangle = 0$. While this is not a theorem, it seems very difficult to have any other structure since in light cone quantization P^+ is a kinematic operator and therefore independent of the coupling. There appears to be *no* way to make a physical P^+ from Q^+ . We will use P^+ as given in Eq. (4.11) in what follows. Similarly, we are not able to generally construct P^\perp from Q^+ and Q^- . In fact P^\perp is unphysical in our formalism, leading to $\langle phys|P^\perp|phys\rangle = 0$. Formally we will work in the frame where total P^\perp is zero, so it would appear consistent with this result. However, $P^\perp = 0$ was a choice and a non-zero value is equally valid and not consistent with the matrix element.

Despite these difficulties we find a physical Q^- which gives us $P_{SDLCQ}^- \xrightarrow{a \rightarrow 0} P_{cont}^-$.

The expression for Q^- and P_{SDLCQ}^- are, respectively,

$$\begin{aligned}
Q^- &= 2^{3/4} g \cdot a \sum_{i=1}^{N_{sites}} \int dx^- \text{tr}(J_i^+ \partial_-^{-1} \psi_i) \\
&\xrightarrow{a \rightarrow 0} 2^{3/4} \int dx^- dx^\perp \text{tr} [\partial_\perp A^\perp \psi + g (i[A^\perp, \partial_- A^\perp] + 2\psi\psi) \partial_-^{-1} \psi],
\end{aligned} \tag{4.22}$$

$$\begin{aligned}
P_{SDLCQ}^- &\equiv \frac{\{Q^-, Q^-\}}{2\sqrt{2}} \\
&= a \sum_i \int dx^- \text{tr} \left[-\frac{g^2}{2} J_i^+ \frac{1}{\partial_-^2} J_i^+ - \frac{i}{2a^2} (\psi_{i+1} M_i^\dagger - M_i^\dagger \psi_i) \partial_-^{-1} (M_i \psi_{i+1} - \psi_i M_i) \right] \\
&\xrightarrow{a \rightarrow 0} \int dx^- dx^\perp \text{tr} \left[-\frac{g^2}{2} J^+ \frac{1}{\partial_-^2} J^+ - \frac{i}{2} D_\perp \psi \frac{1}{\partial_-} D_\perp \psi \right] \equiv 2\sqrt{2} P_{cont}^-.
\end{aligned} \tag{4.23}$$

Notice that this Hamiltonian is only 4th order in the fields. Furthermore, one can check that this Q^- commutes with P^+ obtained from \mathcal{L} ; $[Q^-, P^+] = 0$. Thus, it follows that,

$$\langle phys | [Q^-, M^2] | phys \rangle = \langle phys | [Q^-, 2P^+ P_{SDLCQ}^-] | phys \rangle = 0 \tag{4.24}$$

in our SDLCQ formalism, where $M^2 \equiv 2P^+ P_{SDLCQ}^- - (P^\perp)^2$. The fact that the Hamiltonian is the square of a supercharge will guarantee the usual supersymmetric degeneracy of the massive spectrum, and our numerical solutions will substantiate this. Unfortunately one needs a Q^+ to guarantee the degeneracy of the massless bound states.

The expression for Q^- is

$$\begin{aligned}
: Q^- : &= \frac{i2^{-1/4}ag}{\sqrt{\pi}} \sum_i \int dk_1 dk_2 dk_3 \delta(k_1 + k_2 - k_3) \left[\right. \\
&\frac{k_2 - k_1}{k_3 \sqrt{k_1 k_2}} (-b_i^\dagger d_i a_i + d_i^\dagger a_i^\dagger b_i - b_i^\dagger a_{i-1} d_{i-1} + a_{i-1}^\dagger d_{i-1}^\dagger b_i) \\
&+ \frac{k_2 + k_3}{k_1 \sqrt{k_2 k_3}} (-d_i^\dagger b_i d_i + b_i^\dagger d_i^\dagger d_i - a_{i-1}^\dagger b_i a_{i-1} + b_i^\dagger a_{i-1}^\dagger a_{i-1}) \\
&+ \frac{k_3 + k_1}{k_2 \sqrt{k_3 k_1}} (a_i^\dagger a_i b_i - a_i^\dagger b_i^\dagger a_i + d_{i-1}^\dagger d_{i-1} b_i - d_{i-1}^\dagger b_i^\dagger d_{i-1}) \\
&\left. + \left(\frac{1}{k_1} + \frac{1}{k_2} - \frac{1}{k_3} \right) (b_i^\dagger b_i^\dagger b_i + b_i^\dagger b_i b_i) \right], \tag{4.25}
\end{aligned}$$

where $k^+ \equiv k$, $a^\dagger a \equiv \text{Tr}(a^\dagger(k_1)a(k_2))$, $a^\dagger a a \equiv \text{Tr}(a^\dagger(k_3)a(k_1)a(k_2))$, and $a^\dagger a^\dagger a \equiv \text{Tr}(a^\dagger(k_1)a^\dagger(k_2)a(k_3))$. Notice that from this explicit expression for Q^- it is clear that cyclic states do not get mixed with non-cyclic states under Q^- , as advertised at the end of Section 4.2. Notice also that the winding number introduced in the last section evidently commutes with Q^- and, thus, with P_{SDLCQ}^- .

Now we are in a position to solve the eigenvalue problem $2P^+ P_{SDLCQ}^- |phys\rangle = m^2 |phys\rangle$. We impose the periodicity condition on M_i , M_i^\dagger and ψ_i in the x^- direction giving a discrete spectrum for k^+ :

$$k^+ = \frac{\pi}{L} n \quad (n = 1, 2, \dots), \quad \int_0^\infty dk^+ \rightarrow \frac{\pi}{L} \sum_{n=1}^\infty.$$

We impose a cut-off on the total longitudinal momentum P^+ i.e. $P^+ = \pi K/L$, where K is an integer also known as the ‘harmonic resolution’, which indicates the coarseness of our numerical results. For a fixed P^+ i.e. a fixed K , the number of partons in a state is limited up to the maximum, that is K , so that the total number of Fock states is *finite*, and, therefore, we have reduced the infinite dimensional eigenvalue problem to a finite dimensional one. We should note here that since the matrix

$\langle phys|P_{SDLCQ}^-|phys\rangle$ to be diagonalized does not depend on N_{sites} , the resulting spectrum does not depend on N_{sites} , either. This means there is no need to keep the site index of operators even in numerical calculations; the sum over all the sites is implicitly understood and when one needs to restore the site indices for some reason, one should do so in such a way that physical constraint (4.10) is satisfied. Henceforth we will suppress the sum and the site indices, unless otherwise noted.

In the following two sections we will give the numerical results for the cyclic ($W \neq 0$) states and non-cyclic ($W = 0$) states separately.

4.4 Numerical results for the cyclic ($W \neq 0$) states

For the cyclic states, it is easy to see that $K \geq |W|$. In fact if $K = |W|$, only two states are possible and both are bosonic. They are $\text{tr}(a_{i+N_{sites}-1}^\dagger \cdots a_{i+1}^\dagger a_i^\dagger)|0\rangle$ and $\text{tr}(d_i^\dagger d_{i+1}^\dagger \cdots d_{i+N_{sites}-1}^\dagger)|0\rangle$, Therefore we will focus on $K > |W|$. Since there is an exact Z_2 symmetry between positive W and negative W , it suffices to consider the case where W is positive. Table 4.1 shows the number of eigenstates with different K and W for various types of states. Since the spectrum starts at $K = W$, it is natural to take $K - W$ as the independent variable. Therefore we tabulate the number of eigenstates with W and $K - W$ rather than W and K and we plotted m^2 as a function of $1/(K - W)$ rather than of $1/K$

The massive degenerate fermion and boson states are related by $Q^- |F\rangle \equiv |B\rangle$. The same is not true of massless states. There is no direct connection through Q^- between massless fermionic states and massless bosonic states, leading to a supersymmetry breaking for massless states. Nevertheless, Table 4.1 shows that we have

K-W	1	2	3	4	5	6	7
W	massive fermion or boson states						
1	0	1	5	18	62	208	706
2	0	2	10	38	138	492	
3	0	3	17	68	268	1023	
4	0	4	24	110	470		
5	0	5	33	166	770		
	massless boson states						
1	0	1	1	3	3	8	8
2	1	2	2	5	5	12	
3	1	2	2	5	5	15	
4	1	2	2	6	6		
5	1	2	2	6	6		
	massless fermion states						
1	1	1	2	2	4	4	9
2	1	1	2	2	5	5	
3	1	1	2	2	5	5	
4	1	1	2	2	6		
5	1	1	2	2	6		

Table 4.1: Number of massive and massless cyclic eigenstates.

the exact supersymmetry for massless states when $K - |W| = 2n - 1$ for $n = 2, \dots$

The boson state with $W = 1$ is anomalous since $\text{tr}(a^\dagger) = 0$ in our formulation.

Also notice that there is a jump in the number of massless states with every increment by two in K . This seems to be the case because we need to increase K by two to allow for the addition of an operator like $d_i^\dagger(1)a_i^\dagger(1)$, so as to make a new physical massless state. The requirement that we add a pair of bosons relates back to the Gauss's law constraint. We see here that two bosons are behaving as a single boson. This is additional evidence that Gauss's law and supersymmetry are working together to restrict the number of effective boson degrees of freedom. It is particularly reassuring to see this effect in the massless bound states since it is in this

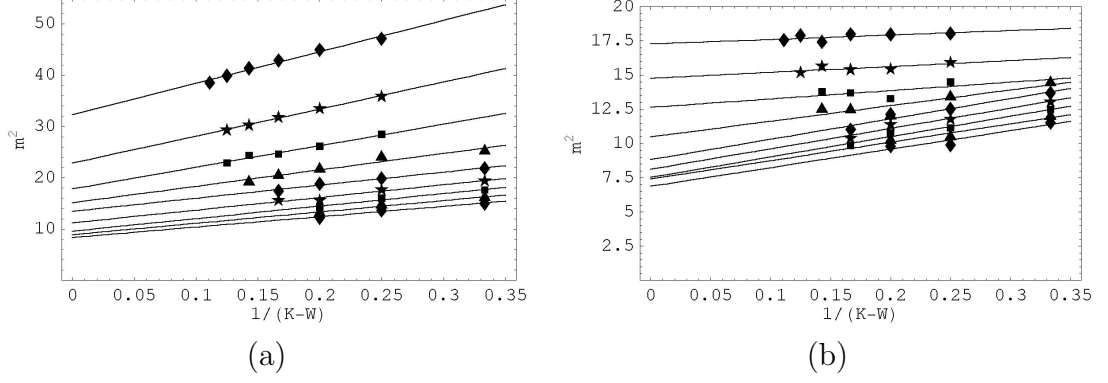


Figure 4.2: Plots of m^2 in units of $\frac{N_c g^2}{\pi a}$ of low energy cyclic states versus $1/(K - W)$ with a linear fit for $W=1$ (top diamond), 2 (top star), 3 (top square), 4 (top triangle), 5 (middle diamond), 6 (bottom star), 7 (bottom square), 8 (bottom triangle), 9 (bottom diamond), (a) state A and, (b) state B.

sector where breaking of the supersymmetric spectrum occurs. We also notice some other interesting properties of our massless states. We find that the Fock states that occur in bosonic massless states have *no* fermionic operators, whereas the Fock states that occur in fermionic massless states have only *one* fermionic operator, which seems to explain the relative shift between the number of massless fermions and bosons.

In Fig. 4.2(a) and (b) we give plots of m^2 for two low-energy states as a function of $1/(K - W)$ and extract m_∞^2 as a $K \rightarrow \infty$ limit of the linear fit. We identify an energy eigenstate with different K 's according to dominant Fock states. Looking at both bosonic and fermionic counterpart also helps distinguish states. We present two states we could easily identify. For the state in (a) the dominant fock component has the form $b^\dagger(n)a^\dagger(1) \cdots a^\dagger(1)b^\dagger(1) + b^\dagger(1)a^\dagger(1) \cdots a^\dagger(1)b^\dagger(n)$ while the state in (b) has the dominant component $b^\dagger(n)a^\dagger(1) \cdots a^\dagger(1)b^\dagger(1) - b^\dagger(1)a^\dagger(1) \cdots a^\dagger(1)b^\dagger(n)$.

In Fig. 4.3 we present m_∞^2 , obtained in Fig.4.2(a) and (b), as a function of $1/W$. We see that state with larger W get lighter. From the discussion of the fock structure

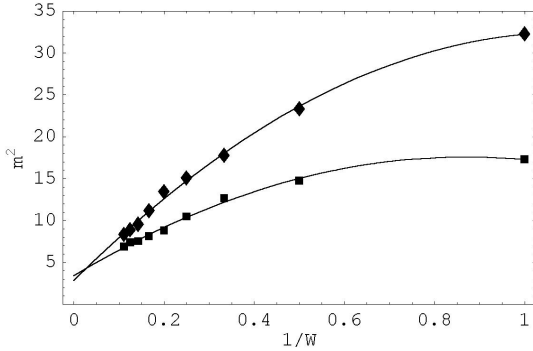


Figure 4.3: Plots of $K \rightarrow \infty$ limit of m^2 in units of $\frac{N_c g^2}{\pi a}$ of low energy cyclic states versus $1/W$ with a quadratic fit to the data. The diamonds correspond to state A and squares correspond to the state B in Fig. 4.2

of these states in the previous paragraph, it is clear that the states with larger W are also longer. Previously in SDLCQ calculations [55, 67] we have seen this unique behavior in SYM theories. We have seen that as we increase K we uncover longer states that have lower masses. Supersymmetric theories like to have light states with long strings of gluons. In the full SDLCQ calculation of $\mathcal{N} = 1$ SYM theory in 2+1 dimensions [20] we have seen these long, light states as well. Here these states of different length are being identified as the same state because of their global fock structure and the length of the fock chain translates to a large W . Therefore we see that states with larger W are lighter.

We see in Fig. 4.3 that the data is fit very well with a quadratic fit in $1/W$. A possible physical argument that compliments the argument above follows if we think of these states as a set of partons in a box of size $2\pi L$ in the transverse direction. The expression for Q^- in 2+1 continuum theory [20] is $Q^- = \alpha_i k_{i,\perp} + g\beta$, where α_i, β are parton operators and $k_{i,\perp}$ is the transverse momenta of the partons. In fact $k_{i,\perp} \propto$

$K =$	3	4	5	6	7	8
massive fermion or boson states						
	2	6	22	72	238	792
massless boson states						
	1	3	3	7	7	17
massless fermion states						
	1	1	3	3	7	7

Table 4.2: Number of massive and massless non-cyclic eigenstates

$1/L \sim 1/W$. Hence we would expect the energy $m^2 \sim (Q^-)^2 = A + B/W + C/W^2$. This is the form of the fit we use in Fig.4.2(a) and (b).

4.5 Numerical results for the non-cyclic ($W = 0$) states

Let us now discuss numerical results for the non-cyclic states. Table 4.2 shows the number of mass eigenstates of massive bosons or fermions, massless bosons, and massless fermions with different K .

From the table we see once again that there are some differences in the number of the massless bosonic and fermionic states and the same dependence on K that we saw for the cyclic states. The reason for this behavior is the same as in the case of the cyclic states. In Fig. 4.4 we show two states whose boson states with a large two partons component. These states appear at the lowest resolution and are the easiest to follow and identify as a function of the resolution K . The boson bound state denoted by diamonds is composed primarily of two fermions, $b^\dagger b^\dagger$, while the boson bound state denoted by squares is composed primarily of two bosons, $d^\dagger a^\dagger$. Again, we see stringy states which appear as we go to higher K with more partons in their dominant Fock state component.

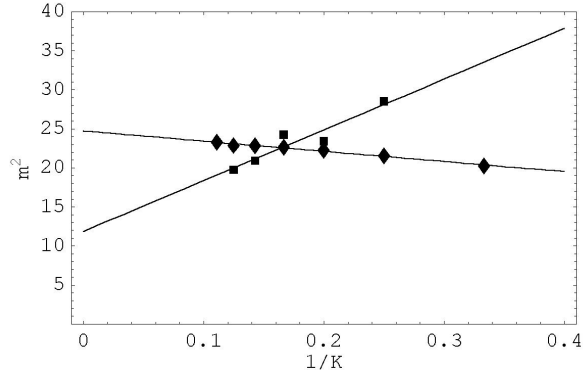


Figure 4.4: Plots of m^2 of low-energy non-cyclic states against $1/K$ with a linear fit in units of $\frac{N_c g^2}{\pi a}$.

We were able to go up to $K = 8$ without making any approximations to the Fock basis, so some of our bound states contained as many as eight partons. However, for $K = 9$ we have truncated the number of partons at 6. We were able to justify this approximation at $K = 9$ for this state by comparing the truncated results with the exact result at $K = 8$. However we were not able to make this approximation for the state denoted by squares.

4.6 Discussion

We have presented a formulation of $\mathcal{N} = (1, 1)$ SYM in 2+1 dimensions where the transverse dimension is discretized on a spatial lattice while the longitudinal dimension x^- is discretized on a momentum lattice. Both x^- and x^\perp are compact. We are able to retain some of the technology of SDLCQ, since this numerical approximation retains one exact supersymmetry. In particular we are able to write the Hamiltonian as the square of a supercharge. Thus there is sufficient supersymmetry in this

formulation to ensure that divergences that appear in this theory are automatically canceled. Furthermore we show that this formulation leads to a fundamentally different and simpler discrete Hamiltonian than the standard Lagrangian approach to the transverse lattice. Since we only have one exact supersymmetry, only the massive fermion and boson bound states in our solution are exactly degenerate. We need an additional supersymmetry to require that the numbers of massless bosons and massless fermions be the same.

As in all transverse lattice approaches, the transverse gauge field is replaced by a complex unitary field, and transverse gauge invariance is maintained. When this complex unitary field is quantized as a general complex linear field, the number of degrees of freedom in the transverse gauge field is improperly represented. In a conventional transverse lattice calculation one tries to dynamically enforce the proper number of degrees of freedom by adding a potential that is minimized by the unitarity constraint. We conjecture that this is not necessary here. Gauss's law requires that color be conserved at every transverse lattice site. This greatly restricts the allowed boson Fock states that can be part of the physical set of basis states and plays an important role in the structure of all bound states. We assert that the combination of the Gauss's law constraint and the one exact supersymmetry are sufficient to approximately enforce the full supersymmetry.

To further support this conjecture we note that in the massless spectrum the number of states changes when we change the resolution by two units indicating that it effectively requires two partons to represent one true degree of freedom. We view solving the theory as a unitary transformation from the constrained basis to a basis free of constraints and very nearly fully supersymmetric.

We should note that this conjecture can not be general since we know of one supersymmetric theory in 1+1 dimensions where the degrees of freedom at the parton level are all fermions [72]. In this model one has to fix the coupling to be a particular value for this miracle to occur. Generally in a supersymmetric theory the coupling is a free parameter. Nevertheless this example provides of word of caution with regard to our assertion.

We found two classes of bound states, cyclic and non-cyclic. The cyclic bound states have color flux that is wrapped completely around the compact transverse space. We were able to isolate two sequences of such states. Each sequence corresponds to a given state with a different number of wrappings. As a function of the winding number W the masses have the form $m^2 = A + B/W + C/W^2$. In the non-cyclic sector we find stringy states as we have in previous SDLCQ calculations. We find good convergence for the bound states we present as a function of K .

Finally we would like to note that the symmetries of this approach and those of Cohn, Kaplan, Katz and Unsal (CKKU)[24] appear to be similar. The formulations are totally different, and these authors consider a two-dimensional discrete spatial lattice as well as extended supersymmetry. Nevertheless there are some similarities. As we have noted several times we have color conservation at each lattice site, thus the symmetry group is $U(N_c)^{N_{sites}}$ similar to CKKU. We have enforced translation invariance for this discrete lattice with N_{sites} sites; therefore, there is a $Z_{N_{sites}}$ symmetry similar to one found by CKKU for their two dimensional lattice. Finally, in this theory there is an orientation symmetry for the trace which is a Z_2 symmetry also similar to CKKU. In addition CKKU have some $U(1)$ symmetries which we seem

to be missing. This may be related to the fundamentally different way chiral symmetry is treated on the light cone[46]. Another similarity appears to be the relation between the number of supersymmetries and the number of fermions on a site. Both approaches have one fermion on a site and one supersymmetry.

Most of our numerical calculation was done using our Mathematica code on a Linux workstation. This was very convenient for our first attempt at a supersymmetric formulation of a transverse lattice problem. We have used our $C++$ code to obtain results for a few of the cyclic states at higher resolution. We are also able to handle the problem of two transverse dimensions with this code as we will do so in chapter 6.

CHAPTER 5

A SOLUTION TO FERMION DOUBLING PROBLEM

5.1 Introduction

When one formulates a theory with chiral fermions on a spatial lattice, one of the most notorious obstacles is the Nielsen-Ninomiya theorem[21] which gives a set of conditions that require species doubling. In our transverse lattice formulation of field theory we use both a spatial lattice and a momentum lattice. The transverse lattice formulations usually has some non-local interaction(s) which voids the Nielsen-Ninomiya theorem however it still seems to have the species doubling problem [73].

In the previous chapter we introduced a super Yang-Mills (SYM) model in 2+1 dimensions on a transverse lattice with one exact supersymmetry [62]. It is well known that in the standard Lagrangian formulation of SYM on the transverse lattice one finds a fermion species doubling problem. We will show however that we are free from species doubling when one uses Supersymmetric Discrete Light Cone Quantization (SDLCQ). This is yet another demonstration of value of maintaining an exact supersymmetry in the numerical approximation. Of course two popular methods of dealing with the doubling, staggered fermions [74] and the Wilson term [75], work for the lagrangian formulation of SYM theories on a transverse lattice. In addition Chakrabarti, De and Harindranath recently proposed the use of the forward

and backward derivatives to remove the species doubling on the light front transverse lattice [76]. However those methods badly break the supersymmetry and it is unclear how many of the unique properties of supersymmetry persist. While our approach can only be used for the transverse lattice formulation of supersymmetric theories, it resolves the doubling problem automatically.

This chapter is organized as follows. In Section 5.2 we will see that the species doubling arises in the standard Lagrangian formulation of the transverse lattice, but can be resolved when one applies the method proposed by Ref. [76]. In Section 5.3 we show that in the SDLCQ formulation of the transverse lattice we do not have any species doubling. In Section 5.4 we discuss some general reasons for this result and give the generalization to 3+1 dimensions. This chapter is based on Ref. [77]

5.2 Fermion species doubling problem on a transverse lattice

To focus on the fermion species doubling problem of the transverse lattice [62], let us consider fermion fields only by setting the coupling $g = 0$ and the link variables $M, M^\dagger = 1$. For this theory one spatial dimension is discretized on a spatial lattice. We work in the light cone coordinates so that $x^\pm \equiv (x^0 \pm x^1)/\sqrt{2}$ with $x^\pm = x_\mp$ and $x^\perp \equiv x^2 = -x_2$ is the dimension that is discretized on the spatial lattice. The Lagrangian is given by

$$\mathcal{L} = \sum_i \text{tr} \left[\bar{\Psi}_i \gamma^\mu \partial_\mu \Psi_i + \frac{i}{2a} \bar{\Psi}_i \gamma^\perp (\Psi_{i+1} - \Psi_{i-1}) \right],$$

where i is the site index, the trace has been taken with respect to the color indices, $\mu = \pm$, and a is the lattice spacing. The gamma matrices are defined to be $\gamma^0 = \sigma^2$, $\gamma^1 = i\sigma_1$, and $\gamma^\perp = i\sigma^3$ with $\gamma^\pm \equiv (\gamma^0 \pm \gamma^1)/\sqrt{2}$. For $\Psi_i = 2^{-1/4} \begin{pmatrix} \psi_i \\ \chi_i \end{pmatrix}$ we find the

equation of motion

$$\partial_- \chi_i = \frac{1}{2\sqrt{2}a}(\psi_{i+1} - \psi_{i-1}).$$

Inverting the light cone spatial derivative, we eliminate the non-dynamical field χ_i from \mathcal{L} and get

$$\mathcal{L} = \sum_i \text{tr} \left[i\psi_i \partial_+ \psi_i + \frac{i}{8a^2}(\psi_{i+1} - \psi_{i-1}) \partial_-^{-1}(\psi_{i+1} - \psi_{i-1}) \right].$$

Note that the second term is non-local. This is sufficient to avoid the Nielsen-Ninomiya theorem. The equation of motion for ψ_i is

$$\partial_+ \psi_i = \frac{1}{8a^2} \partial_-^{-1}(\psi_{i+2} - 2\psi_i + \psi_{i-2}). \quad (5.1)$$

We substitute the Fourier transformed form of ψ_i ,

$$\psi_j(x) = \int_{-\pi/a}^{\pi/a} dk^\perp \int_0^\infty dk^+ dk^- e^{i(k^+ x^- + k^- x^+ - k^\perp (aj))} \tilde{\psi}_j(k),$$

into Eq. (5.1) to find a dispersion relation

$$k^- = \frac{1}{2k^+} \left(\frac{\sin k^\perp a}{a} \right)^2. \quad (5.2)$$

Clearly, in the continuum limit where $a \rightarrow 0$, we find finite energy not only at $k^\perp \approx 0$, but also at $k^\perp \approx \pm\pi/a$ for $-\pi/a < k^\perp < \pi/a$, yielding *extra* unwanted fermion species, that is, the notorious fermion species doubling problem.

Let us point out that the same equation of motion and thus the same dispersion relation follow if one uses Heisenberg equation of motion $i\partial_+ \psi_{i,rs}(x) = [\psi_{i,rs}(x), P^-]$. This is the approach we will use in the next section. In this calculation we use the equal (light cone) time anticommutation relation $\{\psi_{i,rs}(x^-), \psi_{j,pq}(y^-)\} = \delta(x^- - y^-) \delta_{ij} \delta_{rp} \delta_{sq} / 2a$, where we've explicitly written out the color indices r, s, p, q and

$$P^- \equiv a \sum_i \int dx^- T^{+-} = a \sum_i \int dx^- \text{tr} \left[-\frac{i}{8a^2}(\psi_{i+1} - \psi_{i-1}) \partial_-^{-1}(\psi_{i+1} - \psi_{i-1}) \right].$$

$T^{\mu\nu}$ is the stress-energy tensor.

One might wonder what happens if we tried another difference operator, for instance, the forward/backward derivative in place of the symmetric derivative. Answering this question is instructive since the authors of Ref. [76] have found no fermion doubling for chiral fermions if one uses forward and backward derivatives on the light front transverse lattice. Following their procedure, we get in terms of ψ_i and χ_i

$$\begin{aligned}\mathcal{L} &= \sum_i \text{tr} \left[i\psi_i \partial_+ \psi_i + i\chi_i \partial_- \chi_i - \frac{i}{\sqrt{2}a} (\chi_i(\psi_{i+1} - \psi_i) + \psi_i(\chi_i - \chi_{i-1})) \right] \\ &= \sum_i \text{tr} \left[i\psi_i \partial_+ \psi_i + i\chi_i \partial_- \chi_i - \frac{\sqrt{2}i}{a} \chi_i(\psi_{i+1} - \psi_i) \right].\end{aligned}$$

This yields

$$\partial_- \chi_i = \frac{1}{\sqrt{2}a} (\psi_{i+1} - \psi_i)$$

and

$$\mathcal{L} = \sum_i \text{tr} \left[i\psi_i \partial_+ \psi_i + \frac{i}{2a^2} (\psi_{i+1} - \psi_i) \partial_-^{-1} (\psi_{i+1} - \psi_i) \right].$$

From this we find a dispersion relation

$$k^- = \frac{1}{2k^+} \left(\frac{\sin \frac{k^\perp a}{2}}{a/2} \right)^2.$$

In the continuum limit we find a finite energy only at $k^\perp \approx 0$, meaning that we do not have the doubling problem. Hence, we found that the method to remove the doubling proposed in Ref. [76] works even for adjoint fermions.

5.3 Transverse lattice with SDLCQ

In Ref. [62] we proposed a discrete transverse lattice formulation of the supercharge Q^- , which gives the correct continuum form. In this formulation the P^- obtained from SUSY algebra $\{Q^-, Q^-\} = 2\sqrt{2}P^-$ also gives the correct continuum form. With

this P^- in hand, following the same procedure we did in the previous section, we set $g = 0$ and $M, M^\dagger = 1$ to see whether we suffer from the fermion doubling problem.

This P^- is given by

$$P^- = a \sum \int dx^- \text{tr} \left[-\frac{i}{2a^2} (\psi_{i+1} - \psi_i) \partial_-^{-1} (\psi_{i+1} - \psi_i) \right].$$

Heisenberg equation of motion yields

$$i\partial_+ \psi_{i,rs} = [\psi_{i,rs}, P^-] = \frac{i}{2a^2} \partial_-^{-1} (\psi_{i+1} - 2\psi_i + \psi_{i-1})_{rs}.$$

Hence, it follows that

$$k^- = \frac{1}{2k^+} \left(\frac{\sin \frac{k^+ a}{2}}{a/2} \right)^2.$$

Notice, remarkably, that we have a finite energy *only* at $k^\perp \approx 0$, so that we are *free from the species doubling problem with SDLCQ*.

A word of caution is due here. This P^- happens to be the same as the one obtained in Ref. [76], where the authors used the forward and backward derivatives however we get P^- in a completely different way.

5.4 Discussion

We reviewed the known result that one suffers from a species doubling problem in the transverse lattice Lagrangian formalism with the symmetric derivative in spite of the fact that our adjoint fermions interact non-locally. We applied the method of removing the doubling proposed by the authors of Ref. [76] originally for chiral fermions and found that it works as well even for adjoint fermions. We then showed that we do not suffer from species doubling in the SDLCQ formulation of the transverse lattice [62].

While we did the calculation in 2+1 dimensions, we should note that this doubling persists in 3+1 dimensions. As we will see in the next chapter [78], the standard transverse Lagrangian formulation leads to the following dispersion relation,

$$k^- = \frac{1}{2k^+} \left[\left(\frac{\sin k_1^\perp a}{a} \right)^2 + \left(\frac{\sin k_2^\perp a}{a} \right)^2 \right],$$

where k_i^\perp is the i -th transverse momentum. For a model with SDLCQ formulation of the transverse lattice,

$$k^- = \frac{1}{2k^+} \left[\left(\frac{\sin \frac{k_1^\perp a}{2}}{a/2} \right)^2 + \left(\frac{\sin \frac{k_2^\perp a}{2}}{a/2} \right)^2 \right].$$

Again, we do not have any species doubling with SDLCQ.

In Ref. [62] we found that the color of physical states must be contracted at each site. However, this constraint was derived in the standard Lagrangian formalism, which suffers from the doubling problem. Therefore, one might ask if there is any change in the physical constraint due to the doubling problem. We believe the answer is no. The reason is the following. The physical constraint we found in [62] comes from the equation of motion $\frac{\delta \mathcal{L}}{\delta A_i^-} - \partial_+ \frac{\delta \mathcal{L}}{\delta (\partial_+ A_i^-)} = 0$, where A_i^- is the “-” component of the gauge field A_i^μ residing at the i -th site. However, this equation of motion has nothing to do with the terms involving the difference between fermions at different sites, which are the cause of the doubling. Hence, even if we made some change(s) in the standard Lagrangian e.g. by adding a Wilson term to fix the doubling problem, we would not see any change in the equation of motion which leads to the physical constraint.

It seems that SUSY algebra by itself resolves the species doubling problem. This is indeed expected since we do not have any doubling problems in boson sector and SUSY requires that the number of degrees of freedom be the same for bosons and

fermions. In general it is difficult to maintain exact SUSY on a lattice, but it appears that if it is achieved, then it automatically solves the species doubling problem.

CHAPTER 6

SDLCQ AND TRANSVERSE LATTICE IN 3+1 DIMENSIONS

6.1 Introduction

We have introduced a new approach to solving $\mathcal{N}=1$ SYM in 2+1 dimensions non-perturbatively in Chapter 4. Here, we extend the approach to $\mathcal{N}=1$ SYM in 3+1 dimensions and present a formulation for 3+1 dimensional $\mathcal{N}=1$ SYM with a two dimensional transverse lattice in the large N_c limit, which was the work presented in Ref. [78].

At each site of the two dimensional lattice, we have one gauge boson and one four-component Majorana spinor. Adjacent sites are connected by the link variables. All these fields depend only on the light-cone time and spatial coordinates x^\pm and are associated with two site indices, say (i, j) . In the large N_c limit, however, it turns out that we are allowed to drop the site indices for our calculation. This is in some sense the manifestation of the Eguchi-Kawai reduction [71]. However, it is well known that the naive Eguchi-Kawai reduction encounters a problem due to the violation of one of the assumptions made by Eguchi and Kawai [80]. That assumption is the $U(1)^d$ symmetry. Since we do not have to assume the $U(1)^d$ symmetry to justify our reduction of the transverse lattice degrees of freedom, we believe that we do not have

to introduce quenching [80] or twisted [81] lattices, which were invented to overcome the problem associated with the naive Eguchi-Kawai reduction at weak couplings. For more complete and detailed discussion for this claim, see Sec. 6.7. With this reduction of the transverse degrees of freedom, we can regard all the fields as 1+1 dimensional objects. That is to say that we have some complicated 1+1 dimensional field theory with some highly non-trivial interactions of the fields. Furthermore, since we can always work in the frame where we have zero transverse momenta $P^1, P^2 = 0$, $\mathcal{N}=1$ SUSY algebra in 3+1 dimensions becomes identical to $\mathcal{N}=2$ SUSY algebra in 1+1 dimensions, which is sometimes referred to as $\mathcal{N}=(2,2)$ SUSY in literature, (2,2) for two Q^+ 's and two Q^- 's. We are able to maintain one of this underlying $\mathcal{N}=(2,2)$ SUSY algebra in our formulation, meaning that we are able to preserve one exact SUSY.

We discretize light-cone momentum p^+ by imposing the periodic condition on the light-cone spatial coordinate x^- . Thus, we have two spatial lattices and one momentum lattice in our model. Since we are dealing with spatial lattices, one has to be concerned about the notorious fermion doubling problem. In fact it is well known that the transverse lattice suffers from the doubling problem [73]. However, as we have seen in Chapter 5, SDLCQ formulation of a transverse lattice model is automatically free of the doubling problem [77].

There are some aspects of this calculation that are similar to the 2+1 dimensional model [62] and there are others that are not. What is not the same is that the supercharge Q_α^- has terms which have different powers of the coupling $g' \equiv g\sqrt{N_c}$, where $\alpha = 1, 2$. To be more precise, Q_α^- consists of terms proportional to g' and terms proportional to g'^3 . The different powers of g' give rise to a rich spectrum as

one varies g' , and the wavefunctions depend on g' . This means that it is possible to see wavefunctions which are almost vanishing at small couplings, but become very large at strong couplings, and vice versa.

One more thing which is different from the previous case is that our Q_α^- has terms of third and fifth order in dynamical fields, while all of the terms in Q^- are of third order for 2+1 dimensional case. This leads to a hamiltonian of eighth order in fields, which is of higher order than the hamiltonian of sixth order that we get from the standard formulation of 3+1 dimensional $\mathcal{N}=1$ SYM on the two transverse lattice. We admit that this is a disadvantage of our formulation in 3+1 dimensions compared to that in 2+1 dimensions. Nevertheless, we still think that our approach is more advantageous because in the SDLCQ formulation we use Q_α^- , not the hamiltonian, and this Q_α^- is still of lower order in fields than the hamiltonian obtained from the standard formulation, and also because the standard formulation suffers from the fermion doubling problem.

Similar to the 2+1 dimensional case we are not able to preserve the full supersymmetry algebra. We are able to maintain one exact SUSY. This is attributed to the fact that when quantizing the dynamical fields we have to make the link variable, which is a unitary matrix, a linear complex matrix. One way to compensate for the effects of this “linearization” is to make use of the “color-dielectric” formulation of the lattice gauge theory [45, 64, 82, 63]. In this formulation we consider smeared degrees of freedom \mathcal{M} , which are obtained from the original link variable M by averaging M over some finite volume, say $\sum_{av} M$. In order for this smeared theory to be equivalent to the original one, we must have an effective potential for the \mathcal{M} defined

by integrating out M [64, 82]

$$\exp[-V_{eff}(\mathcal{M})] = \int \mathcal{D}M \delta(\mathcal{M} - \sum_{av} M) \exp[-S_{canonical}(M)].$$

However, this $V_{eff}(\mathcal{M})$ can be very complicated and performing the path integral above is extremely difficult, if not impossible. Thus, one makes some approximations with ansatz to determine V_{eff} . For more detail, we'd refer the reader to the Refs. [45, 64, 82, 63].

To constrain the linearized fields, we require the model to exactly conserve one SUSY as we did for our 2+1 dimensional calculation. That is, we present a physical Q_{α}^{-} that preserves one SUSY. By ‘‘physical’’ we mean a Q_{α}^{-} which transforms one physical state into another physical state. We are not able to fully recover SUSY due to the absence of a physical Q_{α}^{+} . This defect results in a different number of massless states in the bosonic and fermionic sectors. However, we do see the mass degeneracy among the massive bosonic and fermionic states. The linearization doubles the bosonic degrees of freedom, leading to the SUSY breakdown. The partial recovery of SUSY implies that we have cured some but not all of the problems associated with the linearization.

We are numerically able to identify what we call the cyclic states and non-cyclic states by examining the properties of the states. The cyclic states are those whose color flux winds all the way around in one or two of the transverse directions. For the non-cyclic states the color flux is localized in color space. The cyclic bound states have a non-trivial spectrum as a function of the winding number. We find that m^2 for the cyclic bound states can be fit by either $b + c/W_I + d/W_I^2$ or $b + cW_I^2 + d/W_I^2$, where b, c, d are some constants and W_I is the winding number in the x_I -direction with $I = 1, 2$. It could be interesting to know how the form of the m^2 changes from weak

coupling to strong coupling however the complicated spectrum for strong couplings puts this beyond our reach at the present time.

The structure of this chapter is the following. In Sec. 6.2 we present a standard formulation of $\mathcal{N}=1$ SYM with a two dimensional transverse lattice and derive constraint equations on the physical states. We discuss the implications of those in some detail. We give SDLCQ formulation of $\mathcal{N}=1$ SYM in Sec. 6.3 and show that this formulation is free from the doubling problem. The coupling dependence of the mass spectrum is discussed in Sec. 6.4 followed by numerical results for cyclic bound states in Sec. 6.5 and for non-cyclic bound states in Sec. 6.6. Sec. 6.7 is to show how we justify the reduction of transverse degrees of freedom in the large N_c limit. The summary and possible further directions of investigation are given in Sec. 6.8.

6.2 Transverse lattice model in 3+1 dimensions

In this section we present the standard formulation of a transverse lattice model in 3+1 dimensions for an $\mathcal{N}=1$ supersymmetric $SU(N_c)$ theory with adjoint bosons and adjoint fermions in the large- N_c limit. We work in light-cone coordinates so that $x^\pm \equiv (x^0 \pm x^3)/\sqrt{2}$. The metric is specified by $x^\pm = x_\mp$ and $x^I = -x_I$, where $I = 1, 2$. Suppose that there are N_{sites} sites in both the transverse directions x^1 and x^2 with lattice spacing a . With each site, say $n = (i, j)$, we associate one gauge boson field $A_{\nu,n}(x^\mu)$ and one four-component Majorana spinor $\Psi_n(x^\mu)$, where $\nu, \mu = \pm$. $A_{\nu,n}$'s and Ψ_n 's are in the adjoint representation. The adjacent sites, say n and $n + i_I$, where i_I is a vector of length a in the direction x^I , are connected by what we call the link variables $M_n^I(x^\mu)$ and $M_n^{I\dagger}(x^\mu)$. $M_n^I(x^\mu)$ stands for a link which goes from the site n to the site $(n + i_I)$ and $M_n^{I\dagger}(x^\mu)$ for a link from the site $(n + i_I)$ to n . We impose the

periodic condition on the transverse sites so that $A_{N_{sites}i_I+n} = A_n$, $\Psi_{N_{sites}i_I+n} = \Psi_n$, $M_{N_{sites}i_I+n}^I = M_n^I$ and $M_{N_{sites}i_I+n}^{I\dagger} = M_n^{I\dagger}$. Under the transverse gauge transformation [45] the fields transform as

$$gA_n^\mu \longrightarrow U_n gA_n^\mu U_n^\dagger - iU_n \partial^\mu U_n^\dagger, \quad M_n^I \longrightarrow U_n M_n^I U_{n+i_I}^\dagger, \quad \Psi_n \longrightarrow U_n \Psi_n U_n^\dagger, \quad (6.1)$$

where g is the coupling constant and $U_n \equiv U_n(x^\mu)$ is a $N_c \times N_c$ unitary matrix. In all earlier work on the transverse lattice [45] Ψ_n was in the fundamental representation.

The link variable can be written as

$$M_n^I(x^\mu) = \exp\left(ia g A_{n+i_I/2,I}(x^\mu)\right), \quad (6.2)$$

where $A_{n,I}$ is the transverse component of the gauge potential at site n and as $a \rightarrow 0$ we can formally expand Eq. (6.2) in powers of a as follows:

$$M_n^I(x^\mu) = 1 + iag A_{n,I}(x^\mu) + \frac{a^2}{2} \left[ig \partial_I A_{n,I}(x^\mu) - g^2 (A_{n,I}(x^\mu))^2 \right] + O(a^3). \quad (6.3)$$

In the limit $a \rightarrow 0$, with the substitution of the expansion Eq. (6.3) for M_n^I , we expect everything to coincide with its counterpart in *continuum* (3+1)-dimensional theory.

The discrete Lagrangian is then given by

$$\begin{aligned} \mathcal{L} = \text{tr} \left\{ & -\frac{1}{4} F_n^{\mu\nu} F_{n,\mu\nu} + \frac{1}{2a^2 g^2} (D_\mu M_n^I) (D^\mu M_n^I)^\dagger \right. \\ & + \frac{1}{4a^4 g^2} \sum_{I \neq J} (M_n^I M_{n+i_I}^J M_{n+i_J}^{I\dagger} M_n^{J\dagger} - 1) + \bar{\Psi}_n i \Gamma^\mu D_\mu \Psi_n \\ & \left. + \frac{i}{2a} \bar{\Psi}_n \Gamma^I (M_n^I \Psi_{n+i_I} M_n^{I\dagger} - M_{n-i_I}^{I\dagger} \Psi_{n-i_I} M_{n-i_I}^I) \right\}, \end{aligned}$$

where the trace has been taken with respect to the color indices, $F_{n,\mu\nu} = \partial_\mu A_{n,\nu} - \partial_\nu A_{n,\mu} + ig[A_{n,\mu}, A_{n,\nu}]$, $\mu, \nu = \pm$. We choose Majorana representation where Majorana spinors have real component fields and Γ 's are given by

$$\Gamma^0 \equiv \begin{pmatrix} 0 & \sigma_2 \\ \sigma_2 & 0 \end{pmatrix}, \quad \Gamma^1 \equiv \begin{pmatrix} i\sigma_1 & 0 \\ 0 & i\sigma_1 \end{pmatrix}, \quad \Gamma^2 \equiv \begin{pmatrix} i\sigma_3 & 0 \\ 0 & i\sigma_3 \end{pmatrix}, \quad \Gamma^3 \equiv \begin{pmatrix} 0 & -\sigma_2 \\ \sigma_2 & 0 \end{pmatrix},$$

$$\Gamma^+ \equiv \frac{\Gamma^0 + \Gamma^3}{\sqrt{2}} = \begin{pmatrix} 0 & 0 \\ \sqrt{2}\sigma_2 & 0 \end{pmatrix}, \quad \Gamma^- \equiv \frac{\Gamma^0 - \Gamma^3}{\sqrt{2}} = \begin{pmatrix} 0 & \sqrt{2}\sigma_2 \\ 0 & 0 \end{pmatrix}.$$

The covariant derivative D_μ is defined by

$$\begin{aligned} D_\mu \Psi_n &\equiv \partial_\mu \Psi_n + ig[A_{n,\mu}, \Psi_n], \\ D_\mu M_n^I &\equiv \partial_\mu M_n^I + igA_{n,I}M_n^I - igM_n^I A_{n+i_I,\mu} \xrightarrow{a \rightarrow 0} iagF_{\mu I} + O(a^2), \\ (D^\mu M_n^I)^\dagger &\equiv \partial^\mu M_n^{I\dagger} - igM_n^{I\dagger} A_n^\mu + igA_{n+i_I}^\mu M_n^{I\dagger} \xrightarrow{a \rightarrow 0} iagF^{\mu I} + O(a^2). \end{aligned}$$

In the limit $a \rightarrow 0$ we recover the standard Lagrangian as expected. Of course the form of this Lagrangian is slightly different from that in Ref. [45] since the fermions are in the adjoint representation. This Lagrangian is hermitian and invariant under the transformation in Eq. (6.1) as one would expect.

The following Euler-Lagrange equations in the light cone gauge, $A_{n,-} = 0$, are constraint equations.

$$\begin{aligned} \partial_-^2 A_n^- &\equiv gJ_n^+ \xrightarrow{a \rightarrow 0} ig[A_I, \partial_- A_I] + \partial_I \partial_- A_I + 2g\psi_R \psi_R, \\ \partial_- \psi_{Ln} &= \frac{-i}{2\sqrt{2}a} \sigma_2 \beta_I (M_n^I \psi_{Rn+i_I} M_n^{I\dagger} - M_{n-i_I}^{I\dagger} \psi_{Rn-i_I} M_{n-i_I}^I) \xrightarrow{a \rightarrow 0} \frac{-i}{\sqrt{2}} \sigma_2 \beta_I D_I \psi_R, \end{aligned} \quad (6.4)$$

where

$$J_n^+ \equiv \frac{i}{2g^2 a^2} (M_n^I \overleftrightarrow{\partial}_- M_n^{I\dagger} + M_{n-i_I}^{I\dagger} \overleftrightarrow{\partial}_- M_{n-i_I}^I) + 2\psi_n \psi_n, \quad \Psi_n \equiv \frac{1}{2^{1/4}} \begin{pmatrix} \psi_{Rn} \\ \psi_{Ln} \end{pmatrix}, \quad (6.5)$$

$\beta_1 \equiv \sigma_1$, $\beta_2 = \sigma_3$ and $\psi_{L,R}$ are the two-component left-moving, right-moving spinors.

Since these equations only involve the spatial derivative we can solve them for A_n^- and ψ_{Ln} , respectively. Thus the dynamical field degrees of freedom are M_n^I , $M_n^{I\dagger}$ and ψ_{Rn} .

Eq. (6.4) gives a constraint on physical states $|phys\rangle$, since the zero mode of J_n^+ acting on any physical state must vanish,

$$J_n^+ |phys\rangle = \int dx^- J_n^+(x^\mu) |phys\rangle = 0 \quad \text{for any } n = (i, j). \quad (6.6)$$

This means that the physical states must be color singlet at *each* site.

It is straightforward to derive $P^\pm \equiv \int dx^- T^{+\pm}$, where $T^{\mu\nu}$ is the stress-energy tensor. We have

$$P^+ = a^2 \sum_n \int dx^- \text{tr} \left(\frac{1}{a^2 g^2} \partial_- M_n^{I\dagger} \partial_- M_n^I + i \psi_{Rn} \partial_- \psi_{Rn} \right), \quad (6.7)$$

$$P^- = a^2 \sum_n \int dx^- \text{tr} \left[\frac{1}{2} (\partial_- A_n^-)^2 + i \psi_{Ln} \partial_- \psi_{Ln} - \frac{1}{4a^2 g^2} (M_n^I M_{n+i_I}^J M_{n+i_J}^{I\dagger} M_n^{J\dagger} - 1) \right], \quad (6.8)$$

where one should notice that we've kept the non-dynamical fields in the expression for P^- to make it look simpler. When one quantizes the dynamical fields, unitarity of M_n^I is lost and M_n^I becomes an $N_c \times N_c$ complex matrix [45]. One way to compensate for the effects of this ‘‘linearization’’ is to make use of the ‘‘color dielectric’’ formulation of the lattice gauge theory [45, 64, 82, 63]. We will approach this issue using supersymmetry as we've done for the 2+1 dimensional case.

Having linearized M_n^I , we can expand M_n^I and ψ_{Rn} in their Fourier modes as follows; at $x^+ = 0$

$$M_{n,rs}^I(x^-) = \frac{ag}{\sqrt{2\pi}} \int_0^\infty \frac{dk^+}{\sqrt{k^+}} (d_{n,rs}^I(k^+) e^{-ik^+x^-} + a_{n,rs}^{I\dagger}(k^+) e^{ik^+x^-}), \quad (6.9)$$

$$u_{n,rs}^\alpha(x^-) = \frac{1}{2\sqrt{\pi}} \int_0^\infty dk^+ (b_{n,rs}^\alpha(k^+) e^{-ik^+x^-} + b_{n,rs}^{\alpha\dagger}(k^+) e^{ik^+x^-}), \quad (6.10)$$

where r, s indicate the color indices, $\psi_{Rn} \equiv \begin{pmatrix} u_n^1 \\ u_n^2 \end{pmatrix}$, $\alpha = 1, 2$, $a_{n,rs}^{I\dagger}(k^+)$ creates a link variable with momentum k^+ which carries color r at site n to s at site $(n + i_I)$, $d_{n,rs}^{I\dagger}(k^+)$ creates a link with k^+ which carries color r at site $(n + i_I)$ to s at site i and $b_{n,rs}^{\alpha\dagger}$ creates a fermion at the site n which carries color r to s . Quantizing at $x^+ = 0$ we have

$$[M_{ij,rs}^I(x^-), \pi_{Mkl,pq}^J(y^-)] = \left[M_{ij,rs}^I(x^-), \frac{\partial_{-y} M_{kl,pq}^{J\dagger}(y^-)}{2a^2g^2} \right] = \frac{i}{2} \delta(x^- - y^-) \frac{\delta_{ik}}{a} \frac{\delta_{jl}}{a} \delta_{rp} \delta_{sq} \delta_{IJ}, \quad (6.11)$$

$$\{u_{ij,rs}^\alpha(x^-), \pi_{\psi kl,pq}^\beta(y^-)\} = \{u_{ij,rs}^\alpha(x^-), iu_{kl,pq}^\beta(y^-)\} = \frac{i}{2} \delta(x^- - y^-) \frac{\delta_{ik}}{a} \frac{\delta_{jl}}{a} \delta_{rp} \delta_{sq} \delta_{\alpha\beta}, \quad (6.12)$$

where π_M, π_ψ are the conjugate momentum for M, ψ , respectively, and we wrote out the site indices for clarity. Note that we divided δ_{ik} and δ_{jl} by a because $\delta_{ik}/a \rightarrow \delta(x^1 - y^1)$ and $\delta_{jl}/a \rightarrow \delta(x^2 - y^2)$ as $a \rightarrow 0$. Then, one can easily see that these commutation relations are satisfied when a 's, d 's and b 's satisfy the following:

$$[a_{ij,rs}^I(k^+), a_{kl,pq}^{J\dagger}(p^+)] = [d_{ij,rs}^I(k^+), d_{kl,pq}^{J\dagger}(p^+)] = \delta(k^+ - p^+) \frac{\delta_{ik}}{a} \frac{\delta_{jl}}{a} \delta_{rp} \delta_{sq} \delta_{IJ},$$

$$\{b_{ij,rs}^\alpha(k^+), b_{kl,pq}^{\beta\dagger}(p^+)\} = \delta(k^+ - p^+) \frac{\delta_{ik}}{a} \frac{\delta_{jl}}{a} \delta_{rp} \delta_{sq} \delta_{\alpha\beta}, \quad (6.13)$$

with others all being zero. Physical states can be generated by acting on the Fock vacuum $|0\rangle$ with these $a^{I\dagger}$'s, $d^{J\dagger}$'s and $b^{\alpha\dagger}$'s in such a manner that the constraint Eq. (6.6) is satisfied.

Before discussing the physical constraint in more detail, let us point out the fact that this naive Lagrangian formulation is *not free from the fermion species doubling problem*, while our SDLCQ formulation that we will introduce in the next section actually *is* [77]. Nonetheless, the constraint equation would still be valid since the constraint equation (6.4, 6.6) was derived from $\frac{\delta\mathcal{L}}{\delta A_n^-} - \partial_+ \frac{\delta\mathcal{L}}{\delta \partial_+ A_n^-} = 0$ in which we do not have any problematic terms responsible for the doubling problem, i.e. the terms which contains the difference between fermions at different sites. Therefore, we assume that

this physical constraint is valid for our SDLCQ formulation in the next section and we will fully utilize it when we carry out our numerical calculations.

With this subtlety in mind, let us complete this section by discussing the physical constraint (6.6) in more detail. The states are all constructed in the large- N_c limit, and therefore we need only consider single-trace states. In order for a state to be color singlet at each site, *each color index has to be contracted at the same site*. As an example consider a state represented by $|phys\ 1\rangle \equiv d_{n,rs}^{I\dagger} a_{n,rs}^{I\dagger} |0\rangle$, where we've suppressed the momentum carried by $a^{I\dagger}$ and $d^{I\dagger}$ and we'll do so hereafter unless it's necessary for clarity. For this state the color r at site n is carried by $a_n^{I\dagger}$ to s at site $(n+i_I)$ and then brought back by $d_n^{I\dagger}$ to r at site n . The color r is contracted at site n *only* and the color s at site $(n+i_I)$ *only*. Therefore, this is a physical state satisfying Eq. (6.6). A picture to visualize this case is shown in Fig. 6.1a. Diagrammatically, one can say that at every point in color space one has to have either no lines or two lines, one of which goes into and the other of which comes out of the point, so that the color indices are contracted at the same site.

One also needs to be careful with operator ordering. One can show that the state $d_{n,rs}^{I\dagger} a_{n,st}^{I\dagger} b_{n,tr}^{I\dagger} |0\rangle$ is physical, while the state $b_{n,rs}^{I\dagger} a_{n,st}^{I\dagger} d_{n,tr}^{I\dagger} |0\rangle$ is unphysical. This statement is almost obvious when one recalls what each creation operator does.

We should however note that a true physical state be summed over all the transverse sites since we have discrete translational symmetry in the transverse direction. That is, for example, the states $d_{11,rs}^{I\dagger} a_{11,rs}^{I\dagger} |0\rangle$ and $d_{12,rs}^{I\dagger} a_{12,rs}^{I\dagger} |0\rangle$ are the same up to a phase factor given by $\exp(iP^2 a)$. We set the phase factor to one since we take physical states to have $P^1 = P^2 = 0$. The physical state $|phys\ 1\rangle$ is in fact $\sum_{i,j=1}^{N_{sites}} d_{ij,rs}^{I\dagger} a_{ij,rs}^{I\dagger} |0\rangle$ with the appropriate normalization constant. From a computational point of view

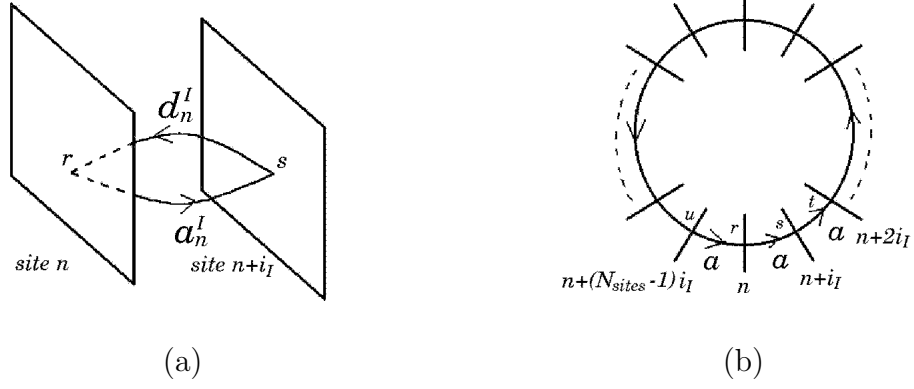


Figure 6.1: (a) The color charge for the state $|phys\ 1\rangle \equiv d_{n,r s}^{I\dagger} a_{n,sr}^{I\dagger} |0\rangle$. The planes represent the color space. $a_n^{I\dagger}$ carries color r at site n to s at site $n + i_I$ and $d_n^{I\dagger}$ carries it back to r at site n . (b) The color charge for the state $|phys\ 2\rangle \equiv a_{n+(N_{sites}-1)i_I,ru}^{I\dagger} \cdots a_{n+i_I,ts}^{I\dagger} a_{n,sr}^{I\dagger} |0\rangle$. The lines which intersect a circle represent the color planes at sites. The color goes all the way around the transverse lattice.

this leads to a great simplification in the large N_c limit. Because as shown in Sec. 6.7 it turns out that in the large N_c limit we can drop the site index n from the expression of the supercharges and thus can practically set $N_{sites} = 1$ for our calculation. This is in some sense the manifestation of the Eguchi-Kawai reduction [71]. Eguchi-Kawai reduction tells us in the usual lattice theory that the large N_c limit allows us to work with only one site in each of the space-time directions in Euclidean space. However, the way we justify this reduction in our transverse lattice formulation is quite different from the way Eguchi and Kawai do in the usual lattice formulation. Therefore, we believe that we do not have to introduce quenching [80] or twisted [81] lattices to overcome the problem that the naive Eguchi-Kawai reduction comes across at weak couplings [80]. See Sec. 6.7 for more detailed support for this claim.

Periodic conditions on the fields allow for physical states of the form $|phys\ 2\rangle \equiv \sum_n a_{n+(N_{sites}-1)i_I,ru}^{I\dagger} \cdots a_{n+i_I,ts}^{I\dagger} a_{n,sr}^{I\dagger} |0\rangle$. The color for this state is carried around the

transverse lattice, as shown in Fig. 6.1b. We will refer to these states as cyclic states. The states where the color flux does not go all the way around the transverse lattice we will refer to as non-cyclic states. We characterize states by what we call the winding number defined by $W_I = n_I/N_{sites}$, where $n_I \equiv \sum_n (a_n^{I\dagger} a_n^I - d_n^{I\dagger} d_n^I)$. For $N_{sites} = 1$, the winding number W_I simply gives us the excess number of $a^{I\dagger}$ over $d^{I\dagger}$ in a state. We use the winding number to classify states since the winding number is a good quantum number commuting with P_{SDLCQ}^- as we will see in the next section. In the language of the winding number the non-cyclic states are those states with $W_I = 0$ and cyclic states have non-zero W_I .

6.3 SDLCQ of the transverse lattice model

The transverse lattice formulation of $\mathcal{N} = 1$ SYM theory in 3+1 dimension presented in the previous section has several undesirable features. First and foremost the naive Lagrangian suffers from the fermion species doubling problem [77]. Second, the supersymmetric structure of the theory is completely hidden. Lastly, the resulting Hamiltonian is 6^{th} order in the dynamical fields. From the numerical point of view a 6^{th} order interaction makes the theory considerably more difficult to solve. In Ref. [62] we found that the (2+1)-dimensional supersymmetric Hamiltonian is only 4^{th} order making this discrete formulation of the theory very different. Unfortunately, it seems this is not the case for 3+1 dimensional model. Instead we seem to have supersymmetric Hamiltonian of 8^{th} order in fields. However, since this SDLCQ Hamiltonian is free from the doubling problem [77] and since the supercharge Q_α^- , where $\alpha = 1, 2$, is of 5^{th} order and it is this Q_α^- that we make use of for our calculations, we think

that this SDLCQ formulation is still more advantageous than the naive DLCQ formulation. There can, of course, be many discrete formulations that correspond to the same continuum theory and it is therefore desirable to search for a better one.

In the spirit of SDLCQ we will attempt a discrete formulation based on the underlying super-algebra of this theory,

$$\{Q_\alpha^\pm, Q_\beta^\pm\} = 2\sqrt{2}P^\pm\delta_{\alpha\beta}, \quad \{Q_\alpha^+, Q_\beta^-\} = 0, \quad (6.14)$$

where $\alpha, \beta = 1, 2$ and the supercharge Q is given by

$$Q \equiv \sum_n \int dx^- j_n^+ \equiv \begin{pmatrix} Q_1^+ \\ Q_2^+ \\ Q_1^- \\ Q_2^- \end{pmatrix}$$

with j_n^μ being the supercurrent at the site $n = (i, j)$, which is a Majorana spinor. For the derivation of the super-algebra in Majorana representation Eq. (6.14), see Sec. 6.7. We've set $P^I = 0$ with $I = 1, 2$ since we're considering the physical states only with $P^I = 0$. Note that this choice of P^I has made Eq. (6.14) coincide with the $\mathcal{N}=2$ super-algebra in 1+1 dimensions also known as $\mathcal{N}=(2,2)$ super-algebra although we are considering $\mathcal{N}=1$ SYM in 3+1 dimensions.

In this effort however there are some fundamental limits to how far one can go. As we discussed in the previous section the physical states of this theory must conserve the color charge at every point on the transverse lattice. Experience with other supersymmetric theories indicates that each term in Q_α^+ has to be either the product of *one* M_n and *one* ψ_n or of *one* M_n^\dagger and *one* ψ_n therefore Q_α^+ is *unphysical*, by which we mean that Q_α^+ transforms a physical state into an unphysical one, so that $\langle phys|Q_\alpha^+|phys\rangle = 0$. While this is not a theorem, it seems very difficult to have any other structure since in light cone quantization P^+ is a kinematic operator and

therefore independent of the coupling. There appears to be *no* way to make a physical P^+ from Q_α^+ . We will use P^+ as given in Eq. (6.7) in what follows. Similarly, we are not able to generally construct physical P^I from Q_α^+ and Q_β^- . In fact P^I is unphysical in our formalism, leading to $\langle phys|P^I|phys\rangle = 0$. Formally we will work in the frame where total P^I is zero, so it would appear consistent with this result. We should note, however, that this is not totally satisfying because $P^I = 0$ was a choice and a non-zero value is equally valid and not consistent with the matrix element.

Despite these difficulties we find a physical Q_α^- which gives us $P_{SDLCQ}^- \xrightarrow{a \rightarrow 0} P_{cont}^-$. The expression for Q_α^- is

$$\begin{aligned} Q_\alpha^- &= i2^{3/4}a^2 \sum_n \int dx^- \text{tr} \left\{ \left[\frac{-i}{2ga^2} \left(M_n^I \overset{\leftrightarrow}{\partial}_- M_n^{I\dagger} + M_{n-i_I}^{I\dagger} \overset{\leftrightarrow}{\partial}_- M_{n-i_I}^I \right) - 2g\psi_{Rn}^T \psi_{Rn} \right] \right. \\ &\quad \times \left. \frac{1}{\partial_-} (\sigma_2 \psi_{Rn})_\alpha + \frac{-i}{2ga^2} (M_n^I M_{n+i_I}^J M_{n+i_I}^{I\dagger} M_n^{J\dagger} - 1) (\beta_I \beta_J \sigma_2 \psi_{Rn})_\alpha \right\} \\ &\xrightarrow{a \rightarrow 0} i2^{-1/4} \int d^3x \left\{ -2gJ^+ \frac{1}{\partial_-} (\sigma_2 \psi_R)_\alpha + F_{IJ} (\beta_I \beta_J \sigma_2 \psi_R)_\alpha \right\}, \end{aligned}$$

where $\beta_1 \equiv \sigma_1$, $\beta_2 = \sigma_3$, $gJ^+ \equiv ig[A_I, \partial_- A_I] + \partial_I \partial_- A_I + 2g\psi_R \psi_R$, and the last line is the continuum form for Q_α^- in 3+1 dimensions.

It is tedious but straightforward to check that $\{Q_1^-, Q_1^-\} \neq \{Q_2^-, Q_2^-\}$, while both $\{Q_1^-, Q_1^-\}$ and $\{Q_2^-, Q_2^-\}$ give the same correct P^- in the limit of $a \rightarrow 0$. In addition, one can show that $\{Q_1^-, Q_2^-\} \neq 0$ in the discrete form but becomes zero as $a \rightarrow 0$. This means that we preserve *only one* supersymmetry algebra, say $\{Q_1^-, Q_1^-\} = P^-$, in our discrete formalism. We cannot use both Q_1^- and Q_2^- at the same time to construct physical states since they do not commute with each other. However, both Q_1^- and Q_2^- separately give us the same mass spectrum when we perform SDLCQ

calculations. Thus, it is sufficient to consider only one of the two and we take Q_1^- for our calculations in the following sessions.

Notice that Q_α^- above is fifth order and, thus, P_{SDLCQ}^- obtained from it is eighth order in fields as we mentioned at the beginning of this section. In fact we find

$$\begin{aligned}
P_{SDLCQ}^- &\equiv \frac{\{Q_1^-, Q_1^-\}}{2\sqrt{2}} \\
&= a^2 \sum_n \int dx \text{tr} \left\{ -\frac{g^2}{2} \frac{i}{2g^2 a^2} \left[\left(M_n^I \overleftrightarrow{\partial} M_n^{I\dagger} + M_{n-i_I}^{I\dagger} \overleftrightarrow{\partial} M_{n-i_I}^I \right) + 2u_n^\alpha u_n^\alpha \right] \right. \\
&\quad \times \frac{1}{\partial^2} \frac{i}{2g^2 a^2} \left[\left(M_n^I \overleftrightarrow{\partial} M_n^{I\dagger} + M_{n-i_I}^{I\dagger} \overleftrightarrow{\partial} M_{n-i_I}^I \right) + 2u_n^\alpha u_n^\alpha \right] \\
&\quad - \frac{i}{2a^2} (u_{n+i_I}^2 M_n^{I\dagger} - M_n^{I\dagger} u_n^2) \partial^{-1} (M_n^I u_{n+i_I}^2 - u_n^2 M_n^I) + \frac{i}{2a^2} \left\{ \right. \\
&\quad (u_{n+i_1+i_2}^2 M_{n+i_2}^{1\dagger} - M_{n+i_2}^{1\dagger} u_{n+i_2}^2) \partial^{-1} (M_n^{2\dagger} u_n^1 M_n^1 M_{n+i_1}^2 - u_{n+i_2}^1 M_{n+i_2}^2 M_{n+2i_2}^1 M_{n+i_1+i_2}^{2\dagger}) \\
&\quad + (u_{n+i_2}^2 M_n^{2\dagger} - M_n^{2\dagger} u_n^2) \partial^{-1} (u_n^1 M_n^1 M_{n+i_1}^2 M_{n+i_2}^{1\dagger} - M_{n-i_1}^{1\dagger} u_{n-i_1}^1 M_{n-i_1}^2 M_{n-i_1+i_2}^1) \\
&\quad + (u_{n+i_1}^2 M_{n+i_1}^2 - M_{n+i_1}^2 u_{n+i_1+i_2}^2) \partial^{-1} (M_{n+i_2}^{1\dagger} M_n^{2\dagger} u_n^1 M_n^1 - M_{n+i_1+i_2}^1 M_{n+2i_1}^{2\dagger} M_{n+i_1}^{1\dagger} u_{n+i_1}^1) \\
&\quad + (u_n^2 M_n^1 - M_n^1 u_{n+i_1}^2) \partial^{-1} (M_{n+i_1}^2 M_{n+i_2}^{1\dagger} M_n^{2\dagger} u_n^1 - M_{n+i_1-i_2}^{2\dagger} M_{n-i_2}^{1\dagger} u_{n-i_2}^1 M_{n-i_2}^2) \left. \right\} \\
&\quad - \frac{i}{4a^2} \left\{ (M_{n+i_1}^2 M_{n+i_2}^{1\dagger} M_n^{2\dagger} u_n^1 - M_{n+i_1-i_2}^{2\dagger} M_{n-i_2}^{1\dagger} u_{n-i_2}^1 M_{n-i_2}^2) \right. \\
&\quad \times \partial^{-1} (u_n^1 M_n^2 M_{n+i_2}^1 M_{n+i_1}^{2\dagger} - M_{n-i_2}^{2\dagger} u_{n-i_2}^1 M_{n-i_2}^1 M_{n+i_1-i_2}^2) \\
&\quad + (M_n^{2\dagger} u_n^1 M_n^1 M_{n+i_1}^2 - u_{n+i_2}^1 M_{n+i_2}^2 M_{n+2i_2}^1 M_{n+i_1+i_2}^{2\dagger}) \\
&\quad \times \partial^{-1} (M_{n+i_1}^{2\dagger} M_n^{1\dagger} u_n^1 M_n^2 - M_{n+i_1+i_2}^2 M_{n+2i_2}^{1\dagger} M_{n+i_2}^{2\dagger} u_{n+i_2}^1) \\
&\quad + (M_{n+i_2}^{1\dagger} M_n^{2\dagger} u_n^1 M_n^1 - M_{n+i_1+i_2}^1 M_{n+2i_1}^{2\dagger} M_{n+i_1}^{1\dagger} u_{n+i_1}^1) \\
&\quad \times \partial^{-1} (M_n^{1\dagger} u_n^1 M_n^2 M_{n+i_2}^1 - u_{n+i_1}^1 M_{n+i_1}^1 M_{n+2i_1}^2 M_{n+i_1+i_2}^{1\dagger}) \\
&\quad + (u_n^1 M_n^1 M_{n+i_1}^2 M_{n+i_2}^{1\dagger} - M_{n-i_1}^{1\dagger} u_{n-i_1}^1 M_{n-i_1}^2 M_{n-i_1+i_2}^1) \\
&\quad \times \partial^{-1} (M_{n+i_2}^1 M_{n+i_1}^{2\dagger} M_n^{1\dagger} u_n^1 - M_{n-i_1+i_2}^{1\dagger} M_{n-i_1}^{2\dagger} u_{n-i_1}^1 M_{n-i_1}^1) \left. \right\} \\
&\quad + \frac{-1}{8a^2} (M_n^1 M_{n+i_1}^2 M_{n+i_2}^{1\dagger} M_n^{2\dagger} - M_n^2 M_{n+i_2}^1 M_{n+i_1}^{2\dagger} M_n^{1\dagger})^2 \left. \right\}.
\end{aligned}$$

One can show that by setting $g = 0$ and $M, M^\dagger = 1$ this P_{SDLCQ}^- gives rise to a dispersion relation

$$k^- = \frac{1}{2k^+} \left[\left(\frac{\sin \frac{k^1 a}{2}}{a/2} \right)^2 + \left(\frac{\sin \frac{k^2 a}{2}}{a/2} \right)^2 \right],$$

which is free from the fermion species doubling problem [77]. Furthermore, one can check that this Q^- commutes with P^+ obtained from \mathcal{L} ; $[Q^-, P^+] = 0$. Thus, it follows that,

$$\langle phys|[Q^-, M^2]|phys\rangle = \langle phys|[Q^-, 2P^+ P_{SDLCQ}^-]|phys\rangle = 0 \quad (6.15)$$

in our SDLCQ formalism, where $M^2 \equiv 2P^+ P_{SDLCQ}^- - (P^1)^2 - (P^2)^2$. The fact that the Hamiltonian is the square of a supercharge will guarantee the usual supersymmetric degeneracy of the massive spectrum, and our numerical solutions will substantiate this. Unfortunately one needs a Q^+ to guarantee the degeneracy of the massless bound states.

Recalling that we set $N_{sites} = 1$ in both transverse directions and that we are in the large- N_c limit, we can write Q_1^- as

$$Q_1^- = \mathcal{Q}_{11}^- + \mathcal{Q}_{12}^- + \mathcal{Q}_{13}^-,$$

where

$$\begin{aligned} \mathcal{Q}_{11}^- &= -\frac{i2^{-1/4}a^2g}{\sqrt{\pi}} \int_0^\infty dk_1 dk_2 dk_3 \delta(k_1 + k_2 - k_3) \\ &\times \left[\frac{k_2 - k_1}{k_3 \sqrt{k_1 k_2}} (-b^{2\dagger} d^I a^I + d^{I\dagger} a^{I\dagger} b^2 - b^{2\dagger} a^I d^I + a^{I\dagger} d^{I\dagger} b^2) \right. \\ &+ \frac{k_2 + k_3}{k_1 \sqrt{k_2 k_3}} (-d^{I\dagger} b^2 d^I + b^{2\dagger} d^{I\dagger} d^I - a^{I\dagger} b^2 a^I + b^{2\dagger} a^{I\dagger} a^I) \\ &+ \frac{k_3 + k_1}{k_2 \sqrt{k_3 k_1}} (a^{I\dagger} a^I b^2 - a^{I\dagger} b^{2\dagger} a^I + d^{I\dagger} d^I b^2 - d^{I\dagger} b^{2\dagger} d^I) \\ &\left. + \left(\frac{1}{k_1} + \frac{1}{k_2} - \frac{1}{k_3} \right) (b^{2\dagger} b^{2\dagger} b^2 + b^{2\dagger} b^2 b^2) \right], \end{aligned} \quad (6.16)$$

$$\mathcal{Q}_{12}^- = -\frac{i2^{-1/4}a^2g}{\sqrt{\pi}} \int_0^\infty dk_1 dk_2 dk_3 \delta(k_1 + k_2 - k_3) \times \left[\frac{-1}{k_3} (b^{2\dagger} b^1 b^1 + b^{1\dagger} b^{1\dagger} b^2) + \frac{1}{k_1} (b^{1\dagger} b^2 b^1 + b^{2\dagger} b^{1\dagger} b^1) + \frac{1}{k_2} (b^{1\dagger} b^{2\dagger} b^1 + b^{1\dagger} b^1 b^2) \right], \quad (6.17)$$

$$\begin{aligned} \mathcal{Q}_{13}^- = & -\frac{i2^{-1/4}a^2g}{\sqrt{\pi}} \frac{a^2g^2}{4\pi} \int_0^\infty dk_1 dk_2 dk_3 dk_4 dk_5 \left\{ \delta(k_1 + k_2 + k_3 + k_4 - k_5) \left[\right. \right. \\ & \frac{1}{\sqrt{k_1 k_2 k_3 k_4}} (b^{1\dagger} d^1 d^2 a^1 a^2 + d^{2\dagger} d^{1\dagger} a^{2\dagger} a^{1\dagger} b^1 - b^{1\dagger} d^2 d^1 a^2 a^1 - d^{1\dagger} d^{2\dagger} a^{1\dagger} a^{2\dagger} b^1) \\ & + \frac{1}{\sqrt{k_2 k_3 k_4 k_5}} (d^{2\dagger} b^1 d^1 d^2 a^1 + b^{1\dagger} d^{2\dagger} d^{1\dagger} a^{2\dagger} d^1 - d^{1\dagger} b^1 d^2 d^1 a^2 - b^{1\dagger} d^{1\dagger} d^{2\dagger} a^{1\dagger} d^2) \\ & + \frac{1}{\sqrt{k_3 k_4 k_5 k_1}} (d^{1\dagger} a^2 b^1 d^1 d^2 + a^{1\dagger} b^{1\dagger} d^{2\dagger} d^{1\dagger} d^2 - d^{2\dagger} a^1 b^1 d^2 d^1 - a^{2\dagger} b^{1\dagger} d^{1\dagger} d^{2\dagger} d^1) \\ & + \frac{1}{\sqrt{k_4 k_5 k_1 k_2}} (a^{2\dagger} a^1 a^2 b^1 d^1 + a^{2\dagger} a^{1\dagger} b^{1\dagger} d^{2\dagger} a^1 - a^{1\dagger} a^2 a^1 b^1 d^2 - a^{1\dagger} a^{2\dagger} b^{1\dagger} d^{1\dagger} a^2) \\ & \left. \left. + \frac{1}{\sqrt{k_5 k_1 k_2 k_3}} (a^{1\dagger} d^2 a^1 a^2 b^1 + d^{1\dagger} a^{2\dagger} a^{1\dagger} b^{1\dagger} a^2 - a^{2\dagger} d^1 a^2 a^1 b^1 - d^{2\dagger} a^{1\dagger} a^{2\dagger} b^{1\dagger} a^1) \right] \right. \\ & + \delta(k_1 + k_2 + k_3 - k_4 - k_5) \\ & \times \left[\frac{1}{\sqrt{k_1 k_2 k_3 k_4}} (d^{1\dagger} a^{2\dagger} a^{1\dagger} a^2 b^1 + a^{1\dagger} b^{1\dagger} d^2 a^1 a^2 - d^{2\dagger} a^{1\dagger} a^{2\dagger} a^1 b^1 - a^{2\dagger} b^{1\dagger} d^1 a^2 a^1) \right. \\ & + \frac{1}{\sqrt{k_2 k_3 k_4 k_5}} (b^{1\dagger} d^{2\dagger} d^{1\dagger} d^1 d^2 + d^{2\dagger} d^{1\dagger} b^1 d^1 d^2 - b^{1\dagger} d^{1\dagger} d^{2\dagger} d^2 d^1 - d^{1\dagger} d^{2\dagger} b^1 d^2 d^1) \\ & + \frac{1}{\sqrt{k_3 k_4 k_5 k_1}} (a^{1\dagger} b^{1\dagger} d^{2\dagger} d^2 a^1 + d^{1\dagger} a^{2\dagger} a^2 b^1 d^1 - a^{2\dagger} b^{1\dagger} d^{1\dagger} d^1 a^2 - d^{2\dagger} a^{1\dagger} a^1 b^1 d^2) \\ & + \frac{1}{\sqrt{k_4 k_5 k_1 k_2}} (a^{2\dagger} a^{1\dagger} b^{1\dagger} a^1 a^2 + a^{2\dagger} a^{1\dagger} a^1 a^2 b^1 - a^{1\dagger} a^{2\dagger} b^{1\dagger} a^2 a^1 - a^{1\dagger} a^{2\dagger} a^2 a^1 b^1) \\ & \left. \left. + \frac{1}{\sqrt{k_5 k_1 k_2 k_3}} (d^{2\dagger} d^{1\dagger} a^{2\dagger} b^1 d^1 + b^{1\dagger} d^{2\dagger} d^1 d^2 a^1 - d^{1\dagger} d^{2\dagger} a^{1\dagger} b^1 d^2 - b^{1\dagger} d^{1\dagger} d^2 d^1 a^2) \right] \right\}, \quad (6.18) \end{aligned}$$

with $k^+ \equiv k$, $a_1 \equiv a(k_1)$,

$$a^\dagger a a \equiv \text{tr}(a_3^\dagger a_1 a_2), \quad a^\dagger a^\dagger a \equiv \text{tr}(a_1^\dagger a_2^\dagger a_3), \quad a^\dagger a a a a \equiv \text{tr}(a_5^\dagger a_1 a_2 a_3 a_4),$$

$$a^\dagger a^\dagger a^\dagger a^\dagger a \equiv \text{tr}(a_1^\dagger a_2^\dagger a_3^\dagger a_4^\dagger a_5), \quad a^\dagger a^\dagger a^\dagger a a \equiv \text{tr}(a_1^\dagger a_2^\dagger a_3^\dagger a_4 a_5), \quad a^\dagger a^\dagger a a a \equiv \text{tr}(a_4^\dagger a_5^\dagger a_1 a_2 a_3).$$

\mathcal{Q}_{11} is the part of \mathcal{Q}_1^- which looks exactly like Q^- in 2+1 dimensional model with the difference being that here we have two types for each of the bosonic fields a and d .

\mathcal{Q}_{12} is a new piece in 3+1 dimensions and mixes two different types of fermionic fields.

\mathcal{Q}_{13} is also new and composed of fields of fifth order. Note that for small couplings, \mathcal{Q}_{11} and \mathcal{Q}_{12} dominate over \mathcal{Q}_{13} , while \mathcal{Q}_{13} dominates in the strong coupling regime. Notice that from this explicit expression for Q_1^- it is clear that the winding number introduced in the last section evidently commutes with Q_1^- and, thus, with P_{SDLCQ}^- . Therefore, cyclic states do not mix with non-cyclic states.

It is always important to look for symmetries of Q^- since the symmetries, if any, will reduce the amount of the computational efforts considerably. To do this, let us consider three cases separately: (i) the intermediate coupling where we have all the three pieces together for Q_1^- ; (ii) the weak coupling limit where we can ignore \mathcal{Q}_{13} ; (iii) the strong coupling limit where we consider \mathcal{Q}_{13} only. For the first case (i) we find two Z_2 symmetries,

- $a_{ij}^1 \leftrightarrow -a_{ij}^2, d_{ij}^1 \leftrightarrow -d_{ij}^2, b_{ij}^1 \leftrightarrow -b_{ij}^1, b^2$ unchanged,
- $a_{ij}^I \leftrightarrow -a_{ji}^I, b_{ij}^\alpha \leftrightarrow -b_{ji}^\alpha$.

The first symmetry implies that states with the winding numbers, say (W_1, W_2) , are equivalent to those with (W_2, W_1) up to the minus sign. On the other hand the second symmetry implies that states with (W_1, W_2) are equivalent to those with $(-W_1, -W_2)$ up to the minus sign.

In the case of the weak coupling limit (ii), we find two more independent Z_2 symmetries;

- $a_{ij}^I \leftrightarrow -a_{ji}^I, d_{ij}^I \leftrightarrow -d_{ji}^I, b_{ij}^\alpha \leftrightarrow -b_{ji}^\alpha$.
- $a_{ij}^1 \leftrightarrow -d_{ji}^1, a_{ij}^2 \leftrightarrow -a_{ji}^2, d_{ij}^2 \leftrightarrow -d_{ji}^2, b_{ij}^\alpha \leftrightarrow -b_{ji}^\alpha$.

The second of these implies, with the help of the second Z_2 symmetry we found in the case of (i), the equivalence of states under $(W_1, W_2) \leftrightarrow (-W_1, W_2) \leftrightarrow (W_1, -W_2)$.

In the strong coupling limit (iii), we do not have any other Z_2 symmetries besides the two we found in the case of (i). However, it is easy to see that Q_{13} commutes with $b^{2\dagger}b^2$, thus the number of $b^{2\dagger}$'s is a good quantum number as well as the two winding numbers.

It is interesting to see what we can find for each of the three different cases (i), (ii) and (iii). However, in this our first attempt to formulate $\mathcal{N} = (2, 2)$ SYM in 3+1 dimensions with SDLCQ on a two dimensional transverse lattice, we constrain ourselves to consider only the most generic case (i) where we have all the three pieces together for Q^- .

Now we are in a position to solve the eigenvalue problem $2P^+P_{SDLCQ}^-|phys\rangle = m^2|phys\rangle$. We impose the periodicity condition on M_n^I , $M_n^{I\dagger}$ and u_n^α in the x^- direction giving a discrete spectrum for k^+ , and ignore the zero-mode:

$$k^+ = \frac{\pi}{L}n \quad (n = 1, 2, \dots), \quad \int_0^\infty dk^+ \rightarrow \frac{\pi}{L} \sum_{n=1}^\infty.$$

We impose a cut-off on the total longitudinal momentum P^+ i.e. $P^+ = \pi K/L$, where K is an integer also known as the ‘harmonic resolution’, which indicates the coarseness of our numerical results. For a fixed P^+ i.e. a fixed K , the number of partons in a state is limited up to the maximum, that is K , so that the total number of Fock states is *finite*, and, therefore, we have reduced the infinite dimensional eigenvalue problem to a finite dimensional one.

For this initial study of the transverse lattice we consider resolution up to $K = 8$ for non-cyclic ($W_1 = W_2 = 0$) states and up to $K = W_I + 6$ and $K = W_I + 5$ for states with $|W_I| = 1$ and $|W_I| = 2, 3, 4, 5$, respectively. We were able to handle these calculations with our SDLCQ Mathematica code and C++ code.

6.4 Coupling dependence of the mass spectrum

In this section we will discuss the mass spectrum as a function of $g' \equiv g\sqrt{N_c}$ for $K = 4, 5, 6$.

It is instructive to see the dependence of m^2 on the coupling since we have terms in Q^- that go like g' and g'^3 . In Fig. 6.2 we show the entire mass spectrum of non-cyclic states in units of $g'^2/\pi a^2$ for $K = 4, 5, 6$ as a function of g' in a log-log plot. In order to see the crossings in more detail we show Fig. 6.2(b), (d), and (f) on a different scale from (a), (c) and (e), respectively. We've set 10^{-8} or less to the numerical zero in our code.

As one can see from Fig. 6.2, there is a rich structure in the mass spectrum as a function of g' , and the origin of this structure for the case where $K = 4$ in Fig. 6.2(a) and (b) is rather easy to understand. We find four types of states; (i) those states which are killed by Q_{13} and whose m^2 in units of $\frac{g'^2}{\pi a^2}$ are independent of g' ; (ii) those states which vanish upon the action of $Q_{11} + Q_{12}$ and thus whose m^2 in units of $\frac{g'^2}{\pi a^2}$ go like g'^4 ; (iii) those states which survive upon the action of $Q_{11} + Q_{12}$ and of Q_{13} independently and whose m^2 in units of $\frac{g'^2}{\pi a^2}$ go like $(A + Bg'^2)^2$, where A, B are some constants; (iv) those massless states which become zero upon the action of $Q_{11} + Q_{12} + Q_{13}$. From Fig. 6.2(a) and (b) it is easy to identify one state each for the second and third type because m^2 of a state of the second type go like g'^4 , giving rise to a straight line with a non-zero slope for all g' in the log-log plot, while m^2 for the third type is $(A + Bg'^2)^2$, leading to some flat, constant line at small g' and a (inclined) straight line at large g' . We should note that for the second kind one should take into account the level crossing. The rest of the states clearly fall into either the first kind or the fourth kind. States of the first type yield g' -independent

m^2 , thus, a flat line in the log-log plot, while states of the fourth type are massless represented by the “dots” below the line of $\log_{10} m^2 = -8$ since the numerical zero is set to 10^{-8} in our code.

This discussion does not however seem to explain the dependence on g' of the mass spectrum with $K = 5, 6$. To get the full understanding of the behavior, we made a toy model. In this model we have a 2×2 matrix R for the boson sector of Q^- given by

$$R = \begin{pmatrix} b_1 + c_1 g'^2 & b_2 + c_2 g'^2 \\ b_3 + c_3 g'^2 & b_4 + c_4 g'^2 \end{pmatrix},$$

where b_i with $i = 1, 2, 3, 4$ is equal to either 0 or 1 and c_i is equal to either 0 or $1/4\pi$. Here one should notice that we've factored out g' from R or Q^- , and therefore g'^2 from P^- . The Q^- for this toy model is thus given by

$$Q^-/g' = \begin{pmatrix} 0 & R \\ R^T & 0 \end{pmatrix},$$

where T stands for the transpose. Thus, the matrix to diagonalize is

$$(Q^-/g')^2 = \begin{pmatrix} RR^T & 0 \\ 0 & R^T R \end{pmatrix},$$

or equivalently RR^T . Among the $2^8 = 256$ possible forms for Q^- , we found sets of parameters that lead to a level crossing, and non-trivial behaviors in the mass spectrum. Some of those non-trivial ones look the same as some of those in Fig. 6.2, while there are others which do not look like any of those in Fig. 6.2. For example see Fig. 6.3, where Fig. 6.3(a) and (b) are the ones that we can see in the actual spectrum in Fig. 6.2, while 6.3(c) and (d) are not. The sets of parameters we used are given in Table 6.1. Of course there are ones which are seen in Fig. 6.2, but cannot be found in our toy model. However, it is very likely that as we increase the size of the matrix

R of our toy model, we would be able to identify those not-yet-seen behaviors in our toy model as well.

	b_1	c_1	b_2	c_2	b_3	c_3	b_4	c_4
Fig. 6.3(a)	0	$1/4\pi$	0	$1/4\pi$	1	0	0	0
Fig. 6.3(b)	0	0	1	$1/4\pi$	1	$1/4\pi$	0	$1/4\pi$
Fig. 6.3(c)	0	0	1	0	1	0	0	$1/4\pi$
Fig. 6.3(d)	0	$1/4\pi$	1	0	1	0	0	$1/4\pi$

Table 6.1: Parameter sets used for our toy model to get each of the spectra in Fig. 6.3.

Using this toy model, we can study wavefunction dependence on the coupling g' . As the simplest example, consider the case of the level crossing shown in Fig. 6.3(a). In this case we can think of a bound state $|m^2\rangle$ as a linear combination of two different states,

$$|m^2\rangle = f(g')|1\rangle + h(g')|2\rangle,$$

where $f(g')$ and $h(g')$ are wavefunctions, which depend on g' . $|1\rangle$ is a state of the first type of the four we considered above and responsible for the constant behavior of the mass spectrum and $|2\rangle$ is a state of the second type responsible for the g'^4 -behavior. In Fig. 6.3(a) the higher energy state stays constant for small g' , where $f(g') \gg h(g')$, and goes like g'^4 for large g' , where $h(g') \gg f(g')$. The opposite behavior of the wavefunctions is true for the lower energy state. That is, the lower energy state goes like g'^4 for small g' , where $h(g') \gg f(g')$, and stays flat for large g' , with $f(g') \gg h(g')$. This observation implies that for more general cases a bound state is a linear combination of states of the four types associated with g' -dependent

wavefunctions, and it is the non-trivial g' -dependence of the wavefunctions that gives rise to such a rich, complicated spectrum in Fig. 6.2.

We expect that the structure of the mass spectrum as a function of g' will persist for the cyclic states and in fact we have numerically confirmed the similar structure for them as well.

Note that since the dominant structure of a bound state changes as one changes g' , there is some sort of “transition” as one goes from weak coupling to strong coupling. It is of great interest to see if the winding number dependence of the mass spectrum varies due to this transition. We are not able to identify any states in strong coupling regime because of the rich and complicated behavior of the spectrum although we are able to find some states in the intermediate region where $g' = 1$.

We discuss the mass spectrum of the cyclic states as a function of the winding number and the resolution with $g' = 1$ in more detail in the next section. The discussion of the mass spectrum of the non-cyclic states is in the following section.

6.5 Numerical results for the cyclic ($W_I \neq 0$) bound states

In principle we can study the case where both of the winding numbers are non-zero and the case where one of them equals zero. However, the size of the Fock basis is much larger for the former case than for the latter. This means that we can reach a higher resolution for the latter case. Thus, in order to get enough data to analyze for our first attempt we restrict ourselves to the case where we set one of the winding numbers to zero. Since we have two Z_2 symmetries, $(W_1, W_2) \leftrightarrow (W_2, W_1)$ and $(W_1, W_2) \leftrightarrow (-W_1, -W_2)$, we can set $W_2 = 0$ without loss of generality and consider only positive W_1 when studying the winding number dependence of the bound states.

As guaranteed by the super-algebra, we find numerically a degeneracy in the mass spectrum between massive fermionic and bosonic states. However, this supersymmetry is broken for the massless states since we do not preserve the entire set of supersymmetry algebra. In this section we only consider the massive bound states, and therefore it suffices to consider only bosonic states.

In Fig. 6.4(a), (b), (c), and (d) we give plots of m^2 with $g' = 1$ for four low-energy bound states as a function of $1/(K - W_1)$ and extrapolate m_∞^2 in the $(K - W_1) \rightarrow \infty$ limit using a linear fit $b + c/(K - W_1)$ for (a) through (c) and a quadratic fit $b + c/(K - W_1) + d/(K - W_1)^2$ for (d), where b, c, d are fitting parameters. We identify a bound state with different K 's from the properties of the bound state, such as the averaged number of partons of a particular type etc. We present here four bound states we could easily identify. The dominant fock component of the bound state in (a) and (c) has the form $b^{1\dagger}a^{1\dagger} \dots a^{1\dagger}b^{1\dagger}$. For the bound state in (b) the dominant component is of the form $b^{1\dagger}a^{1\dagger} \dots a^{1\dagger}b^{2\dagger}$. The bound state in (d) has the dominant component of $d^{2\dagger}a^{1\dagger} \dots a^{1\dagger}a^{2\dagger}$.

In Fig. 6.5 we present m_∞^2 , obtained in Fig. 6.4(a), (b), (c), and (d), as a function of W_1 . We show a fit to the data of the form $b + cW_1^2 + d/W_1^2$ in Fig. 6.5(a) and of the form $b + c/W_1 + d/W_1^2$ in Fig. 6.5(b). As can be seen, it is difficult to say which fit is better from the graphs. The fit of the form $b + cW_1^2 + d/W_1^2$ appears a bit better.

The use of a fit of the form $b + cW_1^2 + d/W_1^2$ has a string theory justification. In the string theory the energy of a string confined in one dimension with a period L is given by the sum of its momentum mode and its winding mode, so that $E = p2\pi/L + qTL$, where p, q are integers and T is the string tension. Now if we consider our cyclic

bound states as a string confined in the x_1 -direction with $L = aW_1$, then it follows that $m^2 = b + cW_1^2 + d/W_1^2$.

We should however remind the reader that we used a fit of the form $b+c/W+d/W^2$ in Ref. [62]. There we argued that the operator has the form $Q^- = b + ck_\perp$ in 2+1 continuous theory and $m^2 \sim (Q^-)^2 = b + c/W + d/W^2$ with $k_\perp \sim 1/L \sim 1/W$. This behavior is consistent with the unique properties of SYM theories that we have seen in previous SDLCQ calculations [55, 67]. We have seen that as we increase K we uncover longer bound states that have lower masses. Supersymmetric theories like to have light bound states with long strings of gluons. We call these bound states with long strings of gluons, stringy bound states. In 3+1 dimensions with two transverse lattices we have seen the stringy bound states as well, and we have $Q^- = b + ck_1 + dk_2$, leading to the fit of the form $b + c/W_1 + d/W_1^2$ in Fig. 6.5(b) for $k_1 \sim 1/L \sim 1/W_1$ and $k_2 = 0$. Up to the numerical resolution we can correctly reach, we can not say for sure which form of m^2 describes $\mathcal{N}=(2,2)$ SYM in 3+1 dimensions. It appears that the form $b + cW_1^2 + d/W_1^2$ is preferable, suggesting that the cyclic bound states in 3+1 dimensions are more like a string with the energy of the form $E = p2\pi/L + qTL$.

6.6 Numerical results for the non-cyclic bound states ($W_I = 0$)

Let us now discuss numerical results for the non-cyclic bound states. Again we follow bound states that we can easily identify from the properties of the bound states. In Fig. 6.6 we show m^2 of three low-energy states in units of $\frac{g'^2}{\pi a^2}$ as a function of $1/K$ with $g' \equiv g\sqrt{N_c} = 1$. The state A denoted by circles is composed primarily of two bosons and two fermions, $b^{1\dagger}d^{1\dagger}a^{1\dagger}b^{1\dagger}$. The state B and C denoted by squares and diamonds are composed primarily of two fermions, $b^{1\dagger}b^{2\dagger}$ and $b^{1\dagger}b^{1\dagger}$, respectively.

	$b^{1\dagger}d^{1\dagger}a^{1\dagger}b^{1\dagger}$	$b^{1\dagger}b^{2\dagger}$	$b^{1\dagger}b^{1\dagger}$
m_∞^2	1.764	4.744	8.204

Table 6.2: Extrapolated values for m^2 in units of $\frac{g'^2}{\pi a^2}$ as $K \rightarrow \infty$ for State A, B, and C in Fig. 6.6 represented by its dominant Fock state.

We show a linear fit to the data and see good conversion as $K \rightarrow \infty$ for all the three states. The extrapolated values for m^2 in the limit of $K \rightarrow \infty$ are given in Table 6.2. We also find the stringy states for the non-cyclic states.

Recall that we found in Sec. 4 that a bound state would be a linear combination of states of the four types we enumerated in Sec. 4. Hence, it is instructive to see if we can identify the three bound states with any of the four types. For $K = 4$ we can identify all the three bound states with those that are killed by \mathcal{Q}_{13} and whose mass in units of $\frac{g'^2}{\pi a^2}$ are independent of g' . However, as K increases, we are not able to classify them into any particular type of the four. This is because as we increase K the number of states becomes very large and the mass spectrum becomes dense. It is likely that these states mix with other nearby states with the same coupling dependence, giving rise to small changes in m^2 but still the same general coupling dependence. At this time however we are not able to resolve the spectrum in an enough detail to study these effects.

6.7 Eguchi-Kawai Reduction

For our numerical calculation we've set $N_{sites} = 1$, in other words, we've dropped the site indices. This reduction of the transverse degrees of freedom has brought a great amount of simplification in our calculation and needs some detailed justification.

Since it is only the supercharges that we need to do our calculation, if the supercharges do not depend on the site indices in the large N_c limit, neither does any quantity that can be computed from Q_α^- , for instance m^2 for our case. Therefore, in order to justify the reduction of the degrees of freedom for our purposes, it suffices to show the independence of Q_α^- of the site indices in the large N_c limit. In this section, in particular, we will show that in the large N_c limit the leading order terms of the supercharges Q_α^- with keeping all the site indices are the same as those with setting $N_{sites} = 1$. We should note that this sort of arguments about the justification of the reduction on a transverse lattice have already been given in literature, for instance see Refs. [45, 64, 82, 63] and our arguments below closely parallel those in the Refs. [45, 63].

In what follows we only consider Q_1^- , however the same arguments apply equally well to Q_2^- . For definiteness let us first consider a Fock state denoted by

$$\sum_n \text{tr}[\dots d_n^{1\dagger}(k_1) a_n^{1\dagger}(k_2) b_n^{1\dagger}(k_3) a_{n-i_1}^{1\dagger}(k_4) \dots] |0\rangle,$$

where we've written $k^+ \equiv k$, $n \equiv (i, j)$ is the transverse lattice site, i_1 is the vector of length a pointing the x^1 direction, a is the lattice spacing, and the dots represent some creation operators. When we act on this state with Q_1^- , we get for example from one of the terms in Q_1^- , say $b^{2\dagger} d^1 a^1 \equiv \sum_n \text{tr}[b_n^{2\dagger}(p_1 + p_2) d_n^1(p_1) a_n^1(p_2)]$ on it

$$N_c \sum_n \text{tr}[\dots b_n^{2\dagger}(k_1 + k_2) b_n^{1\dagger}(k_3) a_{n-i_1}^{1\dagger}(k_4) \dots] |0\rangle.$$

If we set $N_{sites} = 1$, then the Fock state now becomes

$$\text{tr}[\dots d^{1\dagger}(k_1) a^{1\dagger}(k_2) b^{1\dagger}(k_3) a^{1\dagger}(k_4) \dots] |0\rangle,$$

and upon the action of Q_1^- we get from $b^{2\dagger} d^1 a^1 \equiv \text{tr}[b^{2\dagger}(p_1 + p_2) d^1(p_1) a^1(p_2)]$ on it

$$N_c \text{tr}[\dots b^{2\dagger}(k_1 + k_2) b^{1\dagger}(k_3) a^{1\dagger}(k_4) \dots] |0\rangle, \quad (6.19)$$

and one more term

$$\text{tr}[\dots b^{2\dagger}(k_1 + k_4) \dots] \text{tr}[a^{1\dagger}(k_2) b^{1\dagger}(k_3)] |0\rangle. \quad (6.20)$$

Notice that the extra term Eq. (6.20) we get by setting $N_{sites} = 1$ is down by $1/N_c$ compared to the leading order term Eq. (6.19) and thus we can ignore it in the large N_c limit. Of course, in the above example, we could and would have gotten many more terms depending on what we have in those 'dots' inside the trace of the Fock state we considered. However, it is easy to see that our conclusion remains the same; all the extra terms we get by having only one site are down by $1/N_c$ or more powers of $1/N_c$. This all comes down to the fact that we can have only single-traced states in the large N_c limit. Therefore, we find that the leading order terms of Q_α^- are the same whether we keep track of the site indices or not. Although this proof is for finite K , we suspect that the same result would persist at infinite K .

The way to justify the reduction here should be contrasted to the way exploited by Eguchi and Kawai [71]. Eguchi and Kawai showed that in the large N_c limit we can work with only one lattice site in each of the space-time directions in Euclidean space. However, the proof was based on, among others, the assumption that $U(1)^d$ symmetry is not spontaneously broken, where d is the number of the space-time dimensions. This assumption was found to be wrong for $d > 2$ at weak couplings by the authors of Ref.[80]. To resolve this problem, there have been many models proposed, for instance quenching [80] and twisted [81] lattice formulations. Here in our formulation, however, we believe that we do not have to introduce any of the modified lattice formulation since the way we justify the reduction is quite different the way Eguchi and Kawai do. Our proof stands on its own feet regardless of our maintaining the $U(1)^d$ symmetry or not and, therefore, would not suffer from the

problem associated with the naive Eguchi-Kawai reduction as we go from weak to strong couplings.

A question, however, remains. That is the question of how well we've managed to quantize the fields since all our arguments above rely on the fact that we have the quantized fields and true vacuum. Put in another way, how good the reduction procedure is depends on how good our quantization procedure is. Recall that to quantize, we had to “linearize” the unitary link variables, which leads to the breakdown of SUSY. The authors of Refs. [45, 64, 82, 63] make use of the “color-dielectric” formulation to resolve the problem for non-supersymmetric theories. Although this formulation resolves the problem completely, it prevents one from going to small lattice spacings. In our formulation we do not have that constraint on the lattice spacing. However, the price we pay is that we resolve the problem of the linearization partially, not completely. Thus, it is of great importance for one to see to what extent we've resolved the problem and, if possible and necessary, to find a way to get around it completely. Up to this point we are not able to answer this question, but this is one of the crucial steps we should take towards a more sensible supersymmetric model on a lattice within our formulation.

6.8 Discussion

We have presented the standard formulation of $\mathcal{N}=1$ SYM in 3+1 dimensions with a two spatial dimensional transverse lattice. Then we gave the SDLCQ formulation of the theory. We found that the standard formulation suffers from a fermion species doubling problem, while SDLCQ formulation does not. In the frame where the transverse momenta equal to zero, $\mathcal{N}=1$ SUSY in 3+1 dimensions is equivalent

to $\mathcal{N}=2$ SUSY in 1+1 dimensions also known as $\mathcal{N}=(2,2)$ SUSY. We were able to present Q_α^- which has the correct continuum form and yields by the SUSY algebra a discrete form of P^- , where $\alpha = 1, 2$. This P^- then coincides with its continuum form in the continuum limit. Since Q_1^- and Q_2^- don't commute with each other in our formulation, we are to use only one of them to solve the mass eigenvalue problem, preserving one exact SUSY.

We found that this Q_α^- consists of terms which are proportional to $g' \equiv g\sqrt{N_c}$ and terms which go like g'^3 . This led us to investigate in some detail the g' dependence of the mass spectrum. From a simple toy model we concluded that the rich, complicated behavior of the mass spectrum with varying g' is due to some non-trivial coupling dependence of the wavefunctions. This is also responsible for a “transition” in the structure of a bound state when going from weak coupling to strong coupling. Because the dominant structure of a bound state changes with changing g' .

We classified the bound states into two types, the cyclic and non-cyclic as we did in Ref. [62]. The cyclic bound states are those whose color flux goes all the way around in one or two of the transverse directions. The bound states whose color flux is localized and does not wind around are referred to as the non-cyclic bound states. For each type of the bound states, we were able to identify some bound states in the mass spectrum for $g' = 1$ and found the $K \rightarrow \infty$ limit of m^2 .

For the cyclic bound states we were able to present m^2 as a function of the winding number W_I in the x_I direction with $I = 1, 2$. We found two very good fits to the data. The first fit $b + cW_I^2 + d/W_I^2$ is motivated by the string theory, where the energy has the form $E = p2\pi/L + qTL$, where p, q are some integers, T is the string tension and

L is the period of the transverse lattice. The other fit $b + c/W_I + d/W_I^2$ is motivated by the operator structure of Q_α^- . It appeared that $b + cW_I^2 + d/W_I^2$ is preferable,

For the non-cyclic states as $1/K \rightarrow 0$ we saw good linear conversion of m^2 of low-energy bound states that we could identify and gave the extrapolated values for m^2 . We could identify for $K = 4$ the bound states with a state whose m^2 in units of $\frac{g'^2}{\pi a^2}$ are independent of g' though we were not able to do so for higher K 's because of the dense, and complicated spectrum.

In summary, we were able to present a formulation of SYM in 3+1 dimensions with one exact SUSY on a two dimensional transverse lattice and find the mass spectrum nonperturbatively. There remain however a number of important questions to answer. First and foremost it is of great importance to determine the form of m^2 numerically to better precision. It is interesting to see what the winding number dependence of m^2 is if both of the winding numbers are non-zero. We need to invent a method to resolve the dense spectrum at strong couplings. This will help us see if there is any “transition” in the form of m^2 as one goes from weak coupling to strong coupling. However, perhaps most importantly, as discussed in Sec. 6.7 we need to know to what extent we've resolved the problem caused by the linearization of the link variables that we needed to quantize the fields. Knowing this tells us how reliable our numerical results are. Because one of our major simplifications in numerical calculation in the large N_c limit comes about from the reduction of the transverse degrees of freedom whose justification relies upon the presence of the quantized fields and the vacuum. The restoration of SUSY for massive bound states, which has been broken by the linearization gives us some confidence that our formulation indeed provides some sensible results. However, we would still have to clarify the issue to be more certain

and confident. To this end, we need to compare our numerical results with some well-established theoretical predictions and with other numerical results obtained from the usual lattice calculation. Hence, it is of importance to apply our formulation to some other supersymmetric theories in higher than 1+1 dimensions, for instance, Wess-Zumino model, lattice sigma model, and SQED. It appears that the application is relatively straightforward. From more practical point of view, a next question to ask is what happens if one includes scalars and their superpartners in theory. We did not consider this case in here simply because this was the first attempt to formulate SYM in 3+1 dimensions with one exact SUSY on a two dimensional transverse lattice and, thus, we wanted to consider the simplest possible case. However, it is of great interest to consider the question in the future. We believe that when we are able to answer all those questions, we will also be able to test the predictions made by Armoni, Shifman and Veneziano [14, 15].

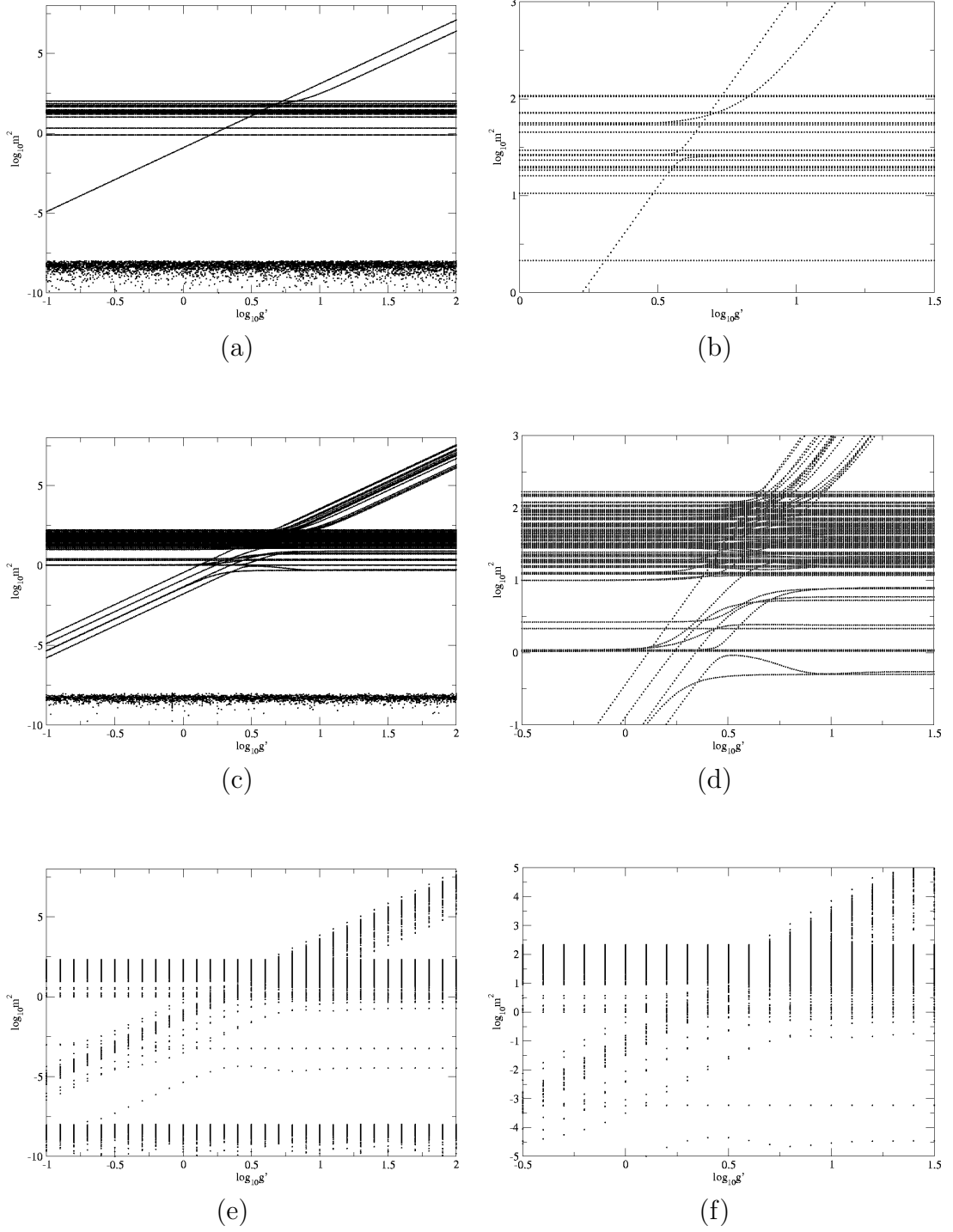


Figure 6.2: Log-log plots of the mass spectrum m^2 in units of $\frac{g'^2}{\pi a^2}$ versus $g' \equiv g\sqrt{N_c}$ with $K = 4, 5, 6$ for (a),(c),(e), respectively. (b), (d), and (f) are the same as (a), (c) and (e), respectively but on a different scale so that one can see the crossings in more detail. 10^{-8} or less is the numerical zero in our code.

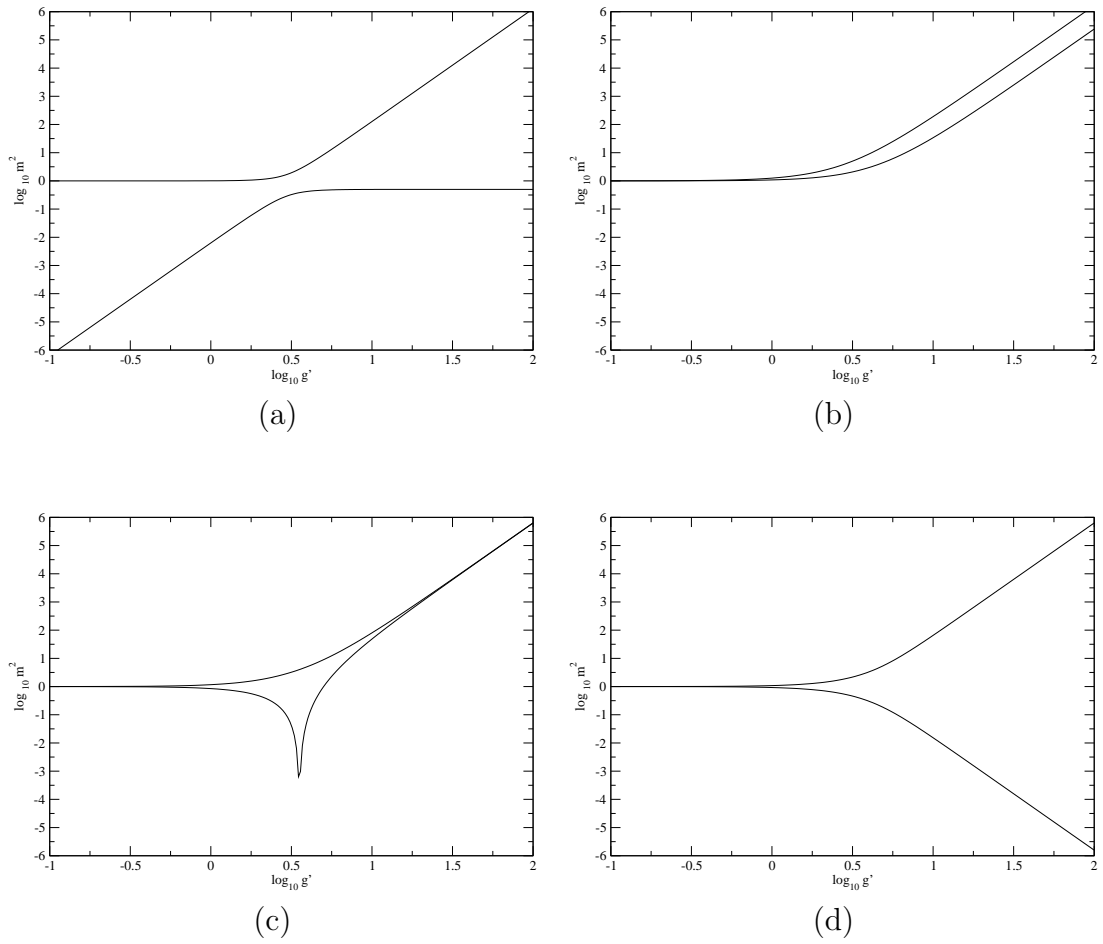


Figure 6.3: Sample spectra obtained from our toy model. (a) and (b) can be seen in the actual full spectrum in Fig. 6.2, while (c) and (d) cannot.

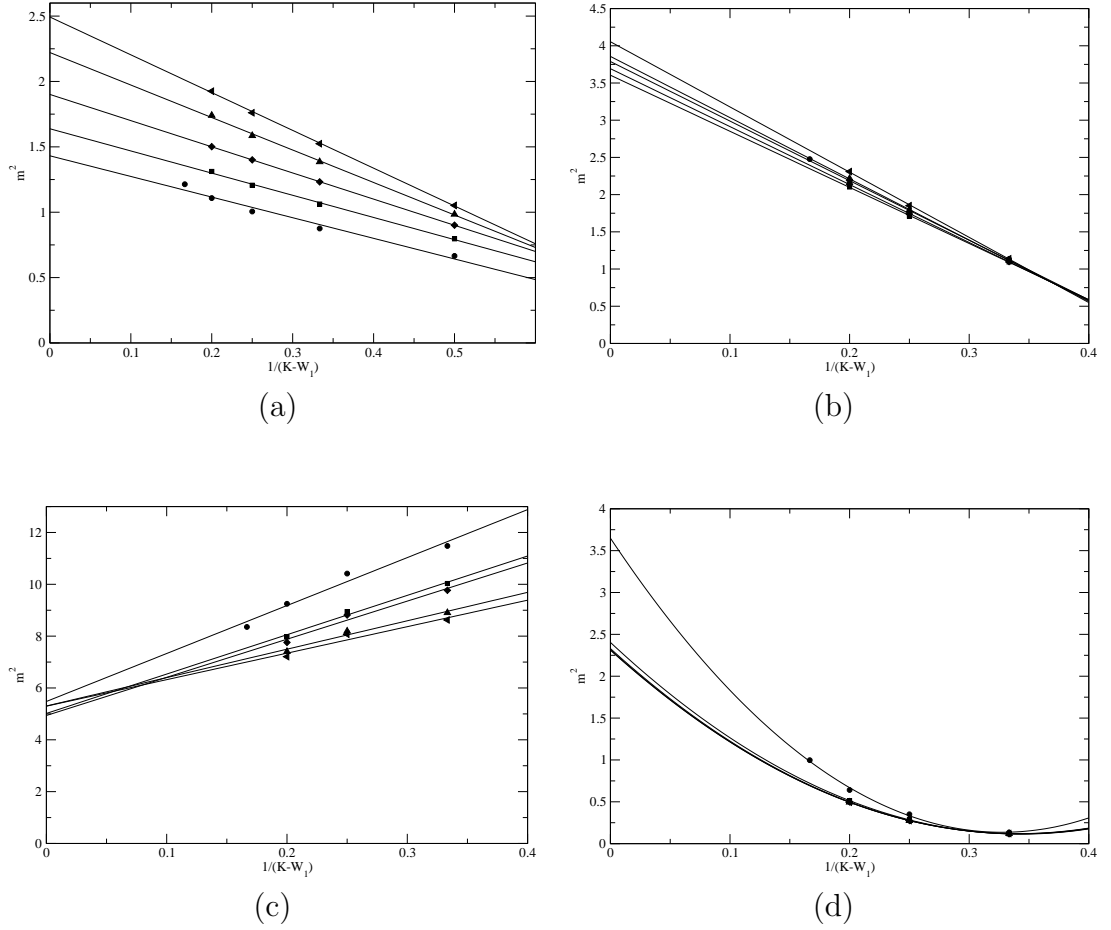


Figure 6.4: Plots of m^2 in units of $\frac{g'^2}{\pi a^2}$ of low-energy cyclic bound states versus $1/(K - W_1)$ for $W_1=1$ (circle), 2(square), 3(diamond), 4(triangle up), 5(triangle left). Also shown are a linear fit for (a), (b), and (c) and a quadratic fit for (d). The coupling $g' \equiv g\sqrt{N_c} = 1$.

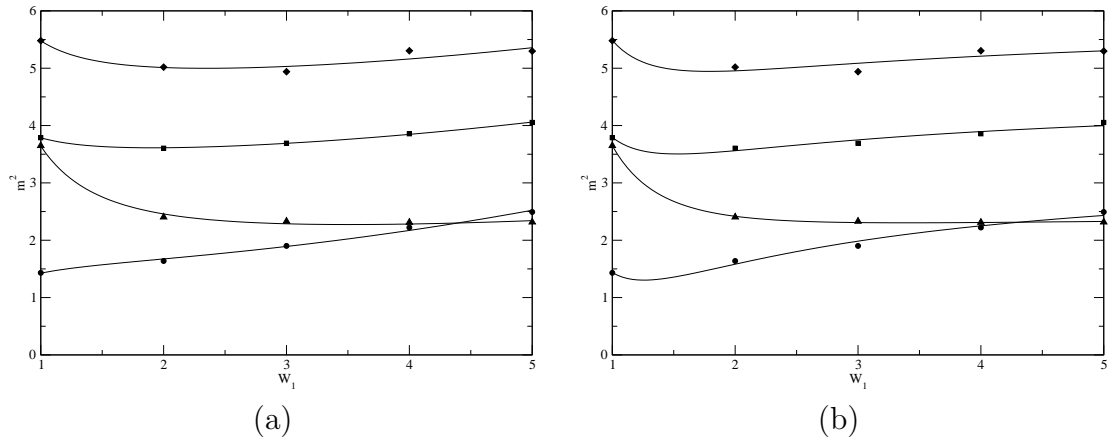


Figure 6.5: Plots of $K \rightarrow \infty$ limit of m^2 in units of $\frac{g'^2}{\pi a^2}$ of low energy cyclic bound states versus W_1 with a fit to the data of the form $b + cW_1^2 + d/W_1^2$ in (a) and of the form $b + c/W_1 + d/W_1^2$ in (b). The circles correspond to the bound state in Fig. 6.4(a), squares in 6.4(b), diamonds in 6.4(c), and triangles in 6.4(d).

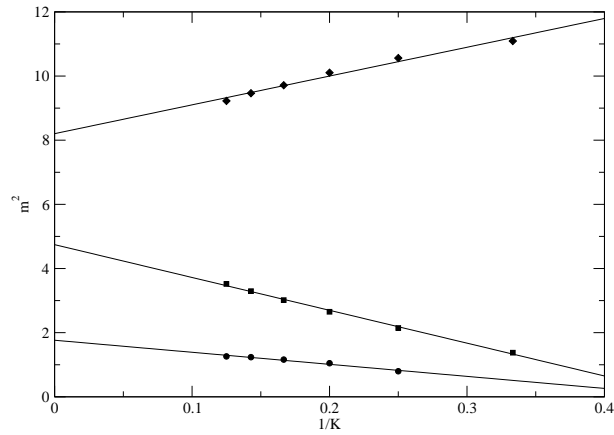


Figure 6.6: Plots of m^2 in units of $\frac{g'^2}{\pi a^2}$ of low-energy non-cyclic bound states against $1/K$ with a linear fit to the data. The coupling $g' \equiv g\sqrt{N_c} = 1$. The circles correspond to bound state A, squares to the state B, diamonds to state C

APPENDIX A

$\mathcal{N}=1$ SUPER-ALGEBRA IN MAJORANA REPRESENTATION

In this appendix we give the super-algebra in Majorana representation in $D + 1$ dimensional light-cone coordinates where $D = 1, 2, 3$.

In Majorana representation Majorana spinors have real component fields, and can be written as

$$\Psi_M = \begin{pmatrix} \theta_L \\ \theta_R \end{pmatrix},$$

where θ_L, θ_R are left-moving, right-moving spinors with real components. This implies that the supercharge Q is also a Majorana spinor with real components of the form

$$Q = \int d^D x j^+ = \begin{pmatrix} Q_L \\ Q_R \end{pmatrix} \equiv \begin{pmatrix} Q^+ \\ Q^- \end{pmatrix},$$

where the integration is taken over the D spatial dimensions, j^μ is the supercurrent, which is a Majorana spinor.

In terms of the Majorana super-charge, the super-algebra is given by

$$\{Q, \bar{Q}\} = 2\Gamma^\mu P_\mu, \tag{A.1}$$

where $\bar{Q} \equiv Q^\dagger \Gamma^0$ in any representation, and thus $\bar{Q} = Q^T \Gamma^0$ in Majorana representation.

A.1 D=1

For 1+1 dimensional case, we have $\Gamma^0 = \sigma^2$ and $\Gamma^1 = i\sigma^1$, so that

$$\Gamma^+ \equiv \frac{\Gamma^0 + \Gamma^1}{\sqrt{2}} = i \begin{pmatrix} 0 & 0 \\ \sqrt{2} & 0 \end{pmatrix}, \quad \Gamma^- \equiv \frac{\Gamma^0 - \Gamma^1}{\sqrt{2}} = i \begin{pmatrix} 0 & -\sqrt{2} \\ 0 & 0 \end{pmatrix}$$

and $\bar{Q} = i(Q^-, -Q^+)$. Thus, Eq. (A.1) reads

$$\{Q, \bar{Q}\} = 2\Gamma^\mu P_\mu = i \begin{pmatrix} 0 & -2\sqrt{2}P_- \\ 2\sqrt{2}P_+ & 0 \end{pmatrix} = i \begin{pmatrix} 0 & -2\sqrt{2}P^+ \\ 2\sqrt{2}P^- & 0 \end{pmatrix},$$

or

$$\{Q^\pm, Q^\pm\} = 2\sqrt{2}P^\pm, \quad \{Q^+, Q^-\} = 0.$$

A.2 D=2

In this case $\Gamma^0 = \sigma^2$, $\Gamma^1 = i\sigma^1$ and $\Gamma^2 = \Gamma^\perp = i\sigma^3$. Therefore,

$$\{Q, \bar{Q}\} = 2\Gamma^\mu P_\mu = i \begin{pmatrix} 2P_\perp & -2\sqrt{2}P_- \\ 2\sqrt{2}P_+ & -2P_\perp \end{pmatrix} = i \begin{pmatrix} -2P^\perp & -2\sqrt{2}P^+ \\ 2\sqrt{2}P^- & 2P^\perp \end{pmatrix},$$

or

$$\{Q^\pm, Q^\pm\} = 2\sqrt{2}P^\pm, \quad \{Q^+, Q^-\} = -2P^\perp.$$

A.3 D=3

In 3+1 dimensions Majorana spinors have four components and thus the supercharge can be written as

$$Q = \begin{pmatrix} Q^+ \\ Q^- \end{pmatrix} \equiv \begin{pmatrix} Q_1^+ \\ Q_2^+ \\ Q_1^- \\ Q_2^- \end{pmatrix}, \quad \bar{Q} = Q^T \Gamma^0 = i(Q_2^-, -Q_1^-, Q_2^+, -Q_1^+).$$

Gamma matrices are 4×4 matrices given by

$$\Gamma^0 \equiv \begin{pmatrix} 0 & \sigma_2 \\ \sigma_2 & 0 \end{pmatrix}, \quad \Gamma^1 \equiv \begin{pmatrix} i\sigma_1 & 0 \\ 0 & i\sigma_1 \end{pmatrix}, \quad \Gamma^2 \equiv \begin{pmatrix} i\sigma_3 & 0 \\ 0 & i\sigma_3 \end{pmatrix}, \quad \Gamma^3 \equiv \begin{pmatrix} 0 & -\sigma_2 \\ \sigma_2 & 0 \end{pmatrix},$$

$$\Gamma^+ \equiv \frac{\Gamma^0 + \Gamma^3}{\sqrt{2}} = \begin{pmatrix} 0 & 0 \\ \sqrt{2}\sigma_2 & 0 \end{pmatrix}, \quad \Gamma^- \equiv \frac{\Gamma^0 - \Gamma^3}{\sqrt{2}} = \begin{pmatrix} 0 & \sqrt{2}\sigma_2 \\ 0 & 0 \end{pmatrix}.$$

Then Eq. (A.1) yields

$$\begin{aligned} \{Q, \bar{Q}\} &= 2\Gamma^\mu P_\mu = 2 \begin{pmatrix} i\sigma^1 P_1 + i\sigma^3 P_2 & \sqrt{2}\sigma^2 P_- \\ \sqrt{2}\sigma^2 P_+ & i\sigma^1 P_1 + i\sigma^3 P_2 \end{pmatrix} \\ &= 2i \begin{pmatrix} -P^2 & -P^1 & 0 & -\sqrt{2}P^+ \\ -P^1 & P^2 & \sqrt{2}P^+ & 0 \\ 0 & -\sqrt{2}P^- & -P^2 & -P^1 \\ \sqrt{2}P^- & 0 & -P^1 & P^2 \end{pmatrix}. \end{aligned}$$

Hence, we find

$$\{Q_\alpha^\pm, Q_\beta^\pm\} = 2\sqrt{2}P^\pm \delta_{\alpha\beta},$$

$$\{Q_1^+, Q_1^-\} = -\{Q_2^+, Q_2^-\} = 2P^1, \quad \{Q_1^+, Q_2^-\} = \{Q_2^+, Q_1^-\} = -2P^2,$$

where $\alpha, \beta = 1, 2$. Note that if $P^1 = P^2 = 0$, then this algebra coincides with the one for $\mathcal{N}=2$ SUSY in 1+1 dimensions also known as $\mathcal{N}=(2,2)$ SUSY.

APPENDIX B

FORMULAS

Here we list some of the formulas we used to derive the anticommutation relations among Q_α^\pm with $\alpha = 1, 2$ in Chapter 6.

$$\{B_1 F_1, B_2 F_2\} = B_2 B_1 \{F_1, F_2\} + B_1 [F_1, B_2] F_2 + B_2 [F_2, B_1] F_1 + [B_1, B_2] F_1 F_2$$

$$[F_1, F_2 F_3] = \{F_1, F_2\} F_3 - F_2 \{F_1, F_3\}$$

$$[F_1 F_2, F_3 F_4] = F_1 \{F_2, F_3\} F_4 - F_1 F_3 \{F_2, F_4\} + \{F_1, F_3\} F_4 F_2 - F_3 \{F_1, F_4\} F_2$$

$$[M_{ij,rs}^I(x), \partial_y M_{kl,pq}^{J\dagger}(y)] = [M_{ij,rs}^{I\dagger}(x), \partial_y M_{kl,pq}^J(y)] = ia^2 g^2 \delta(x-y) \delta_{IJ} \Delta$$

$$[\partial_x M_{ij,rs}^I(x), M_{kl,pq}^{J\dagger}(y)] = [\partial_x M_{ij,rs}^{I\dagger}(x), M_{kl,pq}^J(y)] = -ia^2 g^2 \delta(x-y) \delta_{IJ} \Delta$$

$$[M_{ij,rs}^I(x), M_{kl,pq}^{J\dagger}(y)] = [M_{ij,rs}^{I\dagger}(x), M_{kl,pq}^J(y)] =$$

$$ia^2 g^2 \frac{1}{\partial_y} \delta(x-y) \delta_{IJ} \Delta = -ia^2 g^2 \frac{1}{\partial_x} \delta(x-y) \delta_{IJ} \Delta$$

$$[\partial_x M_{ij,rs}^I(x), \partial_y M_{kl,pq}^{J\dagger}(y)] = [\partial_x M_{ij,rs}^{I\dagger}(x), \partial_y M_{kl,pq}^J(y)] =$$

$$ia^2 g^2 \partial_x \delta(x-y) \delta_{IJ} \Delta = -ia^2 g^2 \partial_y \delta(x-y) \delta_{IJ} \Delta$$

$$\{u_{ij,rs}^\alpha(x), u_{kl,pq}^\beta(y)\} = \frac{1}{2} \delta(x-y) \delta_{\alpha\beta} \Delta$$

$$\{u_{ij,rs}^\alpha(x), \frac{1}{\partial_y} u_{kl,pq}^\beta(y)\} = -\left\{ \frac{1}{\partial_x} u_{ij,rs}^\alpha(x), u_{kl,pq}^\beta(y) \right\} = \frac{1}{2} \frac{1}{\partial_y} \delta(x-y) \delta_{\alpha\beta} \Delta$$

$$\left\{ \frac{1}{\partial_x} u_{ij,rs}^\alpha(x), \frac{1}{\partial_y} u_{kl,pq}^\beta(y) \right\} = \frac{1}{2} \frac{1}{\partial_x \partial_y} \delta(x-y) \delta_{\alpha\beta} \Delta = -\frac{1}{2} \frac{1}{\partial_x^2} \delta(x-y) \delta_{\alpha\beta} \Delta$$

where F 's and B 's are fermionic and bosonic operators, respectively. i, j, k, l are site indices, r, s, p, q color indices, $\alpha, \beta, I, J=1,2$, a the lattice spacing, g the coupling, and

$$\Delta \equiv \delta_{rq} \delta_{sp} \frac{\delta_{ik}}{a} \frac{\delta_{jl}}{a}$$

BIBLIOGRAPHY

- [1] Y. A. Golfand and E. P. Likhtman, JETP Lett. **13**, 323 (1971) [Pisma Zh. Eksp. Teor. Fiz. **13**, 452 (1971)].
- [2] J. Wess and B. Zumino, Nucl. Phys. B **70**, 39 (1974).
- [3] A. Salam and E. Sezgin, “Supergravities In Diverse Dimensions. Vol. 1, 2,”; J. H. . Schwarz, “Superstrings. The First 15-Years Of Superstring Theory. Vol. 1,”.
- [4] M. T. Grisaru, W. Siegel and M. Rocek, Nucl. Phys. B **159**, 429 (1979);
- [5] For a more intuitive proof of the non-renormalization theorem making use of the holomorphy of the superpotential, see N. Seiberg, Phys. Lett. B **318**, 469 (1993) [arXiv:hep-ph/9309335]; arXiv:hep-th/9408013.
- [6] J. D. Lykken, arXiv:hep-th/9612114.
- [7] H. E. Haber and G. L. Kane, Phys. Rept. **117**, 75 (1985).
- [8] S. P. Martin, arXiv:hep-ph/9709356.
- [9] S. Raby, Rept. Prog. Phys. **67**, 755 (2004) [arXiv:hep-ph/0401155].
- [10] S. Dimopoulos, S. Raby and F. Wilczek, Phys. Rev. D **24**, 1681 (1981).
- [11] J. S. Hagelin, S. Kelley and T. Tanaka, Nucl. Phys. B **415**, 293 (1994); F. Gabiani, E. Gabrielli, A. Masiero and L. Silvestrini, Nucl. Phys. B **477**, 321 (1996) [arXiv:hep-ph/9604387]; A. Masiero and L. Silvestrini, arXiv:hep-ph/9711401.
- [12] J. M. Maldacena, Adv. Theor. Math. Phys. **2**, 231 (1998) [Int. J. Theor. Phys. **38**, 1113 (1999)] [arXiv:hep-th/9711200].
- [13] J. R. Hiller, S. S. Pinsky, N. Salwen and U. Trittman, Phys. Lett. B **624**, 105 (2005) [arXiv:hep-th/0506225].
- [14] A. Armoni, M. Shifman and G. Veneziano, Nucl. Phys. B **667**, 170 (2003) [arXiv:hep-th/0302163].

- [15] A. Armoni, M. Shifman and G. Veneziano, Phys. Rev. Lett. **91**, 191601 (2003) [arXiv:hep-th/0307097].
- [16] Y. Matsumura, N. Sakai, and T. Sakai, Phys. Rev. D **52**, 2446 (1995).
- [17] O. Lunin and S. Pinsky, AIP Conf. Proc. **494**, 140 (1999) [arXiv:hep-th/9910222].
- [18] P. Haney, J. R. Hiller, O. Lunin, S. Pinsky and U. Trittmann, Phys. Rev. D **62**, 075002 (2000) [arXiv:hep-th/9911243].
- [19] J. R. Hiller, S. Pinsky and U. Trittmann, Phys. Rev. D **63**, 105017 (2001) [arXiv:hep-th/0101120].
- [20] J. R. Hiller, S. Pinsky and U. Trittmann, Phys. Rev. D **64**, 105027 (2001) [arXiv:hep-th/0106193].
- [21] H. B. Nielsen and M. Ninomiya, Nucl. Phys. B **185**, 20 (1981) [Erratum-ibid. B **195**, 541 (1982)].
- [22] K. Fujikawa, Nucl. Phys. B **636**, 80 (2002) [arXiv:hep-th/0205095].
- [23] D. B. Kaplan, E. Katz and M. Unsal, JHEP **0305**, 037 (2003) [arXiv:hep-lat/0206019].
- [24] A. G. Cohen, D. B. Kaplan, E. Katz, and M. Unsal, JHEP **0308**, 024 (2003) [arXiv:hep-lat/0302017].
- [25] A. G. Cohen, D. B. Kaplan, E. Katz, and M. Unsal, JHEP **0312**, 031 (2003) [arXiv:hep-lat/0307012].
- [26] J. Giedt, Nucl. Phys. B **668**, 138 (2003) [arXiv:hep-lat/0304006]; Nucl. Phys. B **674**, 259 (2003) [arXiv:hep-lat/0307024]; arXiv:hep-lat/0405021.
- [27] F. Sugino, JHEP **0401**, 015 (2004) [arXiv:hep-lat/0311021].
- [28] F. Sugino, JHEP **0403**, 067 (2004) [arXiv:hep-lat/0401017].
- [29] F. Sugino, Nucl. Phys. Proc. Suppl. **140**, 763 (2005) [arXiv:hep-lat/0409036]; JHEP **0501**, 016 (2005) [arXiv:hep-lat/0410035];
- [30] F. Sugino, Phys. Lett. B **635**, 218 (2006) [arXiv:hep-lat/0601024].
- [31] S. Catterall, JHEP **0411**, 006 (2004) [arXiv:hep-lat/0410052]; S. Catterall, JHEP **0603**, 032 (2006) [arXiv:hep-lat/0602004].
- [32] A. D'Adda, I. Kanamori, N. Kawamoto and K. Nagata, Phys. Lett. B **633**, 645 (2006) [arXiv:hep-lat/0507029].

- [33] For a review of the recent approaches and some new results from the deconstruction approach, see J. Giedt, arXiv:hep-lat/0602007.
- [34] W. Bietenholz, Mod. Phys. Lett. A **14**, 51 (1999) [arXiv:hep-lat/9807010]; Y. Kikukawa and Y. Nakayama, Phys. Rev. D **66**, 094508 (2002) [arXiv:hep-lat/0207013]; K. Itoh, M. Kato, H. Sawanaka, H. So and N. Ukita, JHEP **0302**, 033 (2003) [arXiv:hep-lat/0210049]; S. Catterall, JHEP **0305**, 038 (2003) [arXiv:hep-lat/0301028]; S. Catterall and S. Karamov, Phys. Rev. D **68**, 014503 (2003) [arXiv:hep-lat/0305002]; S. Catterall and S. Ghadab, JHEP **0405**, 044 (2004) [arXiv:hep-lat/0311042]; A. D’Adda, I. Kanamori, N. Kawamoto and K. Nagata, Nucl. Phys. B **707**, 100 (2005) [arXiv:hep-lat/0406029]; J. Giedt and E. Poppitz, JHEP **0409**, 029 (2004) [arXiv:hep-th/0407135]; J. Giedt, R. Konik, E. Poppitz and T. Yavin, JHEP **0412**, 033 (2004) [arXiv:hep-lat/0410041].
- [35] For a brief but inclusive review on this subject, see for example A. Feo, Nucl. Phys. Proc. Suppl. **119**, 198 (2003) [arXiv:hep-lat/0210015]; Mod. Phys. Lett. A **19**, 2387 (2004) [arXiv:hep-lat/0410012].
- [36] D. B. Kaplan, Phys. Lett. B **288**, 342 (1992) [arXiv:hep-lat/9206013].
- [37] R. Narayanan and H. Neuberger, Nucl. Phys. B **443**, 305 (1995) [arXiv:hep-th/9411108].
- [38] H. Neuberger, Phys. Lett. B **417**, 141 (1998) [arXiv:hep-lat/9707022].
- [39] E. Witten, Nucl. Phys. B **460**, 335 (1996) [arXiv:hep-th/9510135].
- [40] H.-C. Pauli and S.J. Brodsky, Phys. Rev. D **32**, 1993 (1985); Phys. Rev. D **32**, 2001 (1985).
- [41] J. R. Hiller, M. Harada, S. S. Pinsky, N. Salwen and U. Trittmann, Phys. Rev. D **71**, 085008 (2005) [arXiv:hep-th/0411220].
- [42] N. Arkani-Hamed, A. G. Cohen, and H. Georgi, Phys. Rev. Lett. **86**, 4757 (2001) arXiv:hep-th/0104005; C. T. Hill, S. Pokorski and J. Wang, Phys. Rev. D **64**, 105005 (2001) arXiv:hep-th/0104035.
- [43] W. A. Bardeen and R. B. Pearson, Phys. Rev. D **14**, 547 (1976).
- [44] W. A. Bardeen, R. B. Pearson and E. Rabinocici, Phys. Rev. D **21**, 1037 (1980).
- [45] M. Burkardt and S. Dalley, Prog. Part. Nucl. Phys. **48**, 317 (2002). arXiv:hep-th/0112007.
- [46] S.J. Brodsky, H.-C. Pauli, and S.S. Pinsky, Phys. Rep. **301**, 299 (1998) [arXiv:hep-ph/9705477].

- [47] J. R. Hiller, S. S. Pinsky and U. Trittmann, Phys. Rev. D **65**, 085046 (2002) [arXiv:hep-th/0112151].
- [48] F. Antonuccio, A. Hashimoto, O. Lunin, and S. Pinsky, JHEP **9907**, 029 (1999) [arXiv:hep-th/9906087].
- [49] J. R. Hiller, O. Lunin, S. Pinsky, and U. Trittmann, Phys. Lett. B **482**, 409 (2000) [arXiv:hep-th/0003249].
- [50] J. R. Hiller, Y. Proestos, S. Pinsky and N. Salwen, Phys. Rev. D **70**, 065012 (2004) [arXiv:hep-th/0407076].
- [51] F. Antonuccio, H. C. Pauli, S. Pinsky, and S. Tsujimaru, Phys. Rev. D **58**, 125006 (1998) [arXiv:hep-th/9808120].
- [52] M. Harada, J. R. Hiller, S. Pinsky and N. Salwen, Phys. Rev. D **70**, 045015 (2004) [arXiv:hep-th/0404123].
- [53] D. J. Gross, A. Hashimoto, and I. R. Klebanov, Phys. Rev. D **57**, 6420 (1998) [arXiv:hep-th/9710240].
- [54] J. R. Hiller, S. S. Pinsky, and U. Trittmann, Nucl. Phys. B **661**, 99 (2003) [arXiv:hep-ph/0302119].
- [55] F. Antonuccio, O. Lunin, and S. S. Pinsky, Phys. Lett. B **429**, 327 (1998) [arXiv:hep-th/9803027].
- [56] S. S. Gubser, I. R. Klebanov, and A. M. Polyakov, Phys. Lett. B **428**, 105 (1998) [arXiv:hep-th/9802109].
- [57] E. Witten, Adv. Theor. Math. Phys. **2**, 253 (1998) [arXiv:hep-th/9802150].
- [58] A. Hashimoto and N. Itzhaki, Phys. Lett. B **454**, 235 (1999) [arXiv:hep-th/9903067].
- [59] N. Itzhaki, J. M. Maldacena, J. Sonnenschein, and S. Yankielowicz, Phys. Rev. D **58**, 046004 (1998) [arXiv:hep-th/9802042].
- [60] G. T. Horowitz and J. Polchinski, Phys. Rev. D **55**, 6189 (1997) [arXiv:hep-th/9612146].
- [61] C. Lanczos, J. Res. Nat. Bur. Stand. **45**, 255 (1950); J. Cullum and R. A. Willoughby, *Lanczos Algorithms for Large Symmetric Eigenvalue Computations*, Vol. I and II, (Birkhauser, Boston, 1985).
- [62] M. Harada and S. Pinsky, Phys. Lett. B **567**, 277 (2003) [arXiv:hep-lat/0303027].

- [63] S. Dalley and B. van de Sande, Phys. Rev. D **56**, 7917 (1997) [arXiv:hep-ph/9704408].
- [64] S. Dalley and B. van de Sande, Phys. Rev. D **59**, 065008 (1999) [arXiv:hep-th/9806231].
- [65] S. Dalley and B. van de Sande, Phys. Rev. Lett. **82**, 1088 (1999) [arXiv:hep-th/9810236]; Phys. Rev. D **62**, 014507 (2000) [arXiv:hep-lat/9911035]; Phys. Rev. D **63**, 076004 (2001) [arXiv:hep-lat/0010082].
- [66] S. Dalley, Phys. Rev. D **64**, 036006 (2001) [arXiv:hep-ph/0101318].
- [67] F. Antonuccio, O. Lunin, and S. Pinsky, Phys. Rev. D **58**, 085009 (1998), arXiv:hep-th/9803170; F. Antonuccio, O. Lunin, S. Pinsky, and S. Tsujimaru, Phys. Rev. D **60**, 115006 (1999), arXiv:hep-th/9811254.
- [68] F. Antonuccio, O. Lunin and S. Pinsky, Phys. Rev. D **59**, 085001 (1999), arXiv:hep-th/9811083; P. Haney, J. R. Hiller, O. Lunin, S. Pinsky and U. Trittman, Phys. Rev. D **62**, 075002 (2000), arXiv:hep-th/9911243;
- [69] O. Lunin and S. Pinsky, Phys. Rev. D **63**, 045019 (2001) [arXiv:hep-th/0005282].
- [70] S. Dalley and B. van de Sande, arXiv:hep-ph/0212086.
- [71] T. Eguchi and H. Kawai, *Phys. Rev. Lett.* **48** (1983) 1063.
- [72] D. Kutasov, Phys. Rev. **D48** (1993) 4980, arXiv:hep-th/9306013.
- [73] M. Burkardt and H. El-Khozondar, Phys. Rev. D **60**, 054504 (1999) [arXiv:hep-ph/9805495];
- [74] L. Susskind, Phys. Rev. D **16**, 3031 (1977),
- [75] K. G. Wilson, Phys. Rev. D **10**, 2445 (1974).
- [76] D. Chakrabarti, A. K. De and A. Harindranath, Phys. Rev. D **67**, 076004 (2003) [arXiv:hep-th/0211145].
- [77] M. Harada and S. Pinsky, Phys. Rev. D **70**, 087701 (2004) [arXiv:hep-lat/0408026].
- [78] M. Harada and S. Pinsky, Phys. Rev. D **71**, 065013 (2005) [arXiv:hep-lat/0411024].
- [79] S. Catterall, JHEP **0305**, 038 (2003) [arXiv:hep-lat/0301028].

- [80] G. Bhanot, U. M. Heller and H. Neuberger, Phys. Lett. B **113**, 47 (1982).
- [81] A. Gonzalez-Arroyo and M. Okawa, Phys. Rev. D **27**, 2397 (1983); T. Eguchi and R. Nakayama, Phys. Lett. B **122**, 59 (1983).
- [82] M. Burkardt, AIP Conf. Proc. **494**, 239 (1999) [arXiv:hep-th/9908195].